Spring 1-1-2012

Thermal Analysis of Integrated Radiant Slab Heating and Cooling Systems

Benjamin Park
University of Colorado at Boulder, benjamin.park@colorado.edu

THERMAL ANALYSIS OF INTEGRATED RADIANT SLAB HEATING AND COOLING SYSTEMS

by

BENJAMIN PARK

B.A., University of Seoul, 2007

M.A., University of Colorado at Boulder, 2012

A thesis submitted to the

Faculty of the Graduate School of the

University of Colorado in partial fulfillment

of the requirement for the Master's degree

Department of Civil, Environmental, and Architectural Engineering

2012

This thesis entitled:

Thermal Analysis of Integrated Radiant Slab Heating and Cooling Systems

written by Benjamin Park

has been approved for the Department of Civil, Environmental, and Architectural Engineering, University of Colorado at Boulder

_____

(Moncef Krarti)

_____

(Gregor Henze)

_____

(Junghyon Mun)

Date:_____

The final copy of this thesis has been examined by the signatories, and we Find that both the content and the form meet acceptable presentation standards Of scholarly work in the above mentioned discipline.

Benjamin Park (M.S., Department of Civil, Environmental, and Architectural Engineering)

Thermal analysis of integrated radiant slab heating and cooling systems

Thesis directed by Professor Moncef Krarti

It is reported that the U.S. has seen a significant increase in energy consumption in recent years. According to Department of Energy (DOE), residential buildings in the U.S uses 36 percent more energy than it did 30 years ago (DOE, 2010). In the residential sector, 43 percent of the total energy consumption is used for space heating and space cooling. There is an increasing interest in improving the energy performance of buildings and especially in technologies to reduce building energy consumption for space heating and cooling. Radiant slab heating and radiant cooling systems have been used as alternative options to reduce heating and cooling energy use in residential buildings.

The study presented in this thesis focuses on the analysis of the performance of integrated radiant floor heating and ceiling cooling systems with embedded hot water pipes and chilled water pipes in the building slab. In particular, the study he includes a comprehensive thermal analysis of radiant slab systems with two heat sources to perform as both radiant floor heating and ceiling cooling systems.

To perform the thermal analysis of the integrated radiant slab systems, a two-dimensional transient heat transfer model using implicit finite difference method (FDM) is developed. In addition, to estimate thermal loads for any conditioned zone, an RC network model is developed. Indoor air heat balance algorithm of Energyplus is adopted and implemented in combination with the developed FDM and the RC network model. In terms of control scheme of radiant systems, variable flow control algorithm of Energyplus is adopted.

Several sensitivity analyses and parametric analyses are performed to determine the transient thermal performance of the integrated radiant slab systems under various design and operating conditions. A numerical model of radiant slab has been developed to account for various insulation configurations. The predictions of the numerical model have been validated against reported experimental data. In addition, the results obtained from the developed numerical model for the integrated radiant floor heating and radiant ceiling cooling system have been verified against those with the obtained from Energyplus, a whole building energy simulation program. Using the developed integrated radiant floor and ceiling model, a series of parametric analyses is carried out to examine the transient thermal performance of radiant floor heating and radiant ceiling cooling system for various insulation configurations, building thermal mass, building zoning configurations, and climatic conditions.

ACKNOWLEDGEMENTS

I would like to thank Professor Moncef Krarti and Pyeongchan Ihm for their suggestions and comments to accomplish the study presented in this thesis.

Especially, I sincerely appreciate my advisor, Professor Moncef Krarti. He was not only my academic advisor but also my mentor. He always encouraged me and has not lost faith in me. I am now more confident on how to face and solve research work using his advices. I will never forget his guidance. I also would like to express my gratitude to Professor Pyeongchan Ihm for his comments and kindness. He gave me a sense of how to prepare and solve research problems.

I would like to thank my parents and younger brother for their faith, encouragement and infinite love. Finally, I would like to thank all my colleagues and friends for their encouragement and help.

CONTENTS

FIGURES

TABLES

CHAPTER 1: INTRODUCTION

1.1. Background

It is reported that the U.S. has seen a significant increase in energy consumption in recent years. According to Department of Energy (DOE), residential buildings in the U.S utilize 36 percent more energy than they did 30 years ago (DOE, 2010). In the residential sector, 43 percent of the total energy consumption is used for space heating and space cooling. There is now more interest in techniques and technologies to reduce energy consumption for space heating and cooling. Radiant slab heating and cooling systems represent one of the technologies that can reduce heating and cooling energy consumption for residential buildings.

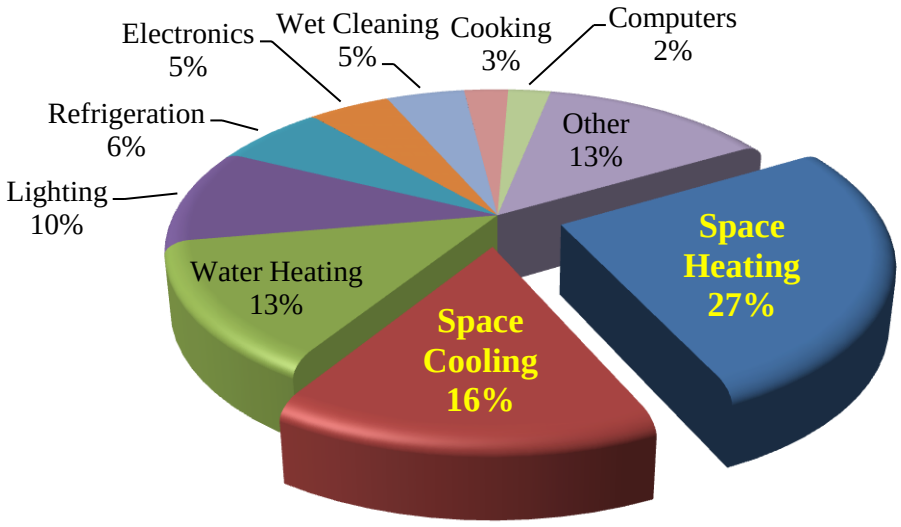

Figure 1.1: Residential energy end-use break down for the U.S. (DOE, 2010)

Radiant panel heating and cooling systems provide heating and cooling energy through temperature-controlled indoor surfaces such as floors, walls, and/or ceilings. The surface temperatures can be controlled by circulating water, air, or electric current through either an embedded circuit or attached circuit. The most common types of panels applied in radiant panel systems are (a) metal ceiling panels, (b) embedded tubing in ceilings, walls, or floors, (c) electric ceiling panels, (d) electrically heated ceilings or floors, and (e) air-heated floors.

In radiant systems, sensible heating or cooling panels transfer heat through temperature-controlled surfaces to or from an indoor space and its enclosure surfaces by thermal radiation and natural convection. Generally more than 50 percent of the heat transfer between panel surface and the space occurs through thermal radiation. Panel heating and cooling systems are used in currently used to maintain thermal comfort in a wide range of buildings including residences, office buildings, classrooms, hospital patient rooms, swimming pool areas, repair garages, and in industrial and warehouse applications.

1.1.1. Overview of radiant heating systems and radiant cooling systems

Residential heating applications usually consist of tubes or electric elements embedded in floors or ceilings. Figure 1.2 illustrates typical subfloor constructions with embedded pipes in concrete or gypsum. The piping is installed on top of the rafters. Heat diffusion and surface temperature can be improved uniformly by adding metal heat transfer plates, which spread heat beneath the finishing material.

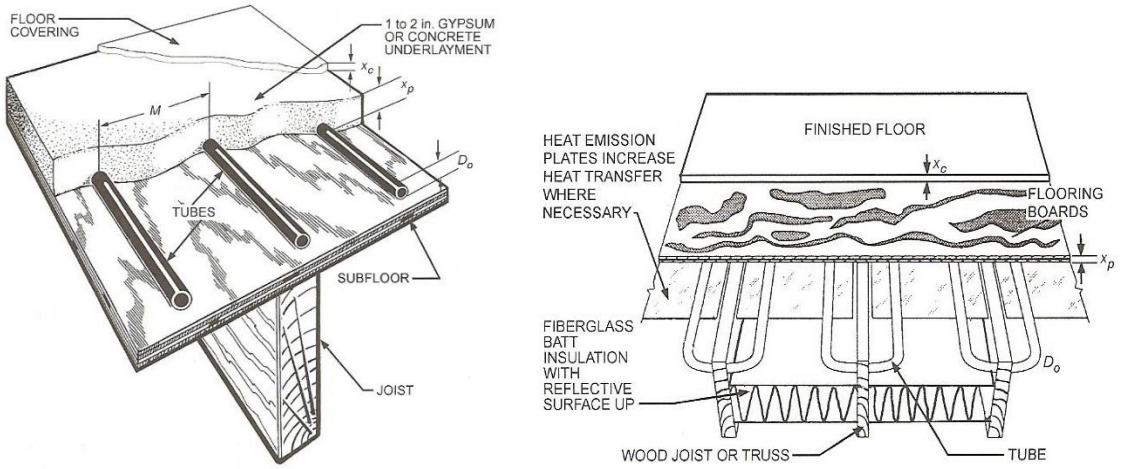

Figure 1.2: A typical embedded tubing in slab and tubing in subfloor (ASHRAE, 2008)

This construction is suitable for zones where thermal loads are stable and for building designs that minimize solar effects. However, in buildings where fenestration is large or where thermal loads change abruptly, the slow response, thermal lag, and override effect of high thermal mass panels are unsatisfactory. Metal ceiling panels with low thermal mass are more suitable since they respond more quickly to sudden thermal load changes (Berglund, 1982).

Radiant floor heating systems (RFH) have become popular due to their potential for energy savings as well as better thermal comfort (uniform cooling and heating distribution). Radiant panel systems have several advantages. Hydronic panel systems may be connected in series increasing exergetic efficiency. Indoor air temperature as well as mean radiant temperature can be controlled with the radiant panels, minimizing air motion within a space. Therefore thermal comfort may be better satisfied than conventional air-conditioning systems. Moreover, radiant panel systems have relatively low initial cost compared to air-conditioning systems. They also require less space for mechanical

equipment and control devices. This feature is especially valuable in hospital patient rooms, offices, and other applications where space is at a premium. Moreover, in-floor heating creates inhospitable living conditions for house dust mites compared to other heating systems. With radiant systems, noise associated with fan-coil or induction units is eliminated. In addition, peak loads are reduced as a result of thermal energy storage in the panel structure, as well as walls and partitions directly exposed to the radiant panels.

Many studies have reported that radiant heating systems can be more energy efficient compared to conventional air systems. Cho and Zaheer-uddin (1997) concluded that radiant floor heating systems can save up to 15 percent of energy usage compared to conventional heating systems. Experimental research analysis (CADDET, 1999) reported that electric radiant panel can achieve 33 percent to 52 percent of heating energy savings compared to air-to-air heat pump and electric baseboard heating systems, respectively. Stetui (1999) concluded that radiant systems can save up to 30 percent of the energy consumption and 27 percent of the peak demand for US office buildings. Watson and Chapman (2002) and Argiriou et al. (2005) reported that radiant systems can benefit from building thermal mass to shift the peak hour and enhance a thermal comfort in the space. Zhai et al. (2009) reported that radiant heating systems can achieve significant energy savings when compared to convective air systems at equal indoor thermal comfort and air quality. Radiant heating systems require less energy due to the fact that unlike the conventional convective air systems, radiant heating systems deliver heat directly to the occupants by radiation; therefore, when heating is required in the conditioned space, the same thermal comfort can be achieved at lower indoor air temperatures. Typically, similar thermal comfort can be accomplished with 3 to 4 degree Celsius lower indoor air temperatures. As a result, air infiltration thermal loads can be reduced for radiant panels

because of lower temperature difference between indoor and outdoor when compared to conventional air systems.

The Radiant Heating and Cooling Handbook (Watson and Chapman, 2002) provides a detailed overview of radiant heating systems including radiant heat transfer, building thermal comfort, design guidelines and typical control strategies. Similarly, ASHRAE Handbook of HVAC Systems and Equipment (2008) provides useful information to analyze, design, and control radiant floor systems. Some basic design guidelines of the radiant floor systems in residential building are outlined in Table 1.1:

Table 1.1: A summary of general design guidelines of the radiant floor heating systems in residential buildings (Adapted from Watson and Chapman, 2002)

Category	Design guideline
Room temperature	65 ~ 72 ˚F (18 ~ 22 ˚C)
Supplied hot water temperature	95 ~ 140 ˚F (35 ~ 60 ˚C)
Floor surface temperature	75 ~ 85 ˚F (24 ~ 30 ˚C)
Temperature drop of water temperature	15 ~ 20 ˚F (8 ~ 11 ˚C)
Maximum length of loop	200 ft. (60 m) in 3/8 inch (1 cm) tube size, 300 ft. (90 m) in 1/2 inch (1.25 cm) tube size
Tube size	3/8 inch (1 cm)
Tube spacing	4 ~ 9 inch (10 ~ 23 cm)

Radiant ceiling cooling (RCC) systems are generally used to provide cooling for either residential or office buildings. RCC systems are commonly used in Scandinavian

countries, Switzerland and Germany. Indeed, RCC systems provide energy efficient alternatives to traditional air conditioning systems, enable to improve thermal comfort.

There are two primary types of radiant cooling systems with a broad range of technologies as illustrated in Figure 1.3. The first type consists of radiant cooling slab systems that deliver cooling using elements of the building structure, commonly slab floors. These systems are generally referred to as thermally activated building systems or TABS (Gwerder, 2008). The second type includes radiant cooling systems that deliver cooling through ceiling panels. Radiant cooling slab systems are cheaper than ceiling panel systems and offer the benefits of thermal mass while ceiling panel systems offer faster temperature control and flexibility due to their low thermal mass level.

Radiant cooling slabs have similar construction elements as heating floors with tubes are embedded within the concrete slab but with thermal insulation placed on the top of the tubes to enhance downward heat transfer exchange with the cooled spaces. The initial cost of these systems is relatively low. However and due to their high thermal inertia, they are difficult to control and exhibit some risks of condensation especially in the case of rapid increases of the relative humidity within the conditioned spaces.

Radiant ceiling panel systems are typically integrated with suspended acoustical ceilings. The ceiling panels are generally made up of steel or copper pipes with diffusion fins. The materials of panels have high thermal conductivity values but they have low thermal inertia. Various theoretical or experimental results show that radiant ceiling panels can achieve energy savings up to 30 percent compared to conventional air systems (Laoudi, 2004). Several factors such as design capacities, temperature settings, and locations of the radiant panels affect the energy efficiency of the systems as well as the thermal comfort of

the occupants. Properly designed systems can produce long term energy savings of up to 30 percent (Conroy, 2001)

In a stand-alone panel cooling system, dehumidification and panel surface condensation may be of a significant concern under specific operating conditions. In particular, preventing condensation problems can affect the selection of the cooling capacity of a radiant cooling system. The surface temperature should not be equal or below the dew point temperature within the space. Some standards suggest a limit for the indoor relative humidity to 60 percent or 70 percent. An air temperature of 26 ℃ (79 ℉) would mean a dew point between 17 ℃ and 20 ℃ (63 ℉ and 68 ℉)(Olesen, 2008). There is, however, evidence that suggests decreasing the surface temperature to below the dew point temperature for a short period of time may not cause condensation issues (Mumma, 2002). As a general rule of thumb, it is recommended to maintain the slab surface higher than 20 ℃. Also, it is recommended to use an additional system, such as a dehumidifier, in order to reduce the indoor relative humidity and allow for increased cooling capacity. A water temperature of 16 ˚C (±1 ˚C) is recommended for radiant cooling systems in order to reduce the risk of condensation.

In terms of economic cost-effectiveness, ceiling cooling panels and chilled beams have been found to have the highest rate of return on investments due to their significant energy savings potential (DOE, 2002).

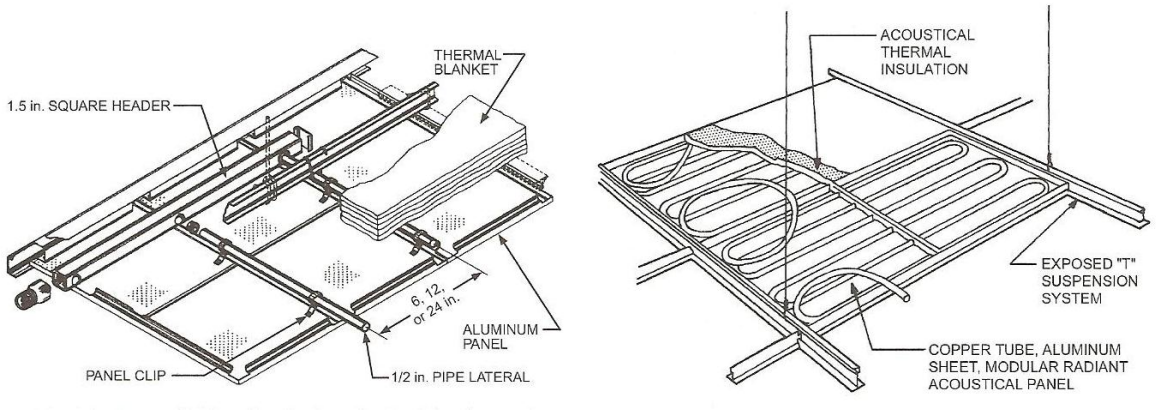

(a)

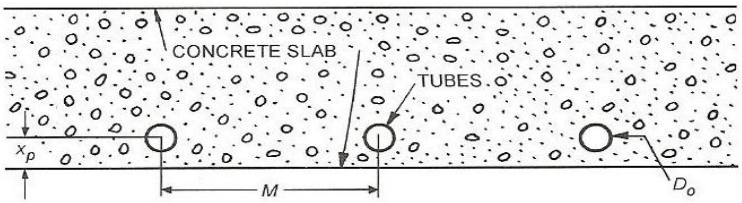

(b)

Figure 1.3: (a) A typical metal ceiling panel with (a) typical piping arrangement and (b) embedded coils in structural concrete slab (Source: ASHRAE, 2008)

Adequate control strategies for radiant systems are rather complicated due to lower operating hot water temperatures, acceptable limits of floor surface temperatures, and characteristics of transient heat transfer especially for slab radiant systems with high thermal mass. Some of the suitable control strategies for radiant systems are especially difficult to implement or to model in detailed whole-building energy simulation tools such as EnergyPlus. Indeed, EnergyPlus can model only some control strategies for radiant systems including the variable flow control scheme.

The control scheme using variable flow for radiant systems as modeled within EnergyPlus is quite simple even though it can be adjusted through the user defined

schedules. The program allows the user to define a setpoint temperature as well as a throttling range through which the water flow rate to the radiant system is varied. The flow rate is varied linearly with 50 % of the maximum flow when the controlling temperature reaches the zone setpoint temperature. The controlling temperature can consist of the mean air temperature, the mean radiant temperature, or the operative temperature of the zone (Energyplus, 2011).

Numerous studies for radiant heating systems consider only on evaluating the performance of systems with one heat sources either for heating only or cooling only. No attempt was reported in the literature to investigate thermal performance and energy efficiency of radiant systems with two heat sources including heating pipes placed on the top of the slab to provide heating energy to the upper conditioned zone and cooling pipes placed on the bottom of the slab to provide cooling energy to the lower conditioned zone. It is the main objective of the work presented in this dissertation to investigate thermal performance and energy efficiency of radiant panel systems with two heat sources that can provide both heating and cooling to conditioned spaces.

1.1.2. Impact of radiant heating and cooling system on energy savings

As noted earlier, radiant systems can provide significant energy savings for heating and cooling buildings compared to the conventional systems. For instance, simulation results obtained for radiant heating slab and radiant ceiling and wall cooling to serve university buildings have shown a 43 % savings in annual energy use of a guest cottage

building compared to the packaged terminal air heat pump system recommended by ASHRAE 90.1 as presented in Figure 1.4 (Krarti and Park, 2011).

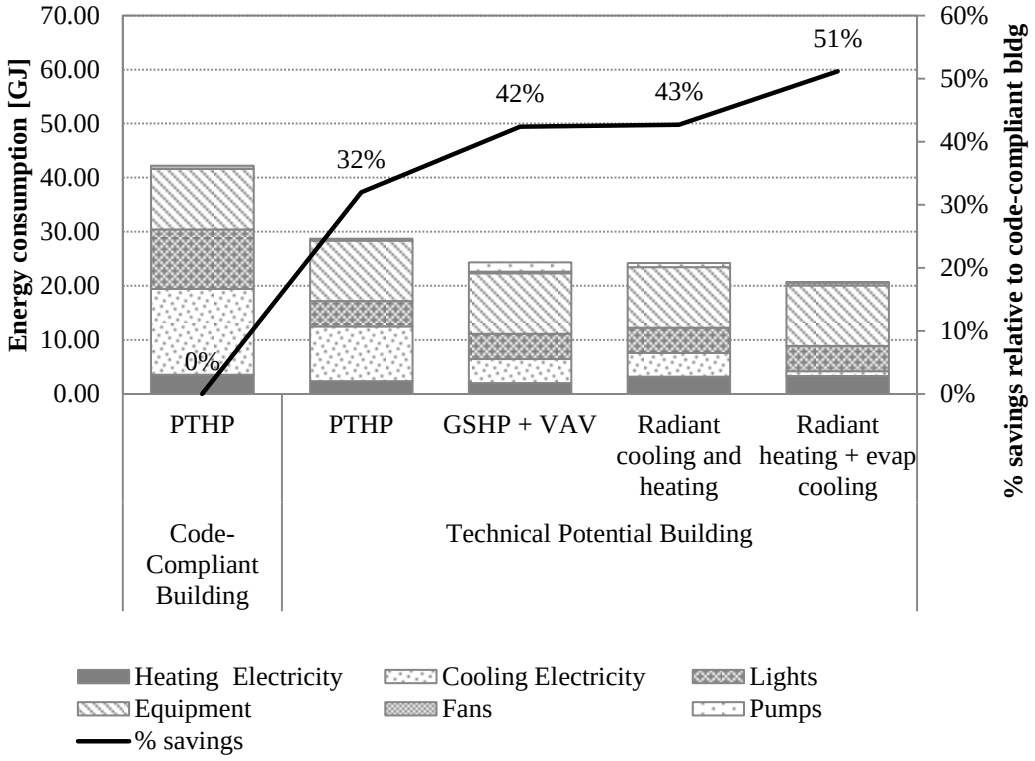

Figure 1.4: Annual energy consumption of various HVAC alternatives and percent savings relative to a code-compliant building for the guest cottage building

For another building, a research laboratory, combined radiant slab heating and radiant ceiling cooling systems have been found to reduce by 27 % the annual energy use compared to the HVAC system specified by ASHRAE 90.1 as shown in Figure 1.5 (Krarti and Park, 2011).

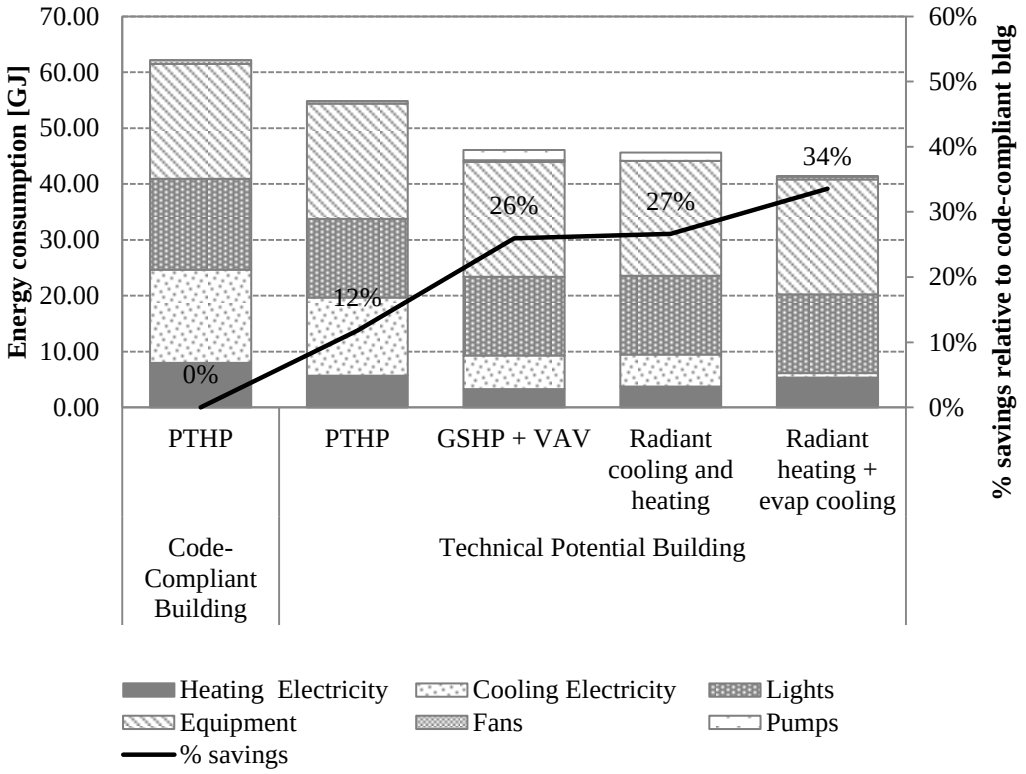

Figure 1.5: Annual energy consumption of various HVAC alternatives and percent savings relative to a code-compliant building for a research laboratory building.

1.2. Objectives

The main purpose of the study presented in this thesis is to evaluate the energy performance of radiant slab heating and cooling systems to maintain thermal comfort within conditioned zones under various design and operating conditions. To achieve this objective, a transient model for radiant floor heating and cooling systems will be first developed using numerical solution technique based on the implicit finite difference method (FDM). The transient model will be then used to develop a standalone building simulation environment tool to predict the energy use of radiant slab heating and cooling systems.

In summary, the main objectives of the project are as follows:

1. To develop a transient floor model for radiant slab heating and cooling system with separately embedded heat sink/sources in one slab construction to analyze heat transfer through the slab.
2. To develop a dynamic simulation environment tool to predict energy use required to maintain thermal comfort within conditioned zones utilizing radiant slab heating and cooling systems. The simulation environment combines the transient two-dimensional radiant slab model and an RC thermal network model for conditioned zones.
3. To validate the predictions from the dynamic simulation environment tool as well as the numerical slab model with the results obtained from experimental measurements as well as Energyplus whole building simulation tool.
4. To investigate the impact of thermal bridging effects on the performance of radiant slab heating and cooling systems for various insulation placement configurations.

   To evaluate the impact of several design and operating parameters on the energy performance of radiant slab heating and cooling systems by using the developed simulation environment tool under various climatic conditions.

1.3. Organization of the Thesis

The thesis provides a summary of a detailed analysis of thermal interactions between outdoor and building indoor environment through radiant slab heating and ceiling cooling systems. The analysis is based on the development of a two-dimensional transient FDM heat transfer model combined with RC thermal network model to constitute a

simulation environment to assess the energy use and thermal comfort level within conditioned zones served by radiant slab heating and cooling systems.

The thesis is organized into five chapters. The following sections describe briefly the scope of each chapter.

Chapter 1 presents an overview of some applications of radiant heating and cooling systems and the current analysis methods and control strategies available to evaluate and operate radiant heating and cooling systems utilized within residential and commercial buildings.

In Chapter 2, a two-dimensional transient heat transfer model for a slab system is developed using the implicit finite difference method (FDM). The predictions from the two-dimensional FDM numerical solution are verified using analytical solutions for simplified slab configurations. A series of parametric and sensitivity analysis is carried out to evaluate the performance of the slab systems. In particular, the thermal exchanges through various slab surfaces are analyzed for various slab insulation placement configurations.

Chapter 3 presents a transient FDM two-dimensional model for radiant slab heating and cooling system with embedded heat sink/sources. The model is validated against reported experimental data obtained for a radiant slab system. A series of sensitivity and parametric analyses is performed to evaluate the thermal performance of radiant slab heating and cooling systems under various design and operating conditions.

Chapter 4 outlines the basic features of the simulation environment developed to assess the energy use and thermal comfort specific to radiant slab heating and cooling systems. The simulation environment includes the transient FDM two-dimensional model for radiant slab heating and cooling system combined with an RC network model for

typical thermal zones in multi-floor buildings. The predictions from the developed simulation environment are validated against results obtained from Energyplus, a detailed whole-building energy simulation tool. Using the simulation environment tool, the impact of thermal bridging effects on energy consumption for radiant slab heating and ceiling cooling systems are evaluated.

Chapter 5 presents some additional applications of the developed simulation environment tool to assess the performance of radiant slab heating and cooling systems under specific design and operation conditions. In particular, a series of parametric analyses are carried out to assess the impact of insulation placement configurations, thermal bridging effects for between two conditioned zones as well as between on conditioned zone and unconditioned spaces, impact of thermal mass location within the building envelope structure, and the effect of climatic conditions on the energy performance of radiant slab heating and cooling systems.

CHAPTER 2: DEVELOPMENT OF NUMERICAL MODEL

2.1. Introduction

Modeling heat transfer within building construction elements is important to understand and predict thermal loads of buildings as well as energy demand, thermal comfort and system control response. Numerous building heat transfer models are reported over the last few decades. Most of these models are based on numerical methods and formulations utilizing using several discretization solution techniques including finite difference, finite element, and control volume approaches. In the analysis work carried out in this thesis, the control volume approach has been chosen. The main advantage of the control volume method is that energy is conserved regardless of the size of the control volume. Thus, a heat conduction problem can be solved quickly utilizing a fairly coarse grid to develop the numerical technique. Finally the control volume method minimizes mathematical complexity of the solution approach for most heat transfer problems (Kreith and Bohn, 2001).

Ho et al. (1995) developed detailed numerical models that rely on a two-dimensional formulation scheme. Zhang (2001) developed a one-dimensional floor model to simulate the dynamic behavior of the under-floor heating system for several control strategies. Laouadi (2004) developed a slab floor model combining a one-dimensional numerical model with a two-dimensional analytical model in order to explore the temperature distribution between the tubes arranged in the serpentine tubing configuration. Weitzman et al. (2005) developed detailed numerical models that rely on a two-

dimensional formulation scheme. In addition, several studies have been carried out using transient numerical modeling of radiant slab floor systems in order to evaluate their thermal performance for a specific set of control strategies under transient conditions. Most existing studies rely on the thermal performance of radiant panel systems with only one heat source to provide either heating only or cooling only.

In this chapter, a two-dimensional numerical solution using implicit finite difference method to evaluate heat transfer within a building slab with two sets of embedded tubes to provide heating and cooling. The stability and the accuracy of the numerical solution is evaluated and verified against results from analytical solution obtained for one-dimensional heat transfer. In particular, the predictions of the numerical solution are assessed for temperature distribution within the slab and the total heat fluxes through the slab surfaces.

2.2. Development of Slab Model

2.2.1. Differential Equation Formulation

Unsteady-state temperature within building elements is generally subject to the time-dependent heat conduction equation. Transient two-dimensional heat conduction equation without heat generation is given as Eq. (2.1):

$$K \cdot \frac{\partial^2 T}{\partial x^2} + K \cdot \frac{\partial^2 T}{\partial y^2} = \rho \cdot c_p \cdot \frac{\partial T}{\partial t} \tag{2.1}$$

Where,

ρ = density [kg/m^3]

c_p = heat capacity [J/kg˚C]

K = thermal conductivity [kg/m^3]

t = time [sec]

2.2.2. Finite Difference Formulation

Control volume approach and pure implicit finite difference technique is typically used to solve the heat conduction equation represented by Eq. (2.1). The control volume and its associated nodal dimensions are shown in Figure 2.1.

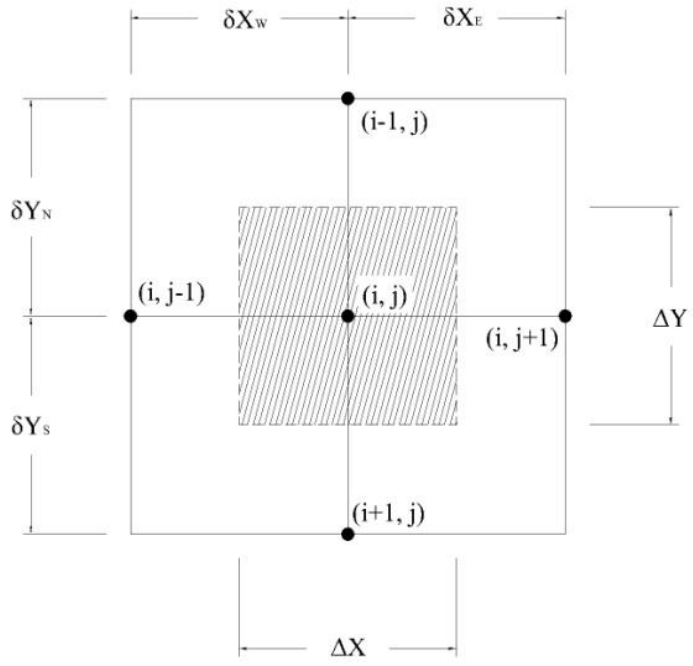

Figure 2.1: Control volume for solving two-dimensional heat conduction equation

The heat conduction equation can be discretized as indicated below:

$$\frac{\partial T}{\partial x_{i,j-\frac{1}{2}}} = \frac{T_{i,j} - T_{i,j-1}}{\delta x_W}$$
$$\frac{\partial T}{\partial x_{i,j+\frac{1}{2}}} = \frac{T_{i,j+1} - T_{i,j}}{\delta x_E}$$
$$\frac{\partial T}{\partial x_{i+\frac{1}{2},j}} = \frac{T_{i,j} - T_{i+1,j}}{\delta y_S}$$
$$\frac{\partial T}{\partial x_{i-\frac{1}{2},j}} = \frac{T_{i-1,j} - T_{i,j}}{\delta y_N}$$

The principle of conservation of energy for the control volume is defined as follows (Kreith and Bohn, 2001):

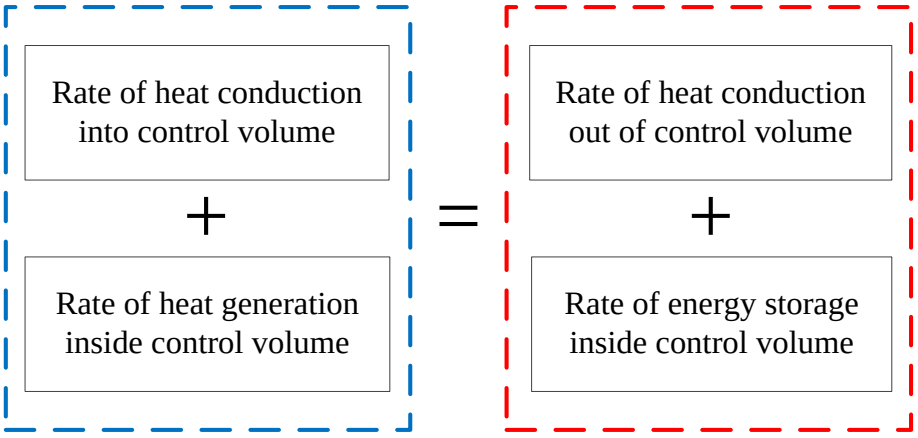

The energy conservation principle can be expressed using Eq. (2.2):

$$-K \cdot A \cdot \left.\frac{dT}{dx}\right|_x - K \cdot A \cdot \left.\frac{dT}{dy}\right|_y + q_G \cdot A \cdot \Delta x$$
$$= -K \cdot A \cdot \left.\frac{dT}{dx}\right|_{x+\Delta x} - K \cdot A \cdot \left.\frac{dT}{dy}\right|_{y+\Delta y} + \rho \cdot Cp \cdot A \cdot \Delta x \cdot \frac{dT(x+\frac{\Delta x}{2}, t)}{dt} \quad (2.2)$$

For two dimensional finite difference grid with non-uniform thermal conductivity (K) values and different nodal distances, this form can be transformed to

$$- K_W \Delta y \frac{T_{i,j}^{p+1} - T_{i,j-1}^{p+1}}{\delta x_w} - K_S \Delta x \frac{T_{i,j}^{p+1} - T_{i+1,j}^{p+1}}{\delta y_S} = -K_E \Delta y \frac{T_{i,j+1}^{p+1} - T_{i,j}^{p+1}}{\delta x_E} - K_N \Delta x \frac{T_{i-1,j}^{p+1} - T_{i,j}^{p+1}}{\delta y_N} + \rho c_p \Delta x \Delta y \frac{T_{i,j}^{p+1} - T_{i,j}^{p}}{\Delta t} \quad (2.3)$$

$$K_E \Delta y \frac{T_{i,j+1}^{p+1} - T_{i,j}^{p+1}}{\delta x_E} - K_W \Delta y \frac{T_{i,j}^{p+1} - T_{i,j-1}^{p+1}}{\delta x_w} + K_N \Delta x \frac{T_{i-1,j}^{p+1} - T_{i,j}^{p+1}}{\delta y_N} - K_S \Delta x \frac{T_{i,j}^{p+1} - T_{i+1,j}^{p+1}}{\delta y_S} = \rho c_p \Delta x \Delta y \frac{T_{i,j}^{p+1} - T_{i,j}^{p}}{\Delta t} \quad (2.4)$$

Where,

$T_{i,j}^{p}$ = temperature as i is noted spatial node and p is for the present time.

Δx = difference between nodes

Δt = time step

Rearranging Eq. (2.4) to put terms with p+1 on the left-hand-side and terms with p on the right-hand-side gives

$$\left(\frac{\rho c_p \Delta x \Delta y}{\Delta t} + \frac{K_E \Delta y}{\delta x_E} + \frac{K_W \Delta y}{\delta x_w} + \frac{K_N \Delta x}{\delta y_N} + \frac{K_S \Delta x}{\delta y_S}\right) T_{i,j}^{p+1} - \left(\frac{K_E \Delta y}{\delta x_E}\right) T_{i,j+1}^{p+1} - \left(\frac{K_W \Delta y}{\delta x_w}\right) T_{i,j-1}^{p+1} - \left(\frac{K_N \Delta x}{\delta y_N}\right) T_{i-1,j}^{p+1} - \left(\frac{K_S \Delta x}{\delta y_S}\right) T_{i+1,j}^{p+1} = \frac{\rho c_p \Delta x \Delta y}{\Delta t} T_{i,j}^{p} \quad (2.5)$$

With some additional rearrangements, Eq. (2.5) becomes as follows:

$$a_p T_p - a_E T_E - a_W T_W - a_N T_N - a_S T_S = a_p^0 T_p^0 \quad (2.6)$$

$$a_p = a_E + a_W + a_N + a_S + a_p^0$$

$$a_E = \frac{K_E \Delta y}{\delta x_E}$$

$$a_W = \frac{K_W \Delta y}{\delta x_W}$$

$$a_N = \frac{K_N \Delta x}{\delta y_N}$$

$$a_S = \frac{K_S \Delta x}{\delta y_S}$$

$$a_p^0 = \frac{\rho C_p \Delta x \Delta y}{\Delta t}$$

2.2.3. Boundary Conditions

Equations for the boundary conditions for a two-dimensional slab heat transfer problem are derived based on the principle of conservation of energy for the control volume. Basically the term in left-hand-side is the rate of heat conduction into a control volume and right-hand-side term presents the rate of heat conduction out of the control volume plus rate of energy storage inside the control volume.

- Left Top Corner

$$-K_S \frac{\Delta x}{2} \frac{T_{i,j}^{p+1} - T_{i+1,j}^{p+1}}{\delta y_S} = -K_E \frac{\Delta y}{2} \frac{T_{i,j+1}^{p+1} - T_{i,j}^{p+1}}{\delta x_E} + h \frac{\Delta x}{2} (T_{i,j}^{p+1} - T_\infty) + \rho c_p \frac{\Delta x}{2} \frac{\Delta y}{2} \frac{T_{i,j}^{p+1} - T_{i,j}^{p}}{\Delta t} \quad (2.7)$$

- Top Edge

$$-K_W \frac{\Delta y}{2} \frac{T_{i,j}^{p+1} - T_{i,j-1}^{p+1}}{\delta x_w} - K_S \Delta x \frac{T_{i,j}^{p+1} - T_{i+1,j}^{p+1}}{\delta y_S} = -K_E \frac{\Delta y}{2} \frac{T_{i,j+1}^{p+1} - T_{i,j}^{p+1}}{\delta x_E} + h \Delta x (T_{i,j}^{p+1} - T_\infty) + \rho c_p \Delta x \frac{\Delta y}{2} \frac{T_{i,j}^{p+1} - T_{i,j}^{p}}{\Delta t} \quad (2.8)$$

- Right Top Corner

$$-K_W\frac{\Delta y}{2}\frac{T_{i,j}^{p+1}-T_{i,j-1}^{p+1}}{\delta x_w}-K_S\frac{\Delta x}{2}\frac{T_{i,j}^{p+1}-T_{i+1,j}^{p+1}}{\delta y_S}=h\frac{\Delta x}{2}(T_{i,j}^{p+1}-T_\infty)+\rho c_p\frac{\Delta x}{2}\frac{\Delta y}{2}\frac{T_{i,j}^{p+1}-T_{i,j}^{p}}{\Delta t} \quad (2.9)$$

- Left Edge (Adiabatic)

$$-K_S\frac{\Delta x}{2}\frac{T_{i,j}^{p+1}-T_{i+1,j}^{p+1}}{\delta y_S}=-K_E\Delta y\frac{T_{i,j+1}^{p+1}-T_{i,j}^{p+1}}{\delta x_E}-K_N\frac{\Delta x}{2}\frac{T_{i-1,j}^{p+1}-T_{i,j}^{p+1}}{\delta y_N}+\rho c_p\frac{\Delta x}{2}\Delta y\frac{T_{i,j}^{p+1}-T_{i,j}^{p}}{\Delta t} \quad (2.10)$$

- Right Edge (Adiabatic)

$$-K_W\Delta y\frac{T_{i,j}^{p+1}-T_{i,j-1}^{p+1}}{\delta x_w}-K_S\frac{\Delta x}{2}\frac{T_{i,j}^{p+1}-T_{i+1,j}^{p+1}}{\delta y_S}=-K_N\frac{\Delta x}{2}\frac{T_{i-1,j}^{p+1}-T_{i,j}^{p+1}}{\delta y_N}+\rho c_p\frac{\Delta x}{2}\Delta y\frac{T_{i,j}^{p+1}-T_{i,j}^{p}}{\Delta t} \quad (2.11)$$

- Left Bottom Corner

$$h\frac{\Delta x}{2}(T_\infty-T_{i,j}^{p+1})=-K_E\frac{\Delta y}{2}\frac{T_{i,j+1}^{p+1}-T_{i,j}^{p+1}}{\delta x_E}-K_N\frac{\Delta x}{2}\frac{T_{i-1,j}^{p+1}-T_{i,j}^{p+1}}{\delta y_N}+\rho c_p\frac{\Delta x}{2}\frac{\Delta y}{2}\frac{T_{i,j}^{p+1}-T_{i,j}^{p}}{\Delta t} \quad (2.12)$$

- Bottom Edge

$$-K_W\frac{\Delta y}{2}\frac{T_{i,j}^{p+1}-T_{i,j-1}^{p+1}}{\delta x_w}+h\Delta x(T_\infty-T_{i,j}^{p+1})=-K_E\frac{\Delta y}{2}\frac{T_{i,j+1}^{p+1}-T_{i,j}^{p+1}}{\delta x_E}-K_N\Delta x\frac{T_{i-1,j}^{p+1}-T_{i,j}^{p+1}}{\delta y_N}+\rho c_p\Delta x\frac{\Delta y}{2}\frac{T_{i,j}^{p+1}-T_{i,j}^{p}}{\Delta t} \quad (2.13)$$

- Right Bottom Corner

$$-K_W\frac{\Delta y}{2}\frac{T_{i,j}^{p+1}-T_{i,j-1}^{p+1}}{\delta x_w}+h\frac{\Delta x}{2}(T_\infty-T_{i,j}^{p+1}) = -K_N\frac{\Delta x}{2}\frac{T_{i-1,j}^{p+1}-T_{i,j}^{p+1}}{\delta y_N}+\rho c_p\frac{\Delta x}{2}\frac{\Delta y}{2}\frac{T_{i,j}^{p+1}-T_{i,j}^{p}}{\Delta t} \quad (2.14)$$

- Between Layers

$$-K_{W_N}\frac{\Delta y}{2}\frac{T_{i,j}^{p+1}-T_{i,j-1}^{p+1}}{\delta x_w}-K_{W_S}\frac{\Delta y}{2}\frac{T_{i,j}^{p+1}-T_{i,j-1}^{p+1}}{\delta x_w}-K_S\Delta x\frac{T_{i,j}^{p+1}-T_{i+1,j}^{p+1}}{\delta y_S} = -K_{E_N}\frac{\Delta y}{2}\frac{T_{i,j+1}^{p+1}-T_{i,j}^{p+1}}{\delta x_E}-K_{E_S}\frac{\Delta y}{2}\frac{T_{i,j+1}^{p+1}-T_{i,j}^{p+1}}{\delta x_E}-K_N\Delta x\frac{T_{i-1,j}^{p+1}-T_{i,j}^{p+1}}{\delta y_N} + \rho c_p\Delta x\Delta y\frac{T_{i,j}^{p+1}-T_{i,j}^{p}}{\Delta t} \quad (2.15)$$

2.2.4. Mesh Generation

A non-uniform geometric discretization scheme is applied to reduce computational CPU time as well as memory requirements. Generally, the discretization grid is very fine near the surface boundaries and/or interactions between two different materials as well as near boundaries of heat sources. The grid is then gradually expanded in the area where relatively smaller temperature changes are expected as illustrated in Figure 2.2 near embedded pipes with a concrete slab.

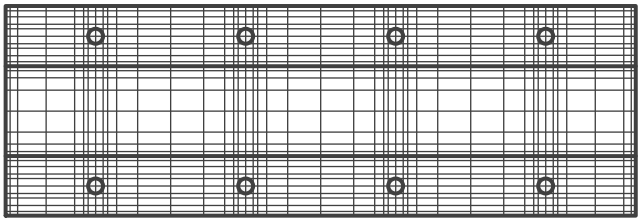

Figure 2.2: Non-Uniform discretization scheme

2.3. Sensitivity Analysis of Numerical Model

2.3.1. Effect of mesh size

In this section, the predictions from the numerical solutions are compared with an analytical solution to assess the accuracy of the numerical solution using the root mean square error defined as follows:

$$\mathrm{RMSE} = \sqrt{\frac{\sum_{i=1}^{n}(x_{\mathrm{numerical},i} - x_{\mathrm{analytical},i})^2}{n}} \tag{2.16}$$

Figure 2.3 summarizes the impact of the number of nodes in the mesh used to obtain the numerical solution on the prediction accuracy defined by the RMSE value defined by Eq. (2.16). Based on the results shown in Figure 2.3, as number of nodes increases numerical solution, the prediction accuracy of the numerical solution improves. However, CPU time required to obtain the numerical solution increases significantly when the number of nodes increases. Therefore, a number of approximately 5000 nodes for the FDM mesh is a reasonable value to achieve reasonable accuracy and computational time for the numerical solution of the two-dimensional slab heat transfer model.

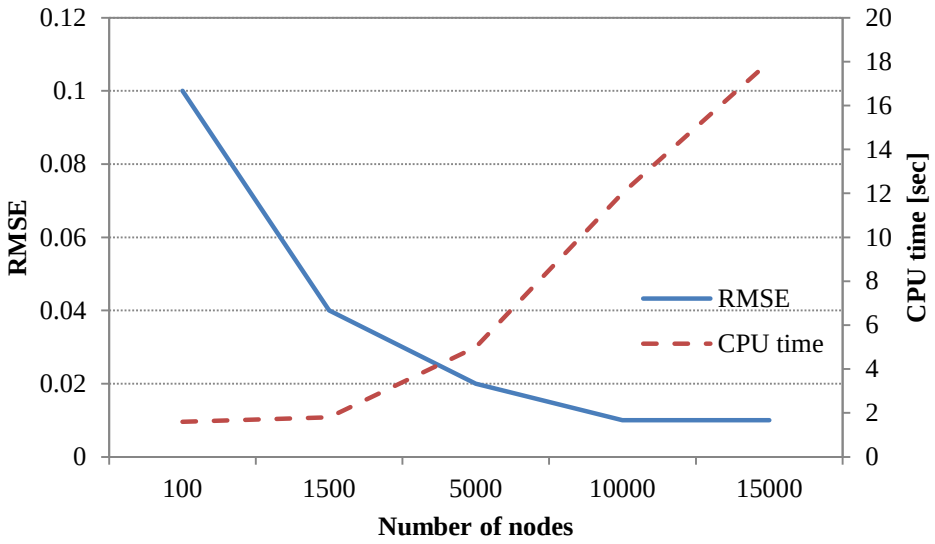

Figure 2.3: Variation of RMSE (root mean square error) and the CPU time vs. the number of mesh nodes

Figure 2.4 presents the mesh generation scheme including above-grade walls and floor. The discretized grid is very fine near the wall and the floor surfaces, and near the interaction between two different materials (such as concrete and insulation material).

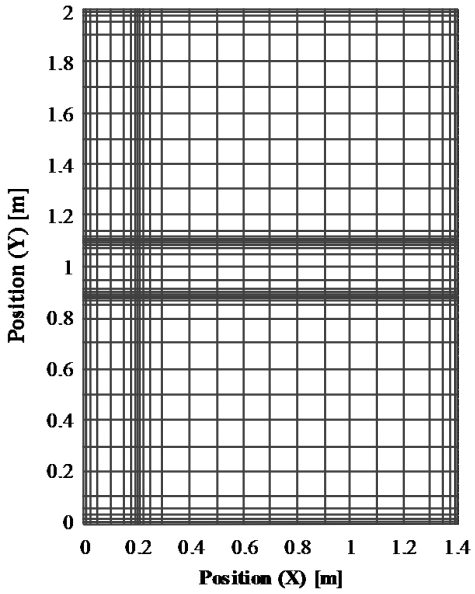

Figure 2.4: Mesh configuration used for two-dimensional slab model

2.4. Thermal Analysis of Numerical Slab Model

2.4.1. One-dimensional slab model

A simplified slab without heat generation two-dimensional heat transfer FDM model is considered in this section. The boundary conditions for the edges of the slab are set to be adiabatic so that one-dimensional heat transfer is achieved within the slab. A time step of 200 seconds is used for the numerical solution. Figure 2.5 illustrates the section view of the simplified slab model considered in this section. Table 2.1 summarizes the properties of the slab materials used for the simplified slab model.

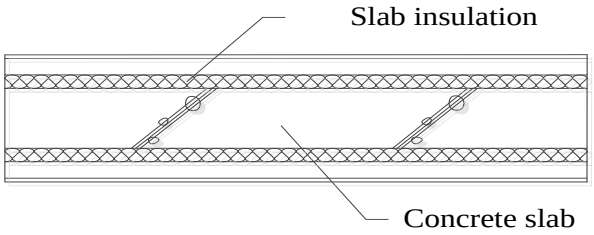

Figure 2.5: Section view of the slab with uniform horizontal insulation considered for the simplified one-dimensional transient heat transfer slab model

Table 2.1: Properties of the layers used in the simplified slab model

Material	Conductivity [W/m-K]	Density [kg/m^3]	Specific Heat [J/kg-K]
Concrete (slab)	0.79	1800	900
Expanded Polystyrene (Slab insulation)	0.052	16	1260

Figure 2.6 illustrates the temperature distribution inside the simplified slab when upper zone air temperature and lower zone air temperature is assumed to be 25 degree Celsius and 15 degree Celsius, respectively. In the case of the simplified slab model, heat exchanges between the slab edges and the outdoors are ignored by setting these boundary conditions to be adiabatic. Therefore, the temperature distribution within the slab follows one-dimensional heat transfer pattern with temperature varying only with depth as shown in Figure 2.6.

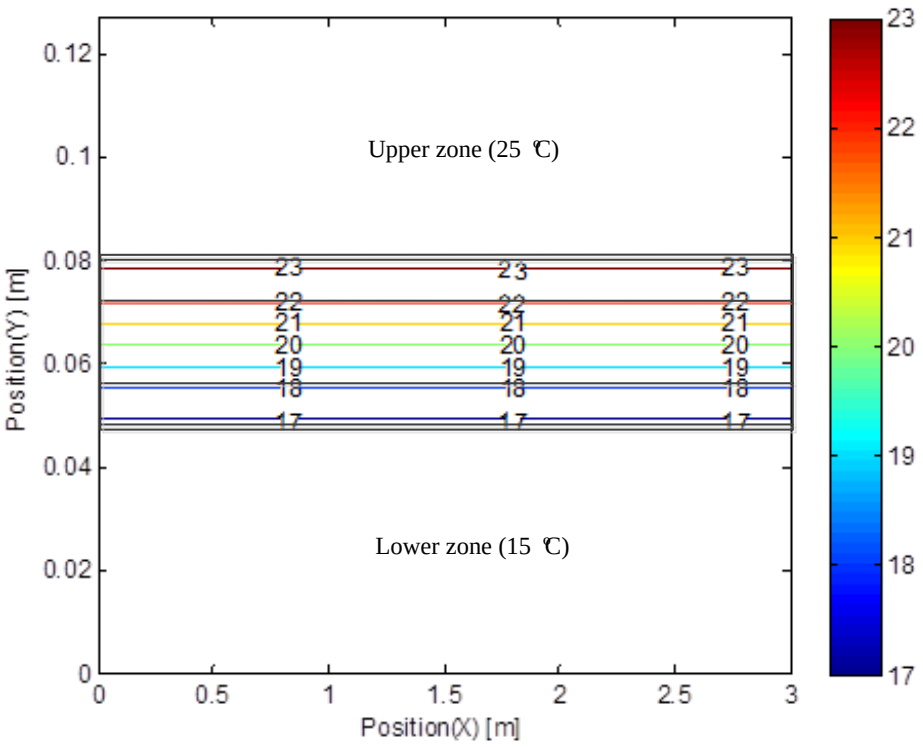

Figure 2.6: Temperature distribution in the simplified slab model

The heat flux q(x) along the slab surface can be estimated from the following expressions:

$$\dot{q}_{Lower}(\mathrm{x}) = h_{Lower}\left(T_{Slab,lower\ surface} - T_{Lower}\right), \quad |x| \le a \tag{2.17}$$

$$\dot{q}_{Upper}(\mathrm{x}) = h_{Upper}\left(T_{Slab,upper\ surface} - T_{Upper}\right), \quad |x| \le a \tag{2.18}$$

Figure 2.7 shows the variation with time of the heat flux of the simplified slab model. As noted earlier, the heat flux along the surface of the simplified slab model is constant regardless of location of node because the slab edges are set to be adiabatic. The results of Figure 2.7 show that the simplified slab reaches to thermal equilibrium state after 18 hours.

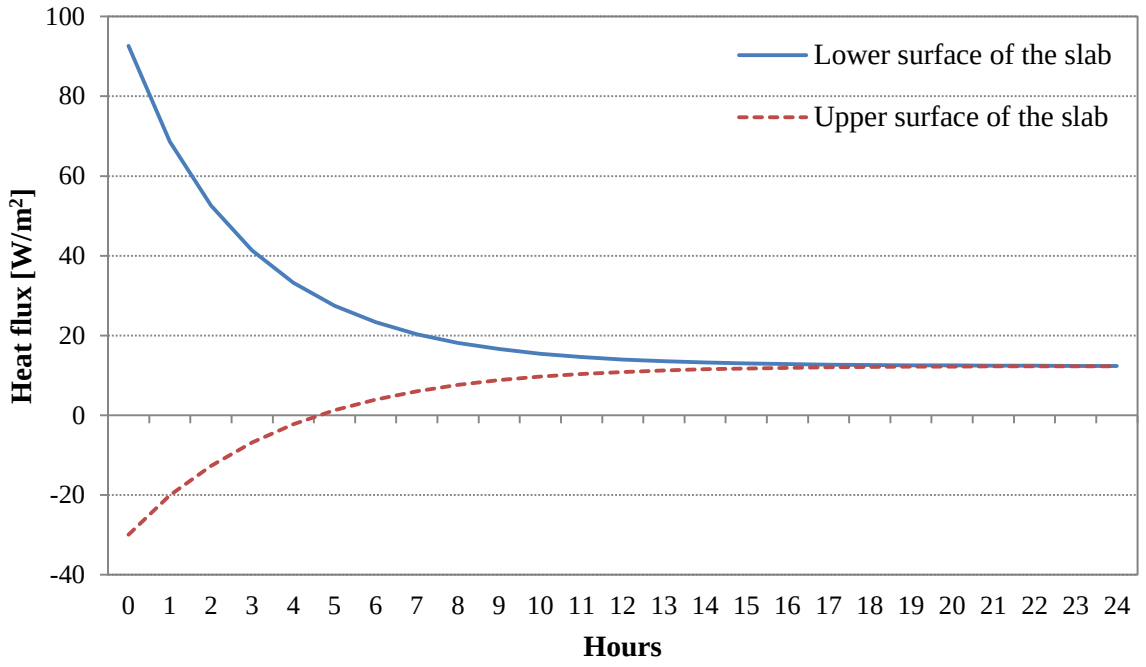

Figure 2.7: Average heat flux from upper and lower surface of slab to zone

2.4.2. Two-dimensional slab model

In this section, exterior walls that are in contact with the outdoors are accounted for in the two-dimensional slab model as illustrated in Figure 2.8. Specifically, vertical sections of 0.9 meter of the exterior walls in contact with the outdoor air are modeled. The construction details of the slab layers are the same as those considered for the simplified slab model. For the two-dimensional slab model, the boundary conditions of the top and bottom of the vertical sections of the exterior walls are set to be adiabatic. The outdoor air temperature is assumed to be constant and is set at 0 degree Celsius. For the upper and lower zones, the indoor air temperature is assumed to be constant and is set at 22.2 degree Celsius. Table 2.2 summarizes the properties of the materials considered for both the slab and the exterior wall constructions used for the two dimensional FDM slab model.

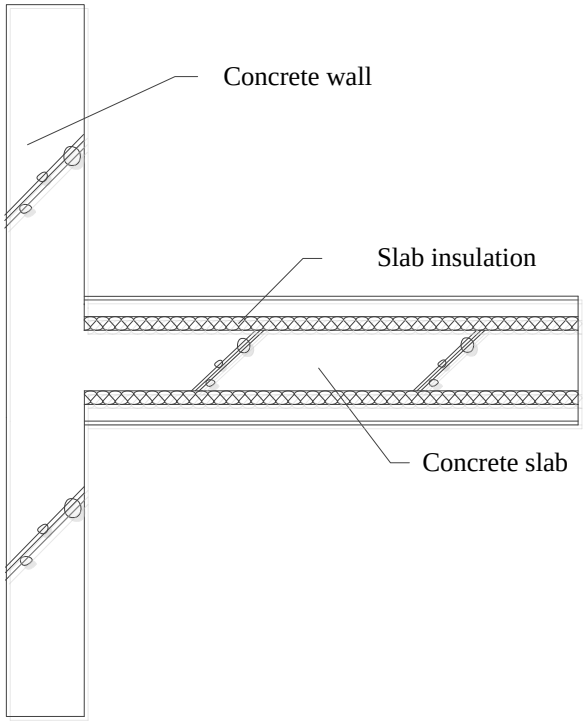

Figure 2.8: Section view of the slab with uniform horizontal insulation and exterior wall sections considered for the two-dimensional heat transfer slab model

Table 2.2: Properties of material constructions used in the two-dimensional slab model

Material	Conductivity [W/m-K]	Density [kg/m^3]	Specific Heat [J/kg-K]
Brick (Exterior wall)	0.89	1920	790
Concrete (Slab)	0.79	1800	900
Expanded Polystyrene (Insulation)	0.052	16	1260

Figure 2.9 illustrates the temperature isotherms obtained for the two dimensional FDM slab model. The two-dimensional nature of the temperature distribution at the slab edges clearly indicates the magnitude of the thermal bridging effect between the slab floor and the exterior walls.

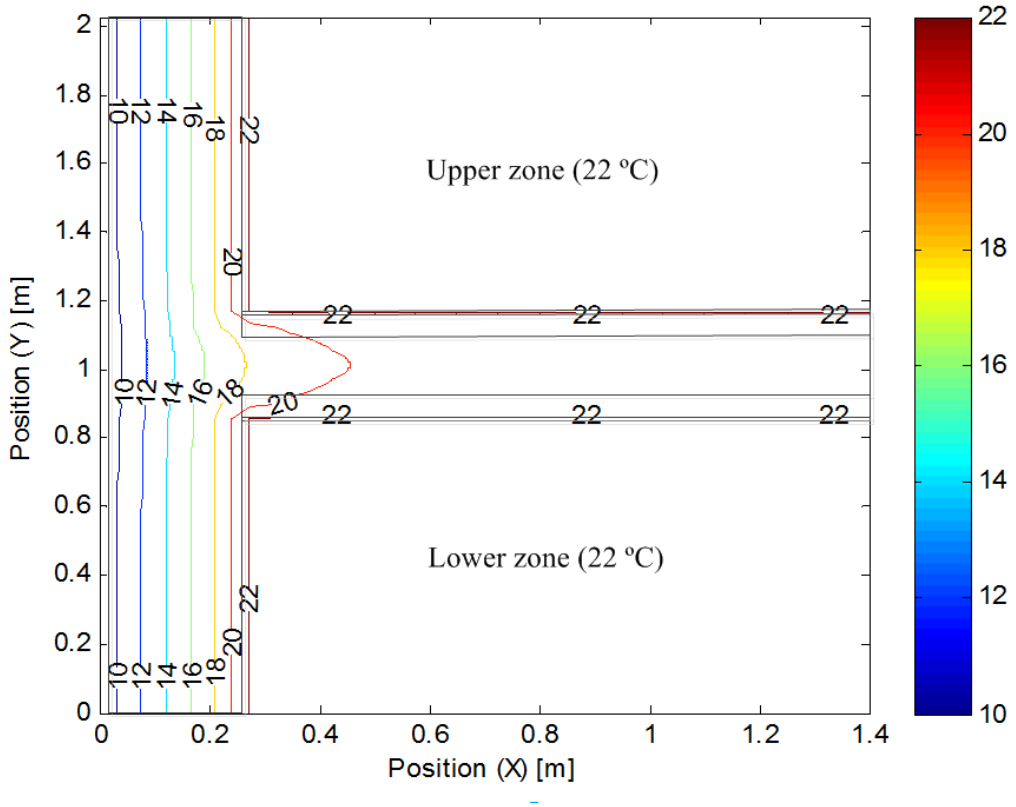

Figure 2.9: Temperature isotherms within the two-dimensional slab model

Heat fluxes along the upper and the lower surface of the slab floor obtained after 24 hours are presented in Figure 2.10. Since the surface convective heat transfer coefficients and the indoor temperatures at the upper and lower zones are assumed to be the same, heat fluxes along the slab are found to be the same. Along the surface of slab, the heat flux is higher near the exterior wall and becomes constant and negligible further away from the wall.

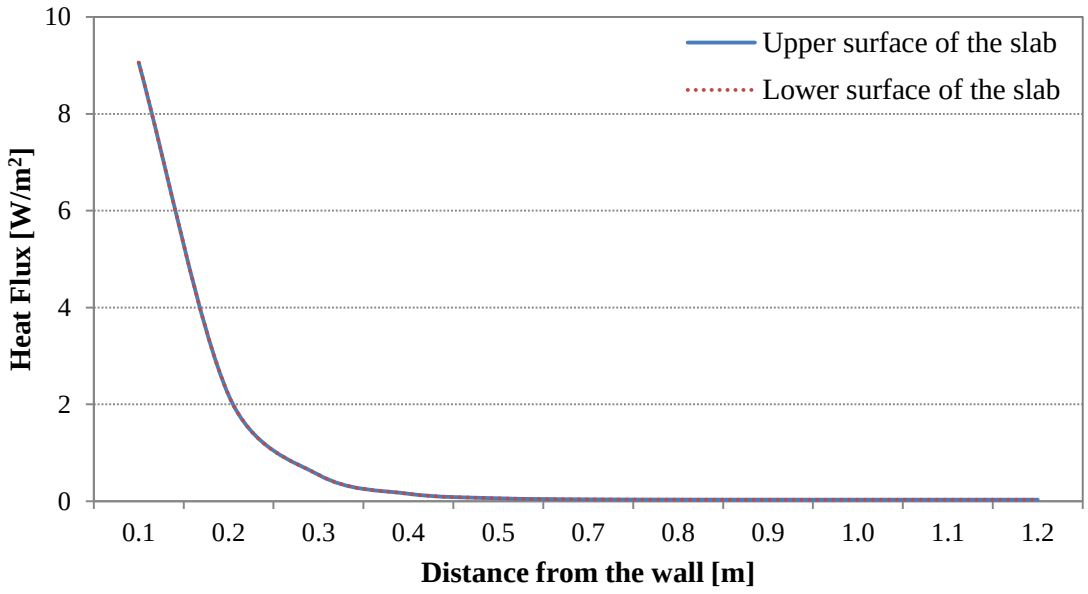

Figure 2.10: Indoor heat flux along slab surfaces (with the upper zone air temperature=22.2 ℃, lower zone air temperature =22.2 ℃, outdoor air temperature=0 ℃)

The temperature distribution within the slab and walls as well as and heat fluxes along the slab surfaces are investigated when the indoor temperatures for the upper and lower zones are different. In this case, the outdoor air temperature is assumed to be 0 degree Celsius (winter conditions). The indoor air temperatures in the upper zone and the lower zone are assumed to be 25 degree Celsius and 15 degree Celsius, respectively. Figure 2.11 shows the temperature isotherms within the slab medium obtained using the numerical solution of the two-dimensional slab model.

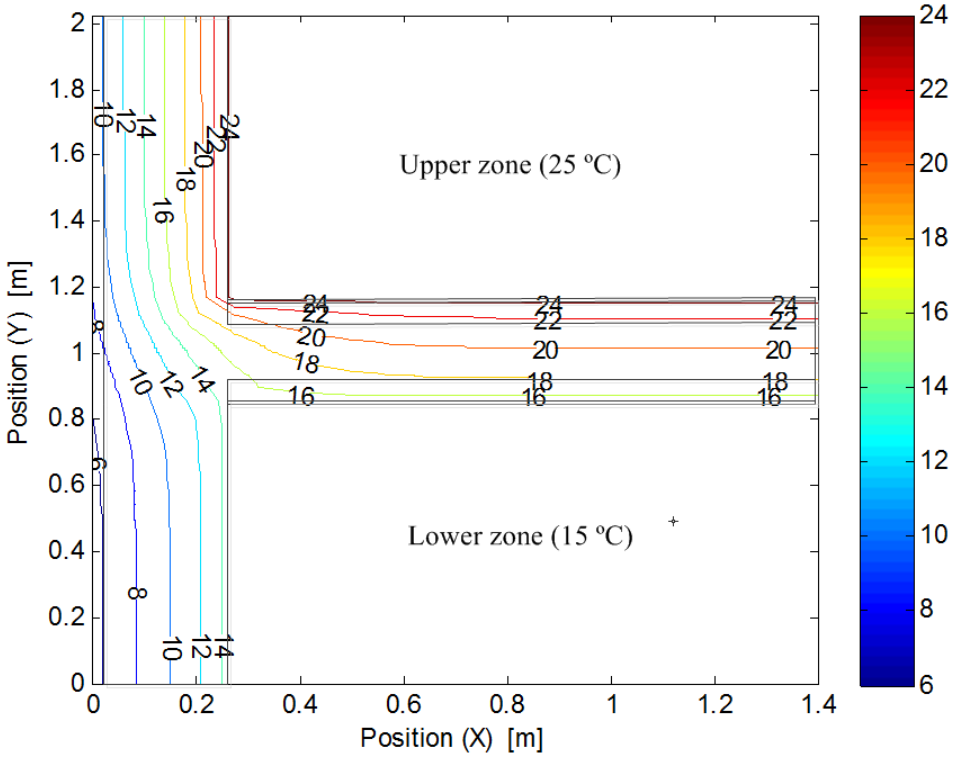

Figure 2.11: Temperature isotherms within the two-dimensional slab model (with the upper zone air temperature=25 ℃, lower zone air temperature=15 ℃, outdoor air temperature=0 ℃)

Heat fluxes along the upper and the lower surfaces of the slab after 24 hours are presented in Figure 2.12. As expected, along the upper slab surface, the heat flux is higher near the exterior wall and becomes constant (but not negligible) further away from the wall. However, along the lower slab surface, the heat flux is lower near the exterior wall because the difference between indoor and outdoor air temperatures is lower for the lower zone than for the upper zone.

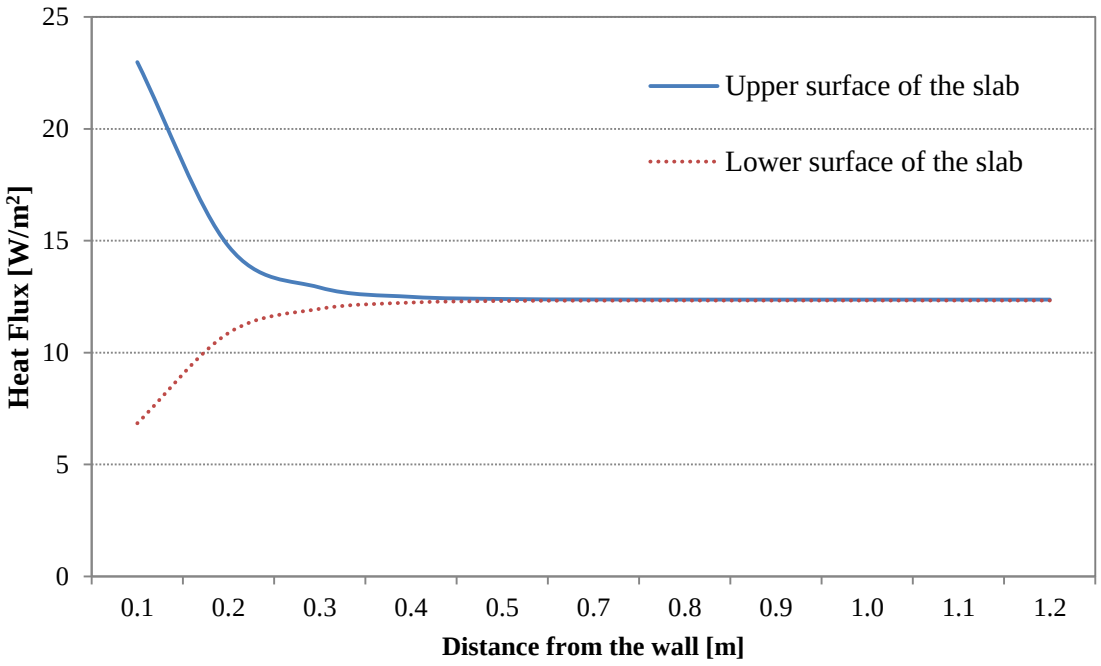

Figure 2.12: Indoor heat flux along the upper and lower slab surfaces (with the upper zone air temperature=22.2 ℃, lower zone air temperature=22.2 ℃, outdoor air temperature=0 ℃)

2.5. Summary and Conclusions

In this chapter, a numerical solution for a two-dimensional slab heat transfer model is developed. The accuracy of the numerical solution is evaluated as a function of the mesh size using an analytical solution obtained for the case of one-dimensional slab heat transfer model.

The predictions of the numerical solution for both the temperature distribution and heat flux along the slab surfaces are analyzed and verified. With the proper section of the mesh size, it is found that a good agreement between the numerical finite difference solution and the analytical solution can be obtained with reasonable computational efforts to solve the transient heat conduction equation for the two-dimensional slab model.

CHAPTER 3: DEVELOPMENT OF NUMERICAL MODEL FOR HEATING AND COOLING RADIANT SLAB

3.1. Introduction

Radiant floor panel system is widely used in several European and Asian countries. Radiant floor panel system consists of embedded water coils in floor slabs of residential and commercial buildings to provide space heating or cooling. Due to their better thermal comfort performance and ventilation control compared to all-air HVAC systems, interest in the radiant systems has increased in the United States.

Nowadays, radiant floor panel systems have a wide range of applications including habitable buildings such as residences, office buildings, classrooms, and hospitals, as well as industrial facilities and warehouses. In addition, the systems are used for snow and ice removal applications instead of chemical and mechanical methods. Heated floor systems are also used to prevent soil heaving beneath foundation of refrigerated warehouses.

Typical radiant slab system consists of a concrete slab with embedded water pipes or electrical resistance wires. Rarely hot air is circulated through a channel underneath the floor. The radiant slab system controls a slab surface temperature to maintain a comfortable environment of zone minimizing air motion within a space. In radiant slab systems, it is known that more than 50 percent of heat is transferred from the controlled surface to other surfaces by radiation (ASHRAE, 1999).

This chapter focuses on the development of a numerical model for a radiant slab system with two heat sources using finite difference method (FDM). The results of the FDM solution are compared against previously reported experimental results.

3.2. Development of Numerical Solution for Radiant Slab Heating and Cooling Systems

3.2.1. Differential equation formulation

Two dimensional numerical solutions for radiant floor heating and cooling systems are developed by adding heat generation and extraction sources using embedded hot and chilled water pipes within the floor slab. By adding these sources, the heat conduction equation can be formulated as follows:

$$K \cdot \frac{\partial^2 T}{\partial x^2} + K \cdot \frac{\partial^2 T}{\partial y^2} + Q = \rho \cdot c_p \cdot \frac{\partial T}{\partial t} \tag{3.1}$$

Where,

ρ = density [kg/m^3]

c_p= heat capacity [J/kg˚C]

K = thermal conductivity [kg/m^3]

t = time [sec]

Q = generated heating or extracted cooling rate [W/m^3]

The heat conduction equation with heat sources represented by Eq. (3.1) can be solved, using a control volume approach and pure implicit finite difference method.

The control volume and its associated nodal dimensions are shown in Figure 3.1 for a typical heat source node.

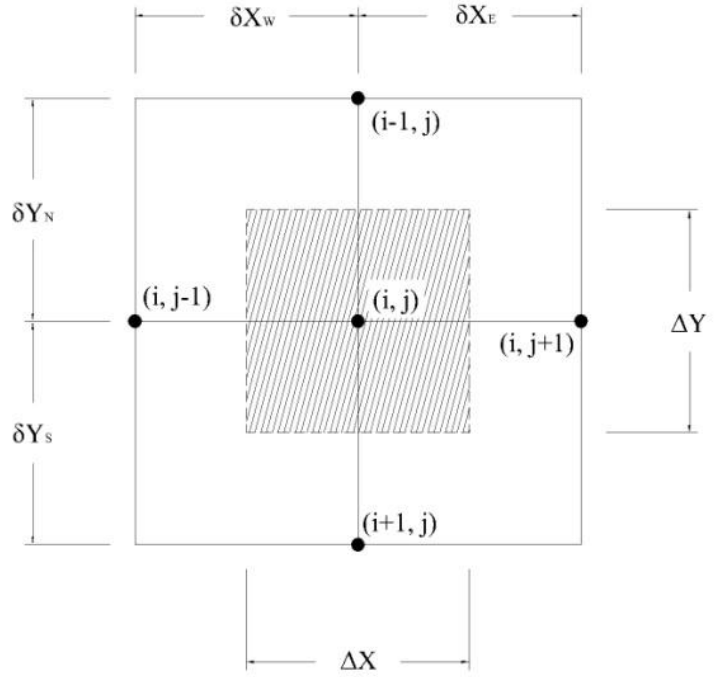

Figure 3.1: Control volume for the two-dimensional heat conduction problem with heat generation source.

3.2.2. Finite Difference Formulation

The differential equation Eq. (3.1) can be discretized as indicated as follows:

$$a_p T_p - a_E T_E - a_W T_W - a_N T_N - a_S T_S = b_p^0 T_p^0 + c_p^0 T_{w,inlet} \quad (3.2)$$

$$a_p = a_E + a_W + a_N + a_S + a_p^0$$

$$a_E = \frac{\Delta Y}{(\frac{1}{h_w} + \frac{\delta x_E}{K_E})}$$

$$a_W = \frac{\Delta Y}{(\frac{1}{h_w} + \frac{\delta x_W}{K_W})}$$

$$a_N = \frac{\Delta X}{(\frac{1}{h_w} + \frac{\delta y_N}{K_N})}$$

$$a_S = \frac{\Delta X}{(\frac{1}{h_w} + \frac{\delta y_S}{K_S})}$$

$$a_p^0 = \frac{\rho C_p \Delta x \Delta y}{\Delta t} + \dot{m} C_{p,w}$$

$$b_p^0 = \frac{\rho C_p \Delta x \Delta y}{\Delta t}$$

$$c_p^0 = \dot{m} C_{p,w}$$

Convective heat flux on a panel system is a function of the panel surface temperature as well as the temperature of the air-layer directly contacting the panel. Various convective heat transfer coefficient correlations have been developed and reported by several researchers. In particular, Awbi and Hatton (1999) conducted laboratory measurements using environmental chambers and developed the following correlation for floor surfaces that are being actively heated.

$$h = \frac{2.175 * |\Delta T|^{0.308}}{D_h^{0.076}} \quad (3.3)$$

Where, $D_h = \frac{4A}{P}$ is the hydraulic diameter of the horizontal surface, A is its area (m^2) and P is the perimeter (m) of the entire zone (all of the adjacent floor surfaces if more than one in the zone).

Karadag (2009) used numerical methods to develop the following equation for convective heat transfer coefficient correlation specific for chilled ceiling surfaces.

$$h = 3.1|\Delta T|^{0.22} \quad (3.4)$$

A correlation to estimate heat transfer coefficient for natural convection along vertical walls can be found in ASHRAE (1999):

$$h = 1.31|\Delta T|^{0.33} \quad (3.5)$$

For radiant slab systems, the fluid circulated within the embedded tubes is generally water. Thus, the convection heat transfer coefficient of the fluid can be determined using the Dittus-Boelter correlation. (Holman, 1986):

$$h_w = \frac{Nu \cdot K_w}{D} \quad (3.6)$$

Where,

$$\text{Nu} = 3.36 \text{ if } (\text{Re} < 2300)$$

$$\text{Nu} = 0.023 Pr^n Re^{0.8} \; else$$

With n=0.4 for heating and n=0.3 for cooling

And,

K_w: Thermal conductivity of the fluid [W/m-K],

D: Diameter of the tube [m]

Nu: Nusselt number

Re: Reynolds number

Pr: Prandtl number

3.2.3. Validation of the numerical model

In this section, the developed numerical radiant floor heating system model is validated against reported experimental data by Harris and Sartain (1957). Figure 3.2 shows the test room set up with a hot water radiant slab heating system that was used by Harris and Sartain to carry out their experimental analysis (Harris and Sartain, 1957). Figure 3.3 illustrates the simplified room model of the radiant floor heating system used for validation analysis.

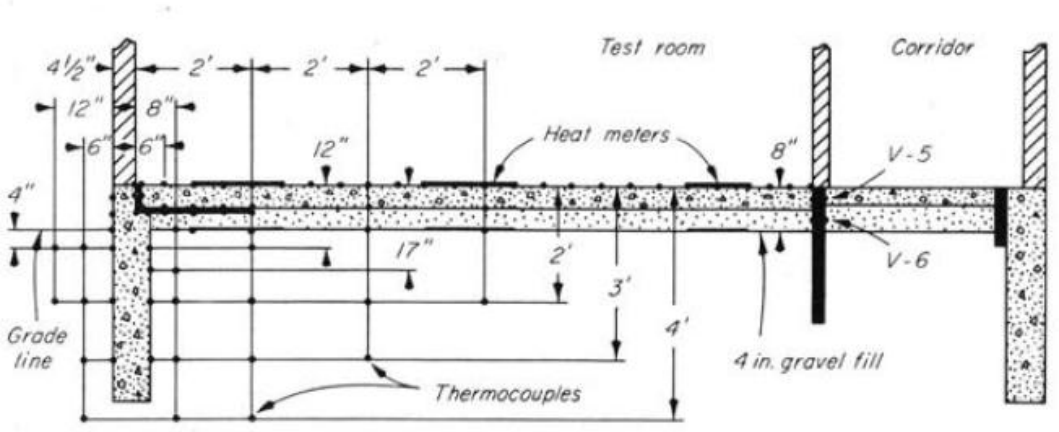

Figure 3.2: A section of the test room with radiant floor heating system used in the validation analysis based on the experimental testing of Harris and Sartain (1957).

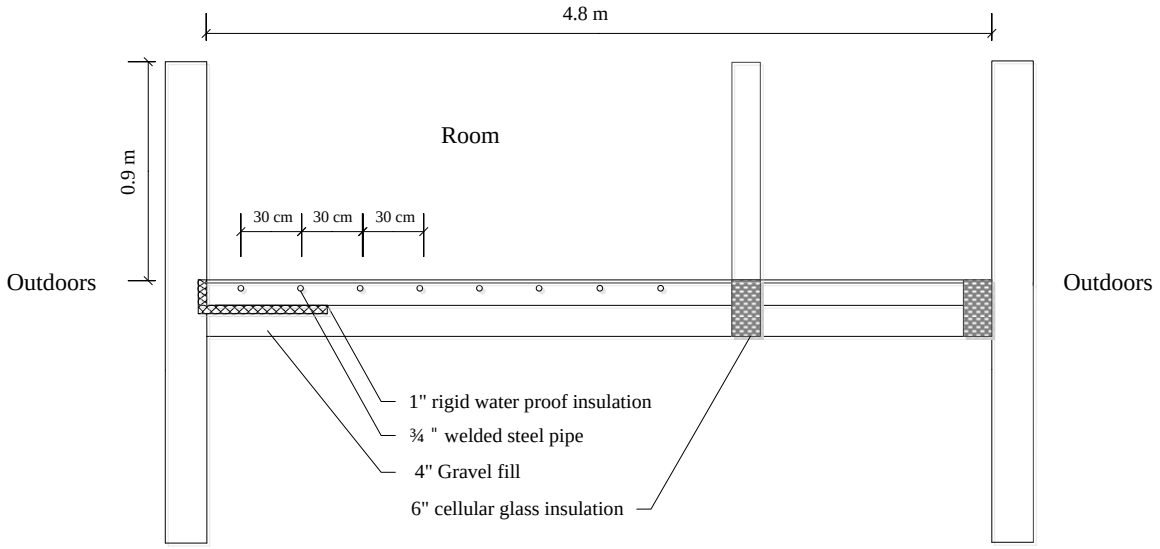

Figure 3.3: Simplified model of the radiant slab heating system used for the validation analysis

Table 3.1 provides material properties used for the simplified model of radiant floor heating system used to validate the numerical solution.

Table 3.1: Material properties used for the simplified model of radiant slab heating system

Material	Conductivity (W/m-℃)	Density (kg/m^3)	specific heat (J/kg-℃)
Concrete	1.731	2300	653
Insulation	0.0648	24.0	1214
Gravel	2.42	2800	840
Soil	0.865	2000	840

The developed room model is the same as the heated floor configuration of Room C used by Harris and Sartain (1957). The space temperature of the room was maintained continuously at 22.2 ℃ with an electric floor heating system. The length of the radiant floor heating panel is 3.6 m. The distance between hot water pipes is 30.4 cm. The pipe is made up of 3/4 inch Schedule 40 steel pipe. Gravel fills the space between the heating panel and

the ground surface. The total radiant floor heating panel area in Room is 14 m^2. The length of the wall exposed to the outdoor environment is assumed to be 0.9 m. The bottom boundary surface of the room is assumed to have a constant temperature. The reported indoor, outdoor and hot water temperatures of the experiments in the room are 22.2 ℃, -3 ℃ and 35.5 ℃, respectively. A boundary condition of 25 ℃ is used for 0.6 m below the gravel. Figure 3.4 compares the predictions from the numerical model and the reported experimental results (Harris and Sartian, 1957). The results provided by Figure 3.4 indicate that the average slab surface temperatures of the experimental data and the numerical solution (26.8 ˚C and 27 ˚C) agree well.

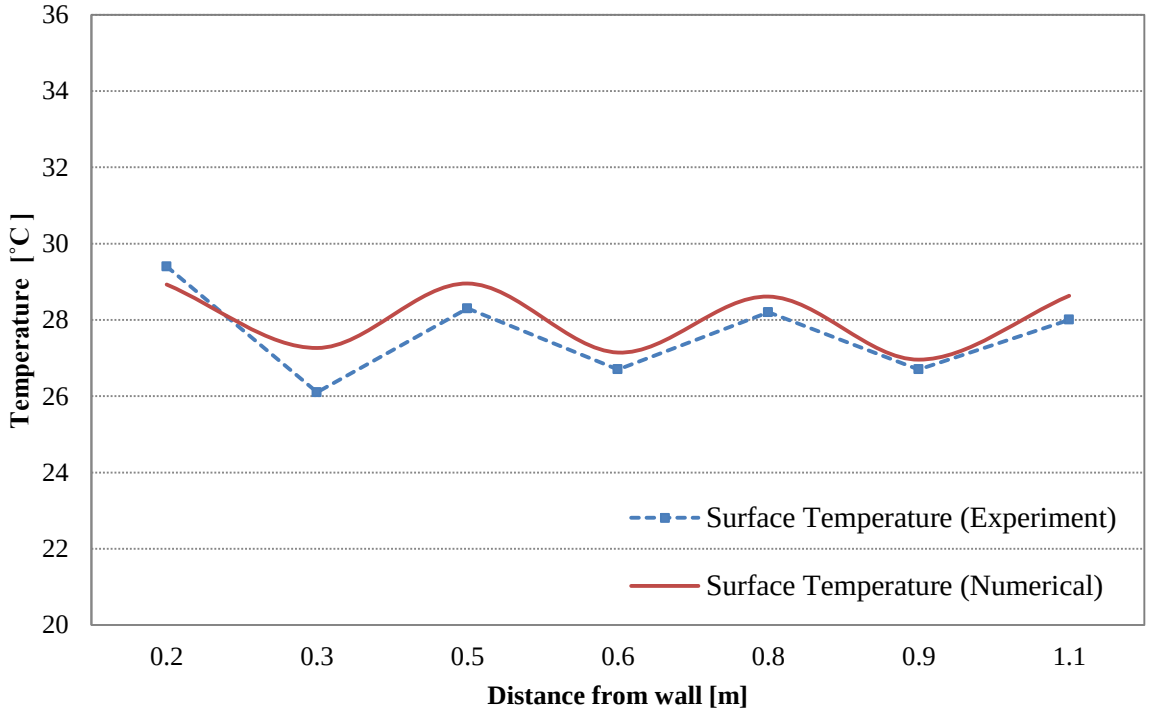

Figure 3.4: Comparison of the upper slab surface temperature predictions of the numerical solution against experimental data

3.3. Parametric Analysis

3.3.1. Effect of pipe pitch

For the analysis presented in this section, a radiant slab with a vertical insulation configuration is considered with three pipe pitches (i.e., distances between two consecutive tubes) of 0.2 m, 0.3 m and 0.4 m. The 35.5 ˚C hot water is supplied with constant mass flow rate of 0.020 kg/s for heating. The 5 ˚C chilled water is supplied with constant mass flow rate of 0.020 kg/s for cooling. Figure 2 illustrates the effect of the pipe pitch on the average slab heat transfer rate at the upper slab surface for a vertically insulated slab. As shown in Figure 3.5, an increase in the pipe pitch results in the reduction of the average slab heat transfer rate due to fewer tubes embedded within the slab.

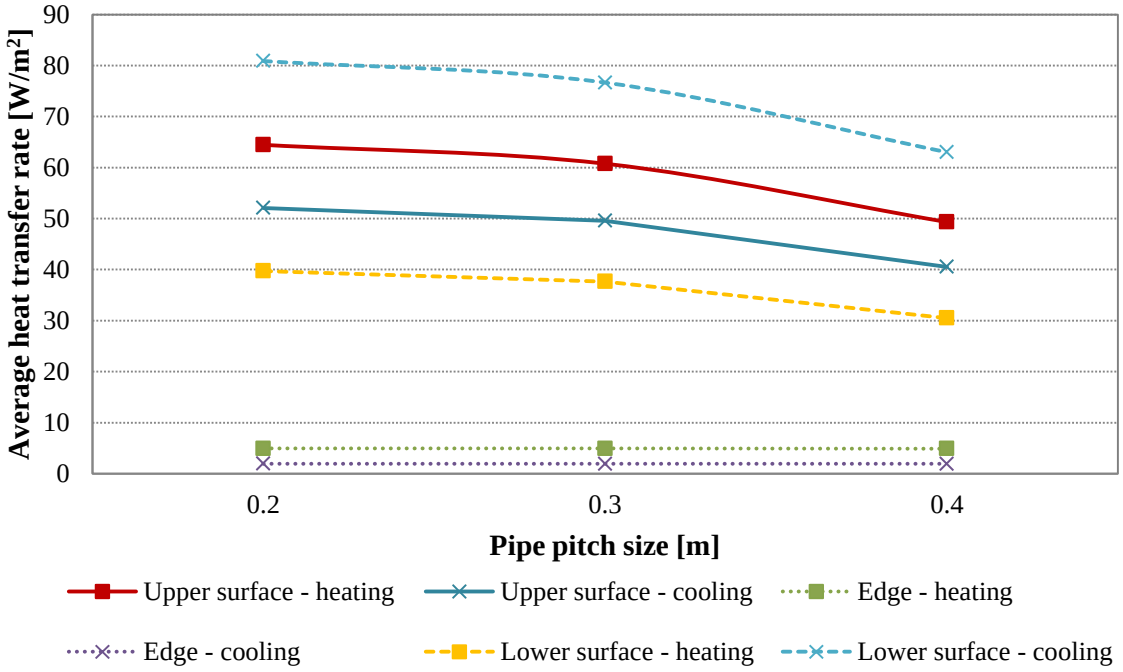

Figure 3.5: Average heat transfer rate through the slab surface with vertical insulation for various pipe pitches

3.3.2. Effect of inlet water temperature

A radiant slab with a vertical insulation is considered in this section. The inlet hot water temperature is varied from 35 ˚C to 65 ˚C with a constant mass flow rate of 0.020 kg/s and a pipe pitch of 0.3 m. Figure 3.6 illustrates the average slab heat transfer rate through the upper slab surface with various inlet hot water temperatures. As expected, the increase in supply hot water temperature results in an increase of the average heat transfer rate.

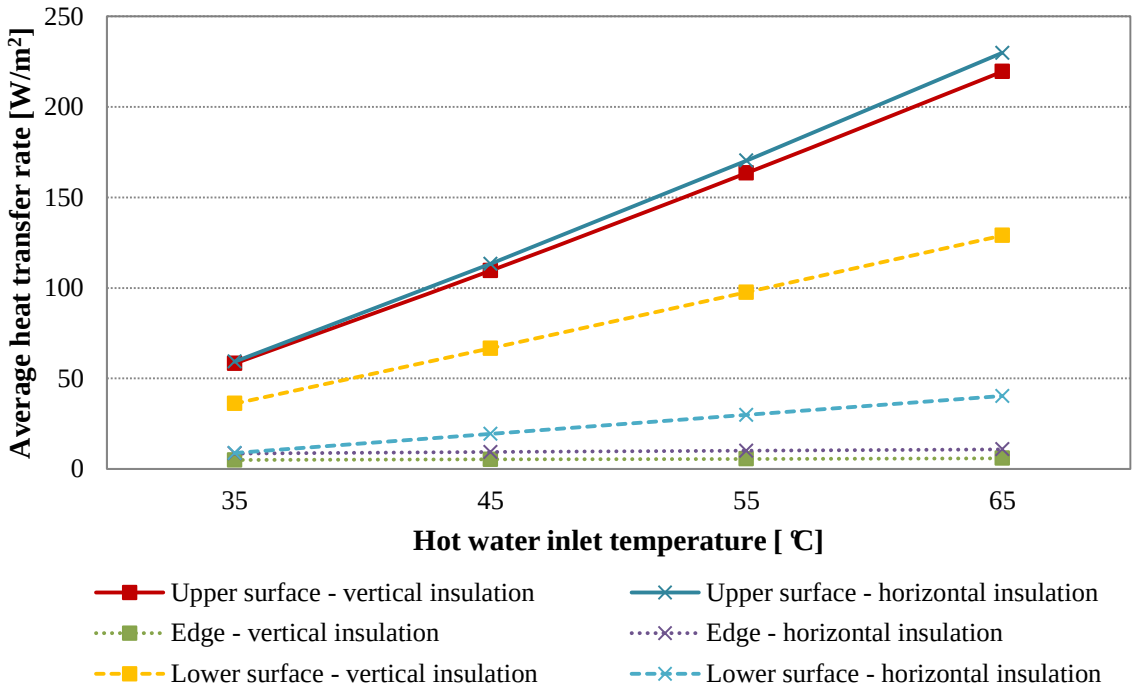

Figure 3.6: Average heat transfer rate through the upper slab surface and average heat loss through the lower slab surface and slab edges for various inlet hot water temperatures

For the same radiant slab configuration, the inlet chilled water temperature is varied from 5 ˚C to 20 ˚C with a constant mass flow rate of 0.020 kg/s and a pipe pitch of 0.3 m. Figure 3.7 illustrates the average slab heat transfer rate through the lower slab surface for various indoor heat transfer coefficients and various inlet chilled water temperatures. The decrease in supply temperature of chilled water increases the average heat transfer rate through the bottom slab surface.

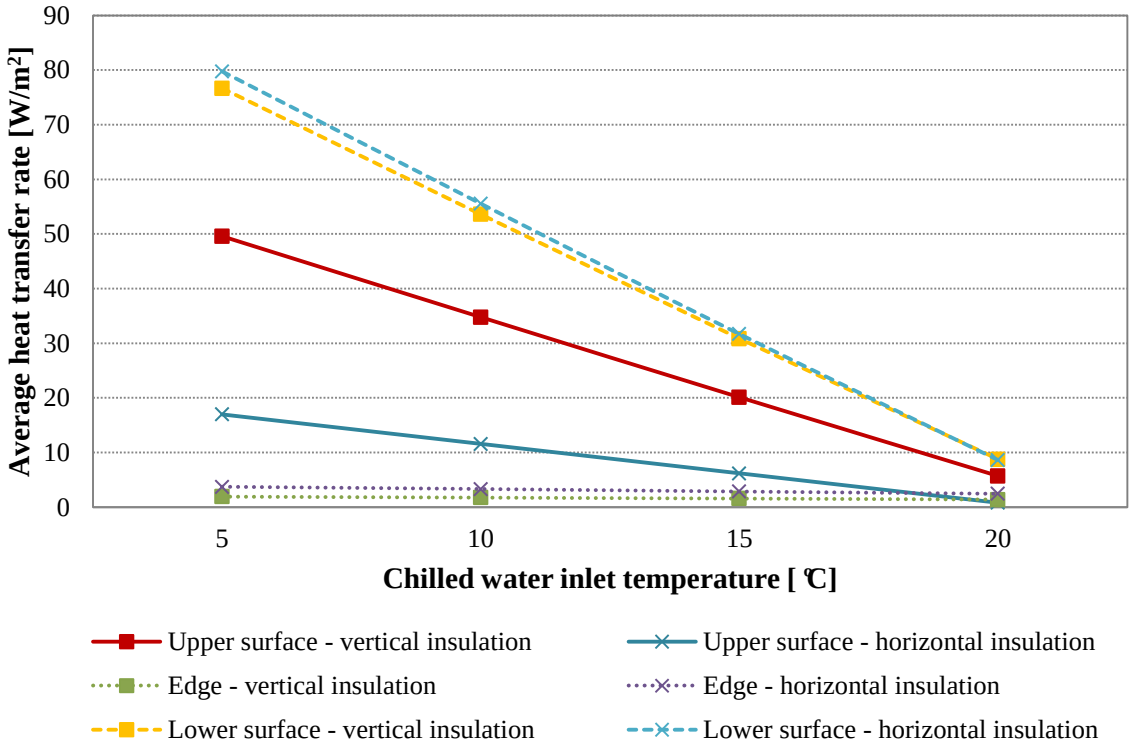

Figure 3.7: Average heat transfer rate through the lower slab surface and average heat loss through the upper slab surface and slab edges for various inlet chilled water temperatures

3.3.3. Effect of water mass flow rate

A vertically insulated radiant slab is considered in this section. The mass flow rate of inlet hot water is varied from 0.01 kg/s to 0.3 kg/s with constant supply temperature of 35.5 ˚C for heating and 5 ˚C for cooling. Figure 3.8 shows the effect of hot water mass flow rate on average slab heat transfer rate at the slab surface. An increase of water mass flow rate increases the average heat transfer at slab surface. It should be noted, however, that when the hot water mass flow rate is larger than 0.15 kg/s, the average slab heat transfer rate is not significantly affected by the mass flow rate.

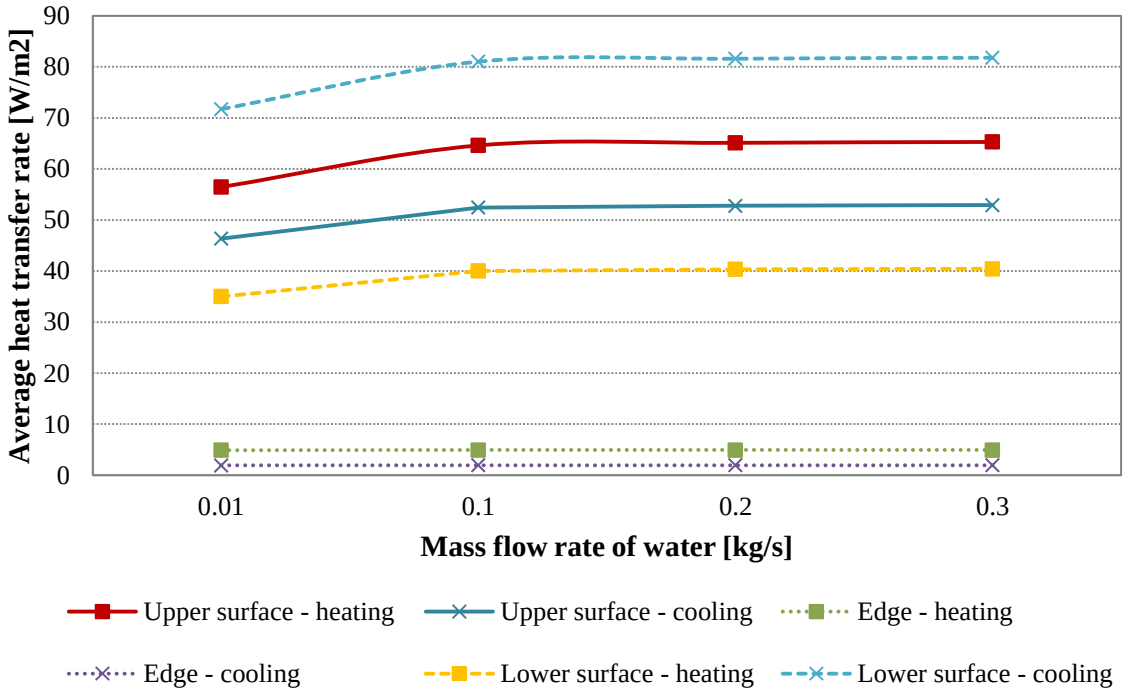

Figure 3.8: Average heat transfer rate through the upper slab surface with a vertical insulation for various hot water mass flow rates

3.3.4. Effect of depth of pipe embedded in fixed thickness of slab

A vertically insulated radiant slab is considered in this section. The depth of pipe embedded in fixed thickness of thermal mass is varied from 0.02 m to 0.07 m with constant supply temperature of 35.5 ˚C for heating and 5 ˚C for cooling. Figure 3.9 shows the effect of depth of pipe on average slab heat transfer rate at the slab surface. An increase in depth of pipe reduces average heat transfer rate through the slab surface.

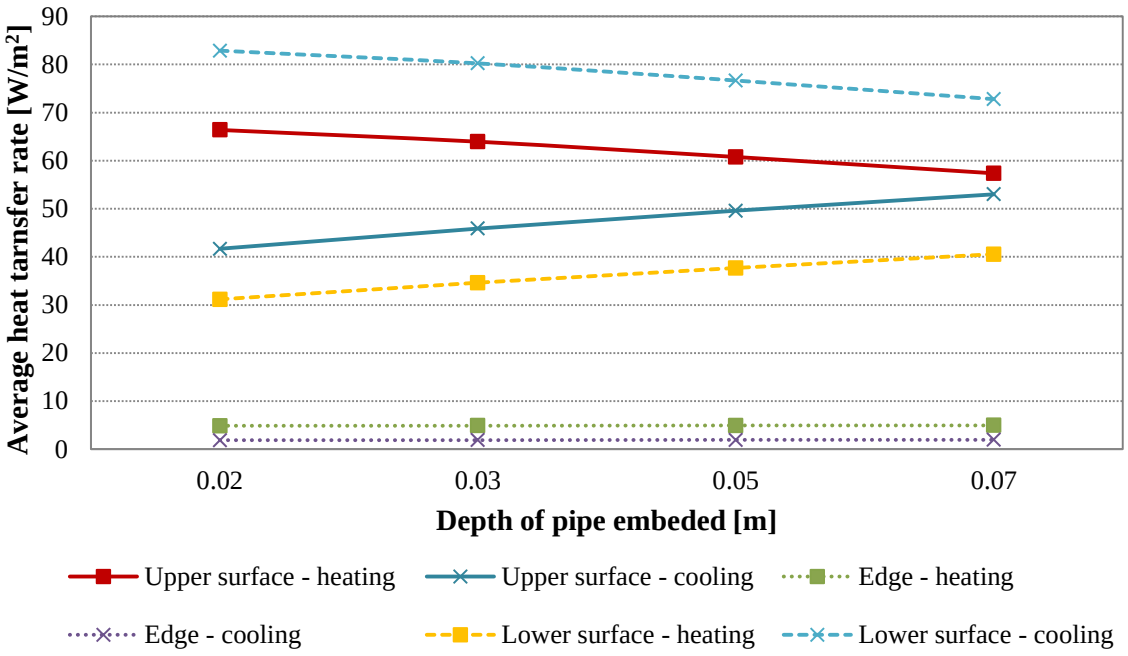

Figure 3.9: Average heat transfer rate through slab surface with vertical insulation for various depths of pipe embedded in fixed thickness of thermal mass

3.3.5. Effect of insulation placement

Four insulation placement configurations are considered in the analysis: no insulation, uniformly horizontal insulation, vertical insulation along edge of slab, and both of uniformly horizontal and vertical insulation as shown in Figure 3.10. In the heating mode, the outdoor air temperature and the indoor air temperature are assumed to be at -3 ˚C and 22.2 ˚C, respectively. For radiant slab heating system, hot water of 35.5 ˚C is supplied with constant water mass flow rate of 0.020 kg/s. In the cooling mode, the outdoor air temperature and the indoor air temperature are set at 30 ˚C and 22.2 ˚C, respectively. For the radiant slab cooling system, chilled water of 5 ˚C is supplied with a constant water mass flow rate of 0.020 kg/s.

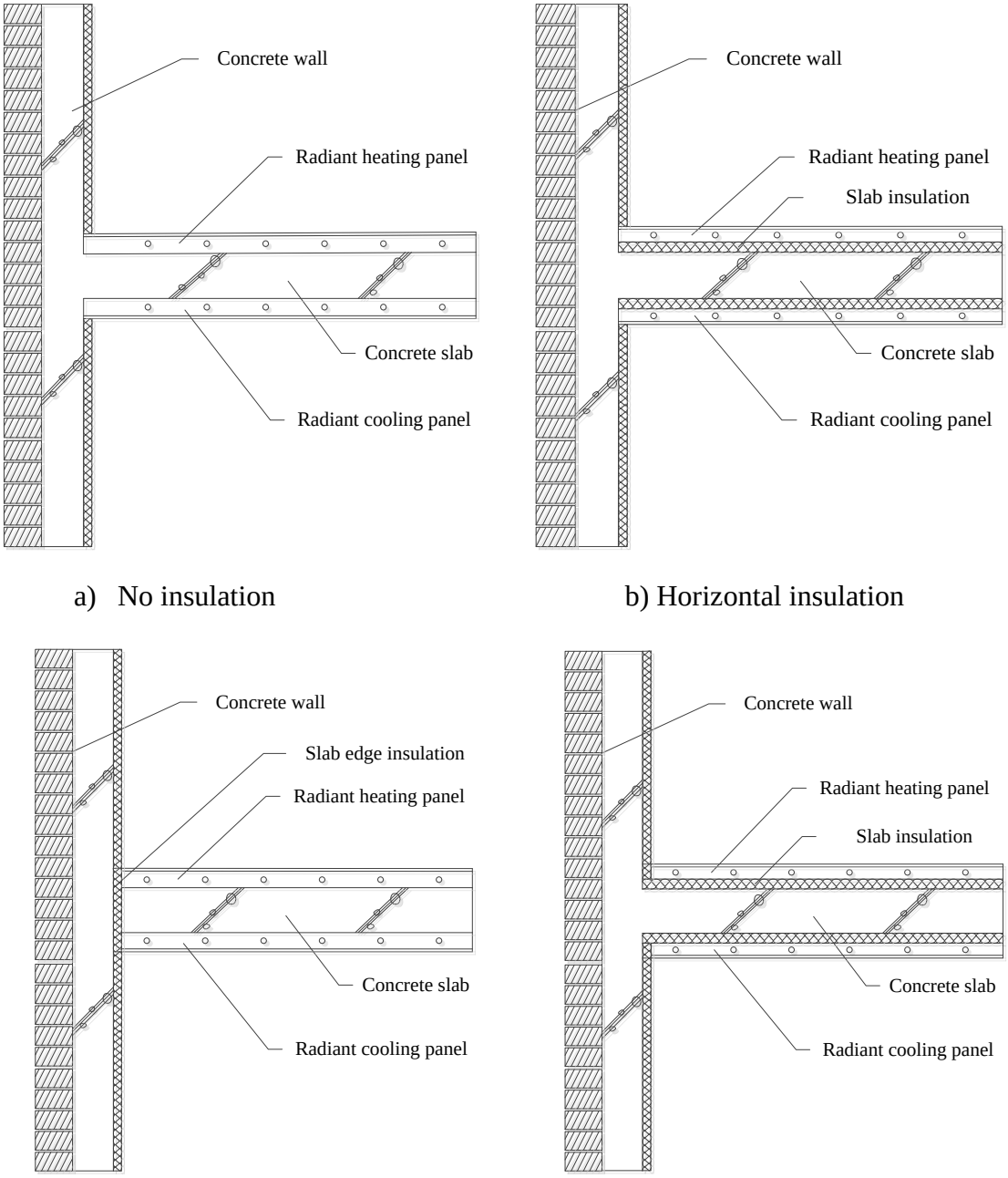

a) No insulation

b) Horizontal insulation

c) Vertical insulation

d) Horizontal and Vertical insulation

Figure 3.10: Various placement configurations of slab insulation

Figure 3.11 shows the effect of insulation type on average heat transfer rate through the upper and lower slab surfaces as well as slab edges. The results indicates that uniform horizontal insulation performs better than vertical insulation

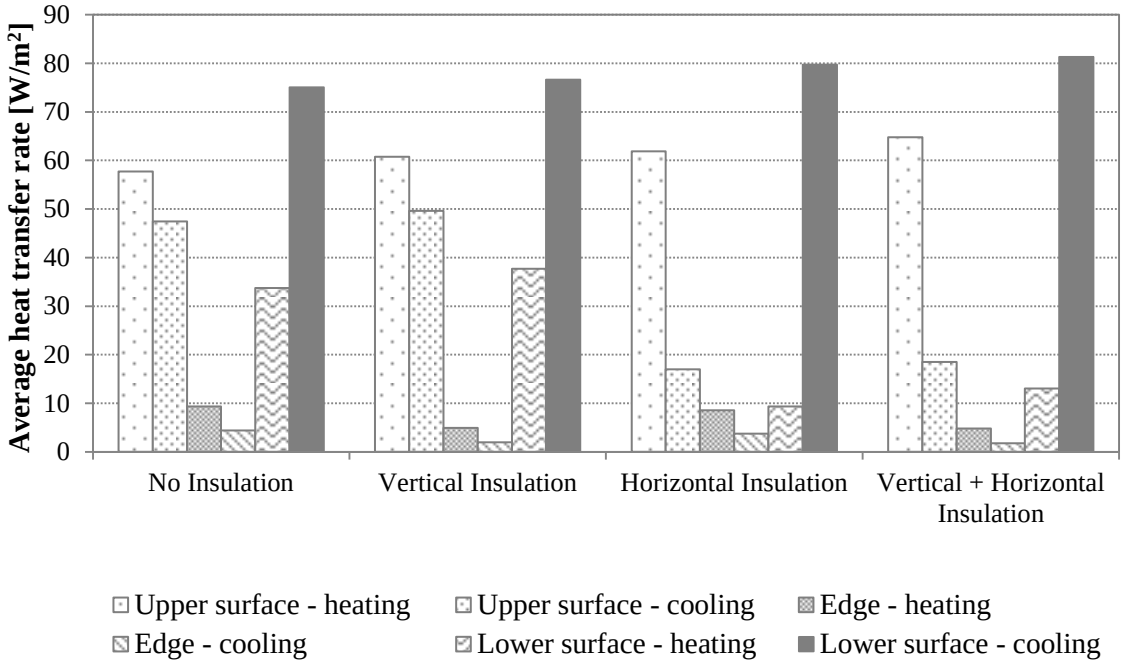

Figure 3.11: Average heat transfer rate through the upper surface of slab for heating and average heat transfer rate through the lower surface of slab for cooling with various insulation placement configurations

Figure 3.12 and Figure 3.13 illustrates the impact of the insulation thickness on average heat transfer rate from slab surfaces to each zone. Thickness of each insulation type is varied from 0.01 m to 0.05 m. As expected, an increase of the insulation thickness of insulation increases the heat transfer rate through the surface of slab.

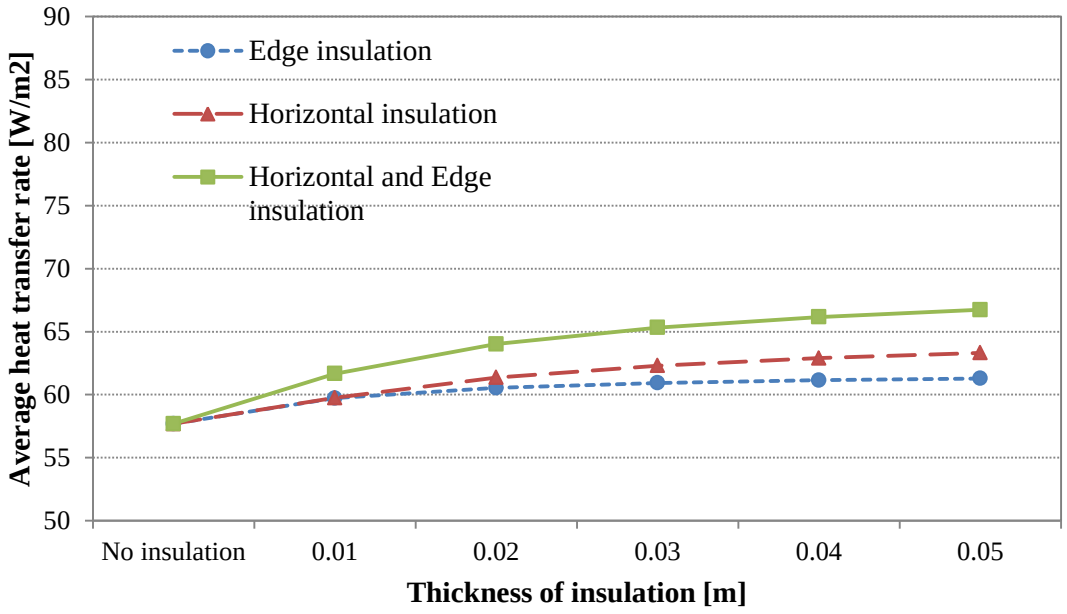

Figure 3.12: Average heat transfer through the upper slab surface with various insulation thicknesses during heating mode

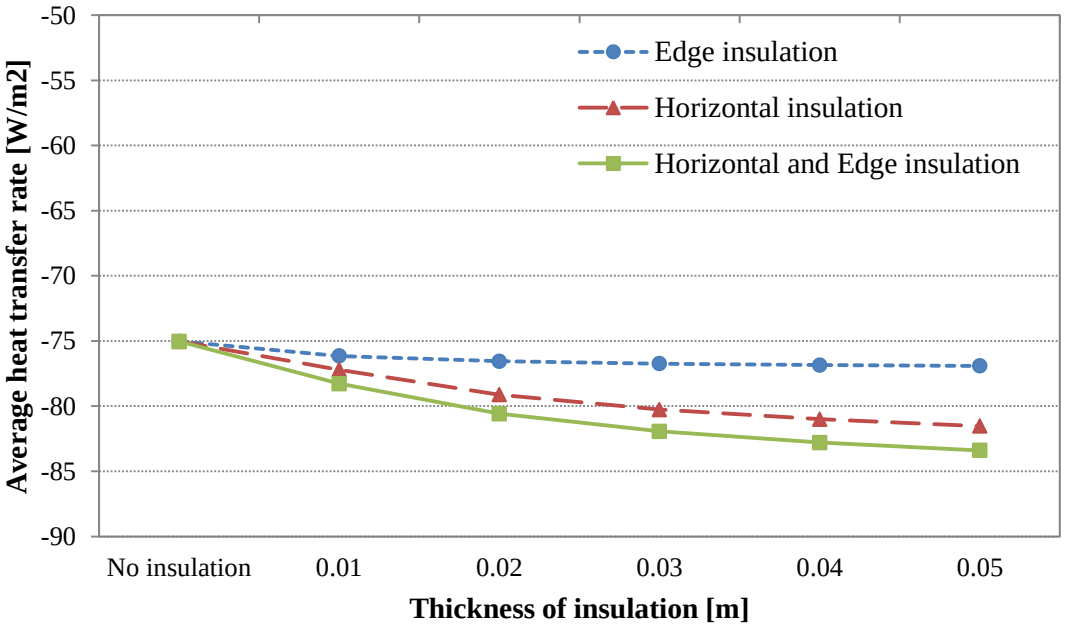

Figure 3.13: Average heat transfer through the lower slab surface with various insulation thicknesses during cooling mode

3.4. Summary and Conclusions

In this chapter, a two-dimensional numerical model for radiant slab with both heating and cooling tubing systems is developed and validated against measured data reported in a previous research study. Several parametric analyses are performed to determine the performance of radiant slab heating and cooling systems under various design and operating conditions. In particular, the parametric analyses include the effect of pipe pitch, water inlet temperature, water mass flow rate, depth of embedded pipes, and insulation placement configurations.

It is found that smaller pipe spacing increases the performance of radiant floor panels for both heating and cooling modes. However, the effect of decreasing the pipe spacing follows a diminishing return pattern with gradually reduced impact. In addition, the total slab heat transfer rate into the indoor space increases proportionally to the increase in hot water inlet temperature during heating mode. However, the total slab heat transfer rate into the zone decreases proportionally to the increase in chilled water inlet temperature during cooling mode.

When the water mass flow rate is larger than 0.15 kg/s, the total slab heat transfer rate to the indoor space is found to be not significantly affected by the mass flow rate in both heating and cooling modes.

As the depth of embedded heating pipe increases, the total slab heat transfer rate along the upper slab surface decreases, but the total slab heat transfer rate on lower slab surface increases. In cooling mode, the total slab heat transfer rate into the upper zone increases almost proportionally to the increase of the depth of the cooling pipe within the concrete slab.

It is found that the slab with both vertical insulation and uniform horizontal insulation placements achieve the best performance of the radiant slab systems. Specifically, it is found that vertical insulation reduces the heat losses through the slab edges and thus reduces thermal bridging impact while horizontal insulation placement reduces the thermal interaction between heated/cooled slab and unconditioned zone. However, the addition of insulation does not significantly affect the total slab heat transfer rate between heated/cooled slab and conditioned zones.

CHAPTER 4: ENERGY USE PERFORMANCE OF RADIANT SLAB HEATING AND RADIANT CEILING COOLING SYSTEMS

4.1. Introduction

Control strategies for radiant slab systems are more challenging than those utilized to operate conventional hot air-heating systems. Due to the inherent time lag of heat transfer associated to the slab thermal mass, controlling the operation of radiant slab system is rather complex in order to maintain indoor space air temperature and/or thermal comfort within acceptable ranges. Previous reported investigations have evaluated control strategies for radiant floor heating panels to maintain space temperature using temperature or heat flux modulation techniques. However, these studies do not consider radiant slab systems with two heat sources (for simultaneous heating and cooling). Therefore, there is a need to explore and possibly develop new control strategies to both improve temperature regulation and save heating energy costs for radiant slab systems with two heat sources.

In this chapter, two control strategies are evaluated including variable flow control and variable temperature control. The evaluation analysis of the control strategies are first carried out using Energyplus simulation tool. Then, a simulation environment developed based on an RC network model and the numerical solution for the two-dimensional heat transfer slab model, and is used to assess the effect of selected control strategies as well as design parameters on energy consumption of conditioned spaces equipped with radiant slab systems to provide both heating and cooling.

4.2. Development of a Simulation Analysis Environment with a Numerical Solution and RC Network Model for Radiant Slab Heating and Cooling Systems

4.2.1. Development of the Simulation Analysis Environment

Figure 4.1 illustrates the schematic of the simulation analysis environment using both an RC thermal network model for two zones and FDM model for the radiant slab. Since FDM is two-dimensional model, RC network only considers two walls to estimate the zones thermal loads. Both the floor and ceiling surface temperatures are obtained using the FDM solution while the radiative and convective heat transfer exchanges between zone surfaces including the walls, the floor and the ceiling are accounted for using the RC network model combined with indoor air heat balance. To account for the incident solar radiation impact on exterior surfaces, the sol-air temperature is assumed to be outdoor air temperature.

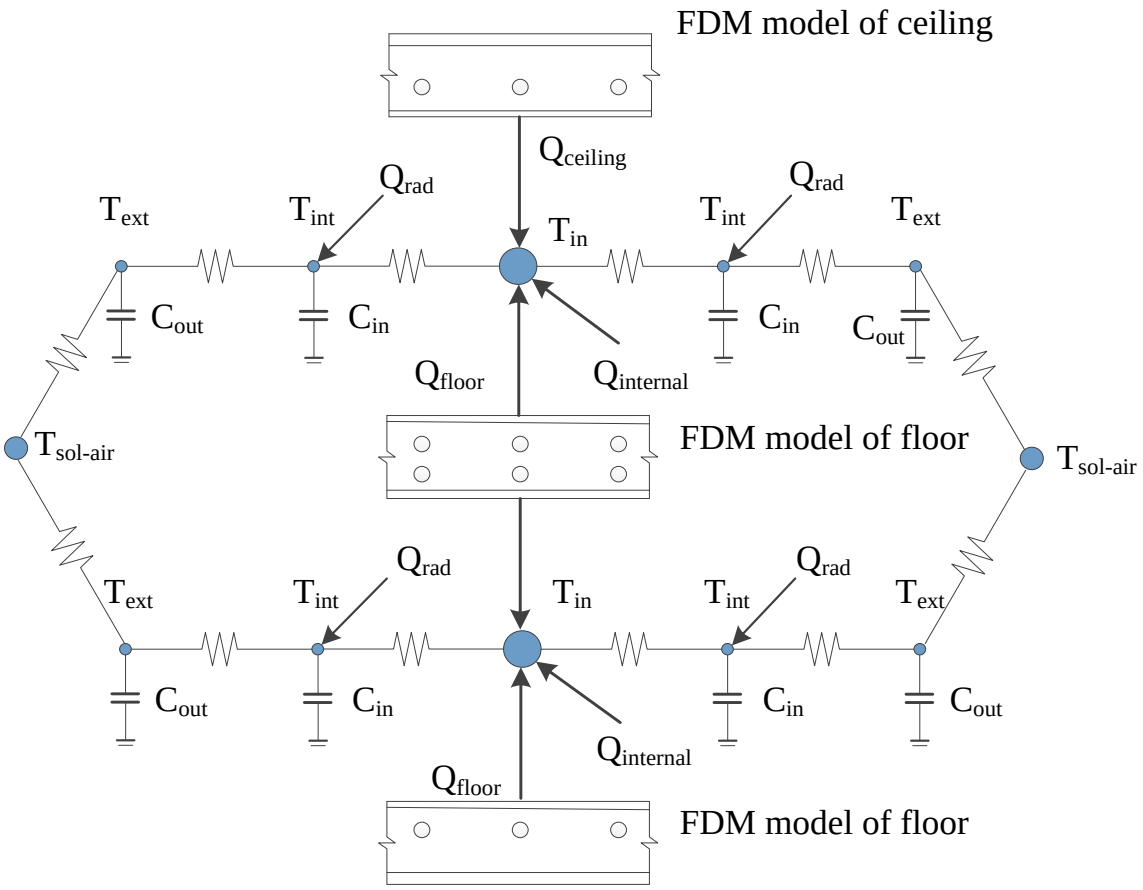

Figure 4.1: Schematic of the FDM+RC simulation environment tool

Figure 4.2 shows the relationship between the heat balance processes for various surfaces using the developed FDM+RC simulation environment of zones equipped with radiant slab systems. The calculation procedure denoted in the top part of Figure 4.2, inside the shaded box, is applied to all exterior surfaces.

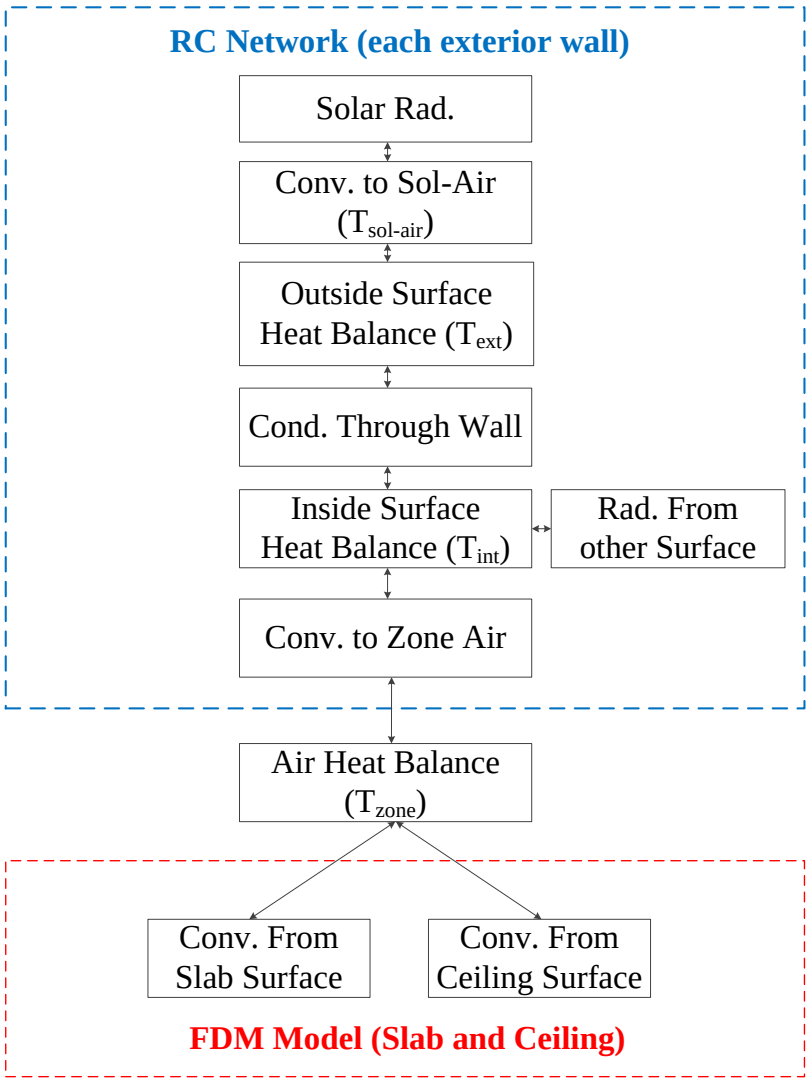

Figure 4.2: Schematic of heat balance calculation procedure applied for one zone

4.2.2. Sol-Air temperature

Sol-air temperature is the outdoor air temperature that, in the absence of all radiation changes gives the same rate of heat entry into the surface as would the combination of incident solar radiation, radiant energy exchange with the sky and other outdoor surroundings, and convective heat exchange with outdoor air. The heat balance at a sunlit surface gives the heat flux into the surface q/A as outlined in Eq. (4.1).

$$\frac{q}{A} = \alpha E_t + h_o(t_o - t_s) - \varepsilon \Delta R \quad (4.1)$$

Where,

α: absorptance of surface for solar radiation

E_t: the total solar radiation incident on surface, W/m2

h_o: coefficient of heat transfer by both radiation and convection at outer surface

t_o: outdoor air temperature

t_s: surface temperature

ε: hemispherical emittance of surface

ΔR: difference between long-wave radiation incident on surface from sky and surroundings and radiation emitted by blackbody at outdoor air temperature

Assuming the rate of heat transfer can be expressed in terms of the sol-air temperature, T_{sol}

$$\frac{q}{A} = h_o(t_{sol} - t_s) \quad (4.2)$$

And from Eq. (4.1), the sol-air temperature can be estimated as follows:

$$T_{sol} = t_o + \frac{\alpha E_t}{h_o} - \frac{\varepsilon \Delta R}{h_o} \quad (4.3)$$

For vertical surfaces, it is common to assume $\varepsilon \Delta R = 0$. Indeed, when solar radiation intensity is high, surfaces of terrestrial objects usually have a higher temperature

than the outdoor air; thus, their long-wave radiation compensates to some extent for the sky's low emittance (ASHRAE, 2005).

4.2.3.Outside-face heat balance

The heat balance on the outside surfaces can be expressed using Eq. (4.4). Typically, the incident solar radiation is considered to occur along the outside-face heat balance. The impact of solar radiation is included in the sol-air temperature for all exterior surfaces considered in the simulation environment utilized in this study.

$$q''_{conv} - q''_{ko} = 0 \tag{4.4}$$

Where,

q''_{conv} = convective exchange flux with outside air

q''_{ko} = conductive flux (q/A) into wall

4.2.4.Inside-face heat balance

The heart of the heat balance method is the internal heat balance. The internal heat balance involving the inside facades of the surfaces can be written as Eq. (4.5) involving several heat transfer components (ASHRAE, 2005):

$$q''_{LWX} + q''_{SW} + q''_{LWS} + q''_{ki} + q''_{conv} = 0 \tag{4.5}$$

Where,

q''_{LWX} = net long-wave radiant flux exchange between zone surfaces

q''_{SW} = net short-wave radiation flux to surface from lights

q''_{LWS} = long-wave radiation flux from equipment in zone

q''_{ki} = conductive flux through the interior surface

q''_{conv} = convective heat flux to zone air

4.2.5. Indoor air heat balance

In heat balance formulations, the capacitance of air in the zone is neglected and air heat balance is calculated as a quasi-steady state balance during each time step. Thermal loads associated with air infiltration and ventilation requirements are also neglected to simplify the analysis considered in this study.

$$q_{conv} + q_{CE} + q_{sys} = 0 \tag{4.6}$$

Where,

q_{conv} = convective heat transfer rate

q_{CE} = convective parts of internal loads

q_{sys} = heat transfer to/from HVAC system

4.2.6. Internal radiation heat exchange

Two surfaces at different temperature will exchange heat energy by thermal radiation. In radiative heat transfer, a view factor between surfaces is defined as the proportion of the radiation from surface i that strikes surface j. Since view factors only depend on the surfaces geometry, it is computed from using established calculation

methods (Yunus, 2001). Once the view factors between all surfaces within a zone are determined, the radiant exchange is calculated for each surface using Eq. (4.7).

$$q_{i,j} = A_i F_{i,j} (T_i^4 - T_j^4) \quad (4.7)$$

4.2.7. Calculation of building foundation heat transfer

A simplified calculation method tool to calculate heat transfer for slabs and basements has been developed by Krarti and Chuangchid (1999). The simplified calculation method is adopted in the developed simulation environment to calculate the seasonal foundation heat transfer using Eq. (4.8) to estimate foundation heat losses or gains.

$$Q_m = U_{eff,m} \cdot A \cdot (T_a - T_r) \quad (4.8)$$

Where,

$U_{eff,m} = m \cdot U_o \cdot D$

The coefficient *m* depends on the insulation placement configuration and is provided in Table 4.1. In this analysis, partial horizontal insulation is commonly used for the slab insulation configuration.

Table 4.1: Coefficients *m* to be used in Eq. (4.8) for foundation heat gain calculations

Insulation Placement	m
Uniform – Horizontal	0.40
Partial – Horizontal	0.34
Partial - Vertical	0.28

The normalized parameters used in Eq. (4.8) are defined as follow:

$$U_o = \frac{k_s}{(\frac{A}{P})_{eff,b}}$$

$$D = ln\left[(1+H)(1+\frac{1}{H})^H\right]$$

$$H = \frac{(\frac{A}{P})_{eff,b}}{k_s R_{eq}}$$

$$R_{eq} = R_f \times \frac{1}{\left[1-(\frac{c}{\frac{A}{P}} \times \frac{R_i}{R_i+R_f})\right]}$$

Where,

A = Basement/slab area, m^2

c = Insulation length of basement/slab, m

k_s = Soil thermal conductivity, W/m^2-K

P = Perimeter of basement/slab, m

Q_m = The annual mean of the total heat loss, W

R_{eq} = Equivalent thermal resistance R-value of entire foundation, m^2-K/W

R_f = Thermal resistance R-value of floor, m^2-K/W

R_i = Thermal resistance R-value of insulation, m^2-K/W

T_a = Ambient or outdoor air temperature, ℃

T_r = Room or indoor air temperature, ℃

$U_{eff,m}$ = Effective U-value for the annual mean method, W/m^2-K

4.2.8. Variable Flow Control Strategies

In the developed simulation environment, Algorithms have been included to control the zone indoor air temperature within selected setpoints and throttling ranges. In particular, variable flow control strategies are considered to modulate the operation of the radiant heating and cooling slab systems. Specifically, the radiant systems can vary the water flow rate from zero up to a specified maximum water flow rate. The flow rate is varied linearly on an hourly basis (or any selected time step). In the analysis presented in this study, the mean indoor air temperature is used as a thermal comfort indicator to control the water flow rate. However, other thermal comfort indicators (such as radiant mean temperature) can be used to control the water flow rate. Since water flow rate is varied, the inlet water temperature remains constantly. Graphical descriptions of the control strategies based on variable water flow rate utilized for the radiant slab systems as implemented in the simulation environment are shown in Figure 4.3.

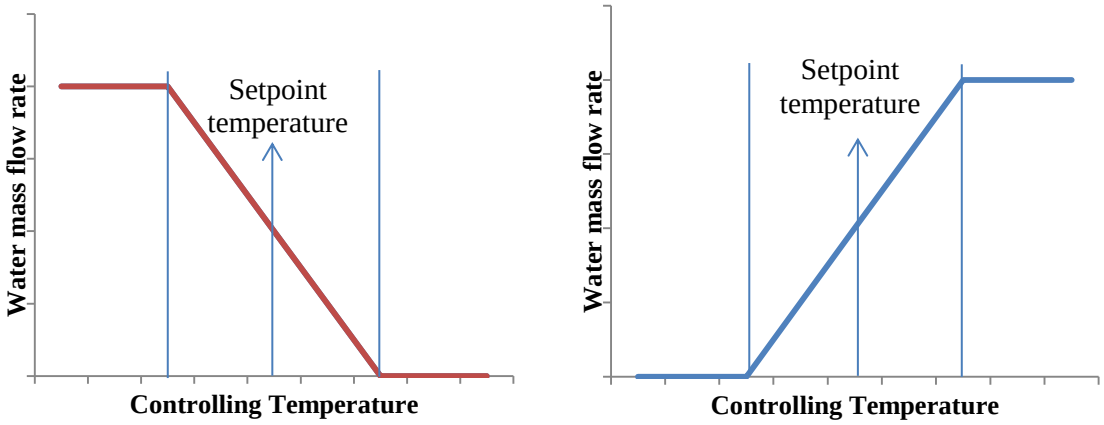

(a) Heating (b) Cooling

Figure 4.3: Variable flow control schemes for (a) heating mode and (b) cooling mode

4.3. Sensitivity Analysis

4.3.1. Mesh Grid Sensitivity

To assess the impact of selecting the grid size used for the numerical slab model on the accuracy of the results from the simulation environment tool, a sensitivity analysis to assess the accuracy in predicting slab inside/outside surface temperatures, temperatures between slab layers, East/West wall inside/outside surface temperatures, zone mean air temperature and water outlet temperature is carried out using a detailed grid with 40,625 nodes as a reference. Figure 4.4 summarizes the results of the assessment analysis to determine the impact of the grid size (expressed in terms of the number of nodes) on both the prediction accuracy (expressed in terms of RMSE between the predictions and the reference case results) as well as on the computational effort (expressed in terms of CPU of processing time). According to the Figure 4.4, when we consider RMSE as well as CPU time 11165 of nodes is the best option by using a computer with Intel® Core ™ i7-2670 QM CPU @ 2.20 GHz.

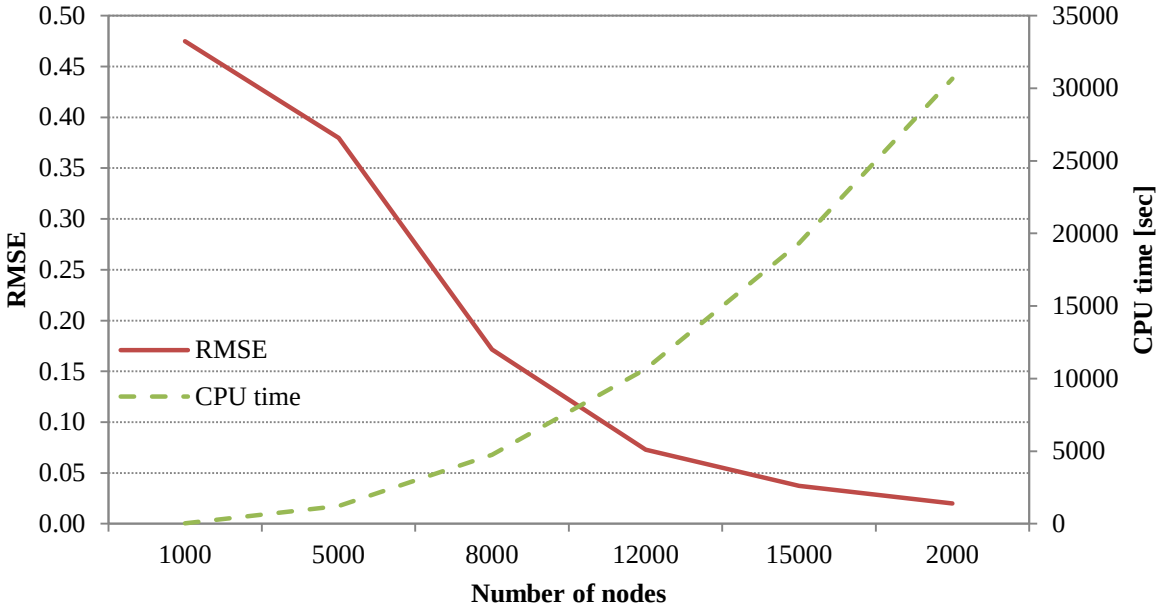

Figure 4.4: Impact of the number of nodes of the grid mesh on the prediction accuracy and computational effort

4.3.2. Timestep Sensitivity

To assess the best timestep to be used in the simulation environment, a sensitivity analysis is performed to determine the impact of the timestep selection on the prediction accuracy of slab inside/outside surface temperatures, temperatures between slab layers, East/West wall inside/outside surface temperatures, zone mean air temperature and water outlet temperature. For the sensitivity analysis, a reference case based on the results obtained from of Energyplus with 10 minute timestep is considered. Various timestep simulations are conducted with the selected grid size (see section 4.6.1). The results of the impact of timestep on both the prediction accuracy and the computational effort are

summarized in Figure 4.5. According to the Figure 4.5, when we consider RMSE as well as cpu time 11165 of nodes is the best option.

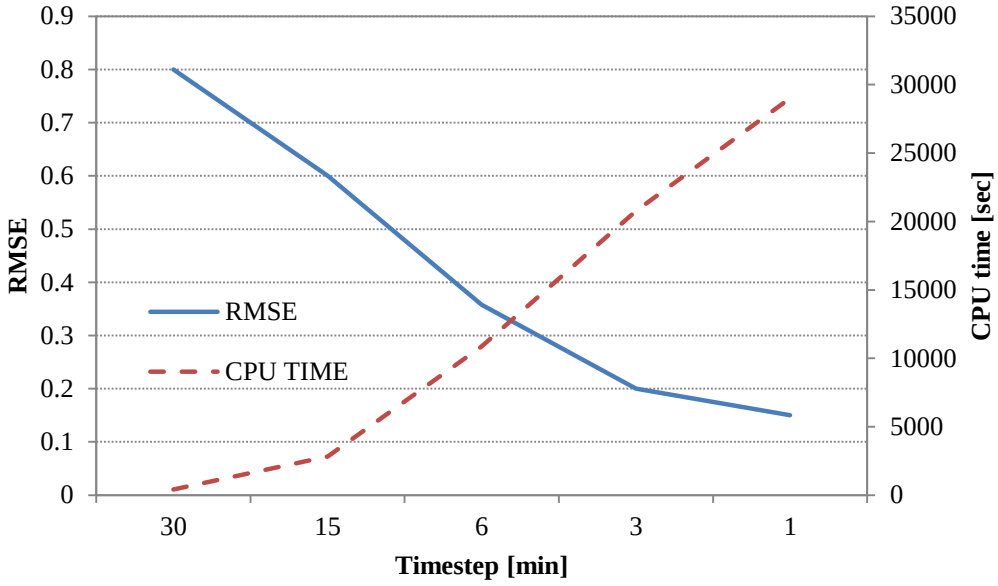

Figure 4.5: Impact of the timestep on the prediction accuracy and computational effort

4.4. Validation with Energyplus

In order to validate the predictions from the simulation environment that combines RC thermal network modeling and two-dimensional FDM analysis of slab heat transfer, predictions from EnergyPlus are utilized as reference results. In particular, predictions from the developed simulation environment and EnergyPlus are compared for the similar zone models. Figure 4.6 presents a section of two thermal zones modeled using both the simulation environment and Energyplus. Specifically, the zone model includes a radiant heating and cooling floor system embedded in a concrete slab with uniform horizontal insulation placed in the middle of slab. The length of the radiant floor panel is 4.3 meter (14

feet). The thickness of the exterior walls is 0.15 meter (0.5 feet). The pipe pitch size is 0.3 meter (12 inch). Embedded pipes are made of 3/4 inch Schedule 40 steel pipe. The total area of radiant slab heating and cooling panels is 18.49 square meter (199 square foot). Heating and cooling setpoint temperature is assumed to be 22 ℃ and 27 ℃, respectively, during 24 hours. The exterior walls are exposed to outdoor air. The roof of the upper zone and the slab of the lower zone are assumed to be adiabatic so that two zones are assumed to be located in the middle of a multi-floor building. For the Energyplus model, the exterior walls on North and South side are set as adiabatic surfaces while the boundaries for the roof and the floor are modeled to be the same as those considered in the developed simulation environment.

Table 4.2 provides a summary of the control parameters for the radiant slab heating and cooling system.

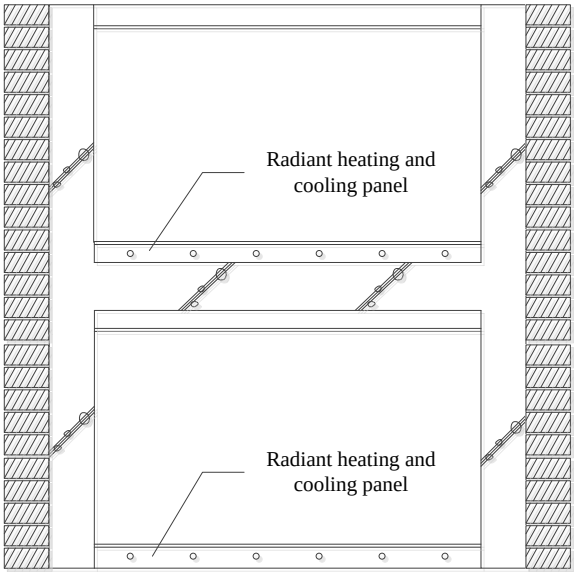

Figure 4.6: A Section view of the building slab and exterior walls for two thermal zones used in the validation analysis

Table 4.2: Summary of control and features of the radiant slab system

Category			Input variable
Radiant heating	Zone setpoint temperature		22 ˚C
	Throttling range		1 ˚C
	Variable flow	Water mass flow rate	0 ~ 0.1 kg/s
		Water inlet temperature	45 ˚C
Radiant cooling	Zone setpoint temperature		27 ˚C
	Throttling range		1 ˚C
	Variable flow	Water mass flow rate	0 ~ 0.1 kg/s
		Water inlet temperature	15 ˚C

The validation analysis is conducted using weather data for Golden, CO obtained from TMY3 weather file (Wilcox and Marion, 2008). The total solar radiation incident on the outside of the exterior wall surfaces are calculated and include several components solar beam, solar sky diffuse, solar ground diffuse, and reflected solar radiations. Figure 4.7 and Figure 4.8 illustrate outdoor dry bulb temperature and exterior surface incident solar radiation on the exterior walls during December 21 and July 21 in Golden, CO, respectively.

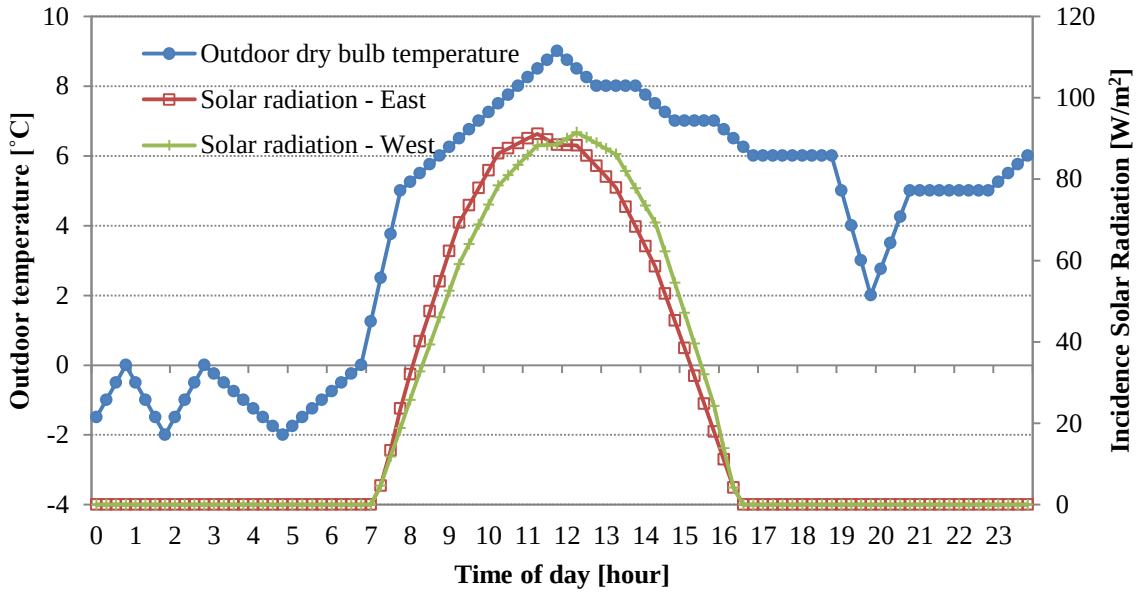

Figure 4.7: Outdoor air temperature and exterior incident solar radiation during December 21 in Golden, CO.

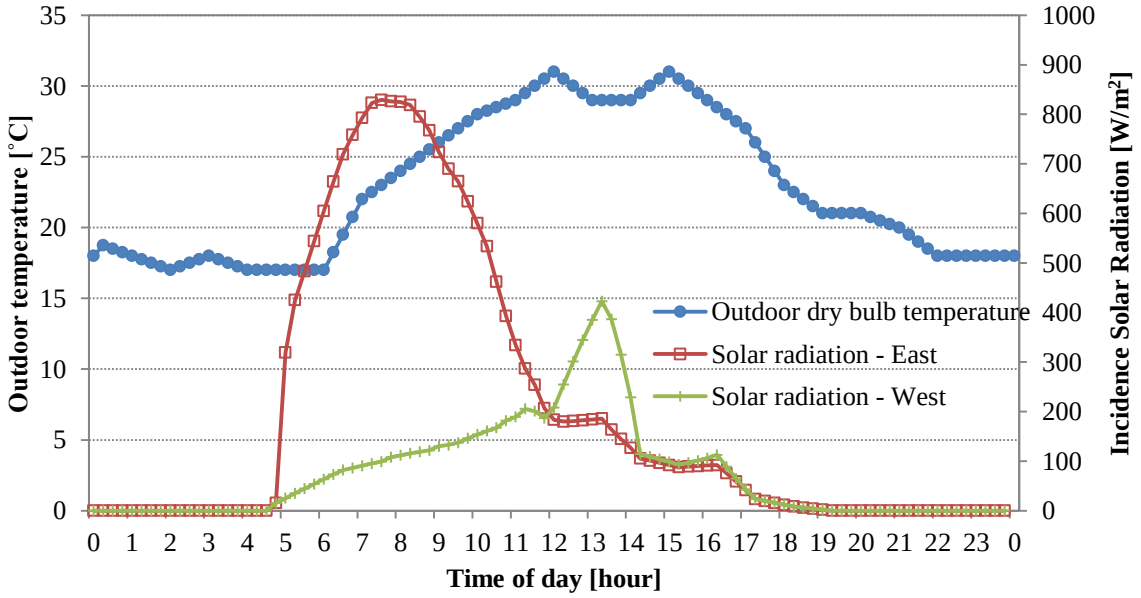

Figure 4.8: Outdoor air temperature and exterior incident solar radiation during July 21 in Golden, CO.

The predictions obtained for the two-zone model from the developed simulation environment (that combines an RC thermal network and a numerical solution of the radiant slab heating and cooling system) are compared against the results obtained from Energyplus simulation tool. Specifically, the results obtained by both simulation tools for zone mean air temperature, mass flow rate for radiant system, and energy consumption are compared.

The results for the hourly radiant heating energy consumption of Energyplus are simply obtained from output report. For the developed simulation environment, the radiant heating energy consumption is calculated for each time step using following equation:

$$E_{heating} = \dot{m}_h C_{p,h}(T_{hot\ water,in} - T_{hot\ water,out})$$

Where,

$E_{heating}$ = Radiant heating energy consumption [J]

$\dot{m}_h$ = Hot water mass flow rate [kg/s]

$C_{p,h}$ = specific heat of hot water [J/kg- ℃]

Radiant cooling energy consumption is similarly calculated using following equation:

$$E_{cooling} = \dot{m}_c C_{p,c}(T_{chilled\ water,out} - T_{chilled\ water,in})$$

Where,

$E_{cooling}$ = Radiant cooling energy consumption [J]

$\dot{m}_c$ = Chilled water mass flow rate [kg/s]

$C_{p,c}$ = specific heat of chilled water [J/kg- ℃]

4.4.1. Radiant heating slab validation

In this section, the predictions obtained during heating season for zone mean air temperature, mass flow rate for radiant system and energy consumption are compared using results from the simulation tool and EnergyPlus.

Figure 4.9 presents the comparative analysis results for zone mean air temperatures. According to the results, the mean air temperature agreed well. Figure 4.10 shows the comparative analysis results for the daily energy consumption. Table 4.3 provides a summary of the total daily radiant heating energy consumption predicted by both simulation tools. The results indicate that the total daily radiant heating energy consumption predicted by the developed simulation environment and Energyplus agreed well within 2 percent difference.

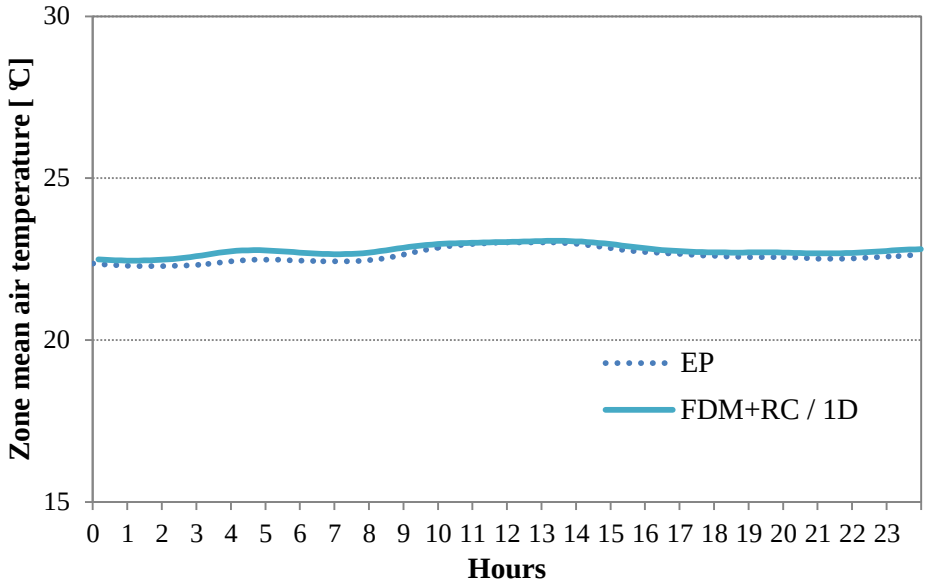

Figure 4.9: Comparison of zone mean air temperature obtained from Energyplus and developed simulation environment during a heating season day

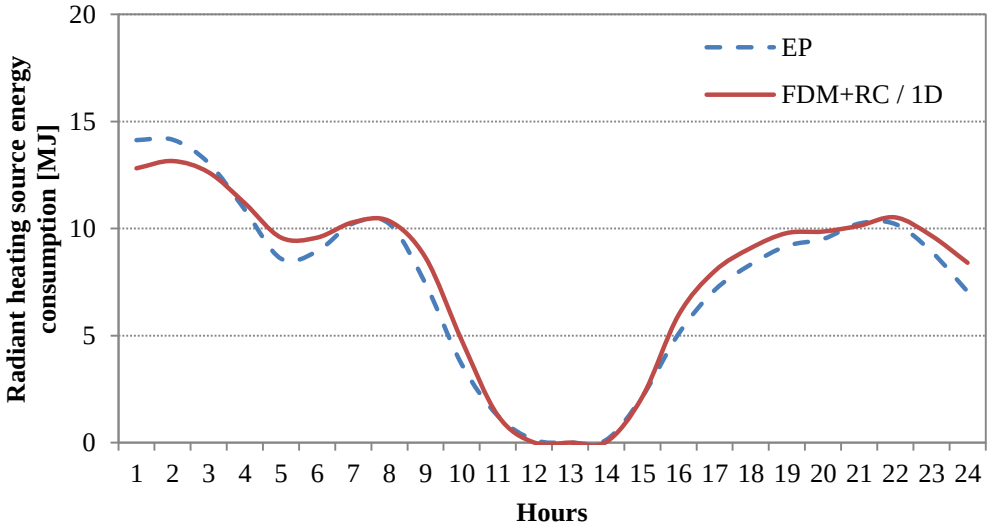

	6 hours	12 hours	18 hours	24 hours
RMSE	0.77	0.34	0.30	0.35

Figure 4.10: Comparative analysis of radiant heating energy consumption obtained by both simulation tools

Table 4.3: Comparison of daily radiant heating energy consumption predicted by both simulation tools

	Daily heating source energy consumption [MJ]
FDM	185
EP	183
Difference	2%

4.4.2. Radiant cooling slab validation with Energyplus

In this section, the predictions obtained for zone mean air temperature and energy consumption are compared using results from the simulation tool and EnergyPlus.

Figure 4.11 present the comparative analysis results for zone mean air temperatures predicted by the two simulation tools. According to the results, the mean air temperature predictions by both simulation tools agree well. Figure 4.12 shows the comparative analysis results for the daily energy consumption. Table 4.4 provides a summary of the total daily radiant cooling energy consumption predicted by both simulation tools. The results indicate that the total daily radiant cooling energy consumption obtained from the developed simulation tool and Energyplus agree well within 3 percent difference.

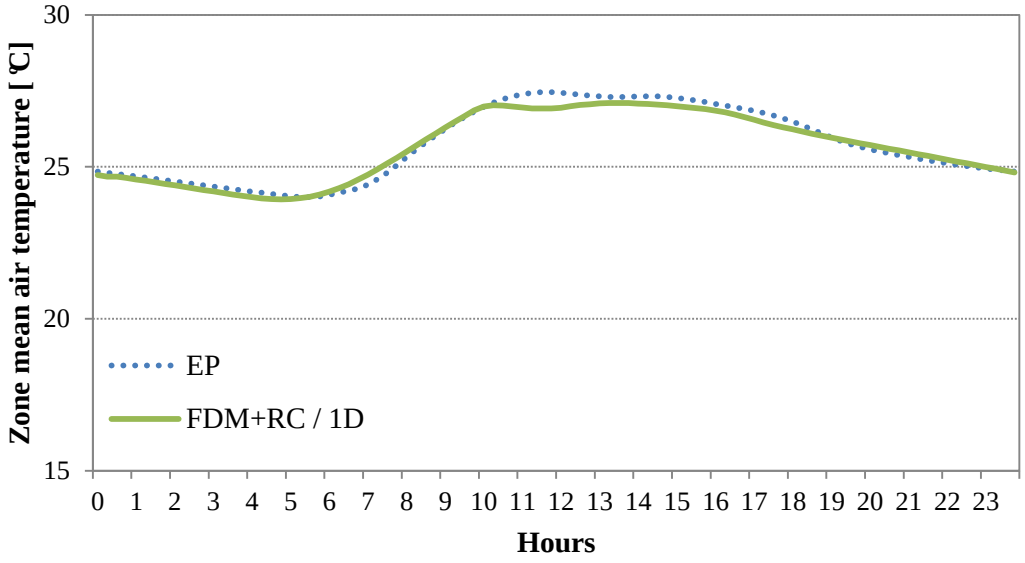

Figure 4.11: Comparison of zone mean air temperature obtained from Energyplus and developed simulation environment during a cooling season day

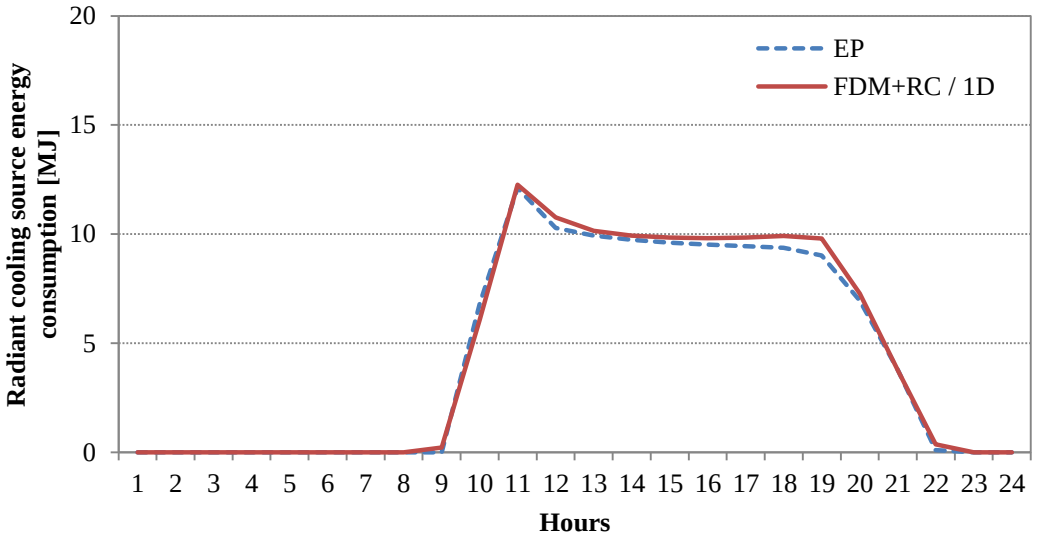

	6 hours	12 hours	18 hours	24 hours
RMSE	0.00	0.37	0.33	0.36

Figure 4.12: Comparative analysis of radiant cooling energy consumption obtained by both simulation tools

Table 4.4: Comparison of daily radiant cooling energy consumption predicted by both simulation tools

	Daily cooling source energy consumption [MJ]
EP	106
FDM	110
Difference	3%

4.5. Impact of Thermal Bridging Effect on Radiant System Performance

4.5.1. Radiant heating slab performance

In this section, the impact of thermal bridging caused by the floor slab-wall joint is investigated by estimating the total daily radiant heating energy consumption of the radiant heating slab operated with variable flow control strategy. To estimate the impact of thermal bridging effect, the results obtained from the developed simulation environment are obtained for both 1-dimensional numerical solution and 2-dimensional numerical solution for the slab heat transfer model. Specifically, the 1-dimensional FDM+RC model does not account for thermal bridging and has no heat losses through the slab edges, but the 2-dimensional FDM+RC model account for the thermal bridging between the floor slab-wall joint and has heat transfer through the slab edges especially in the case where no insulation is utilized.

4.6.1.1. Zone indoor temperature

Figure 4.13 and Figure 4.14 show time variations of zone mean air temperature and radiant heating energy consumption predicted by the simulation environment with 1-dimensional numerical solution and 2-dimensional numerical solution for the radiant slab heat transfer problem. Based on the results, the variations of zone mean air temperatures obtained for both 1-dimensional numerical solution and 2-dimensional numerical solution are almost identical since the variable flow control strategy is maintaining the same desired indoor temperature with the thermal zone. However, there is a significant difference in heating energy use predicted using the two numerical solutions. Indeed, using the 2-dimensional numerical solution, the radiant heating system consumes about 35 percent more energy when compared to the case using the 1-dimensional numerical solution. Therefore, 35 percent more energy is consumed due to heat losses caused by thermal bridging effect in the floor slab-wall joint.

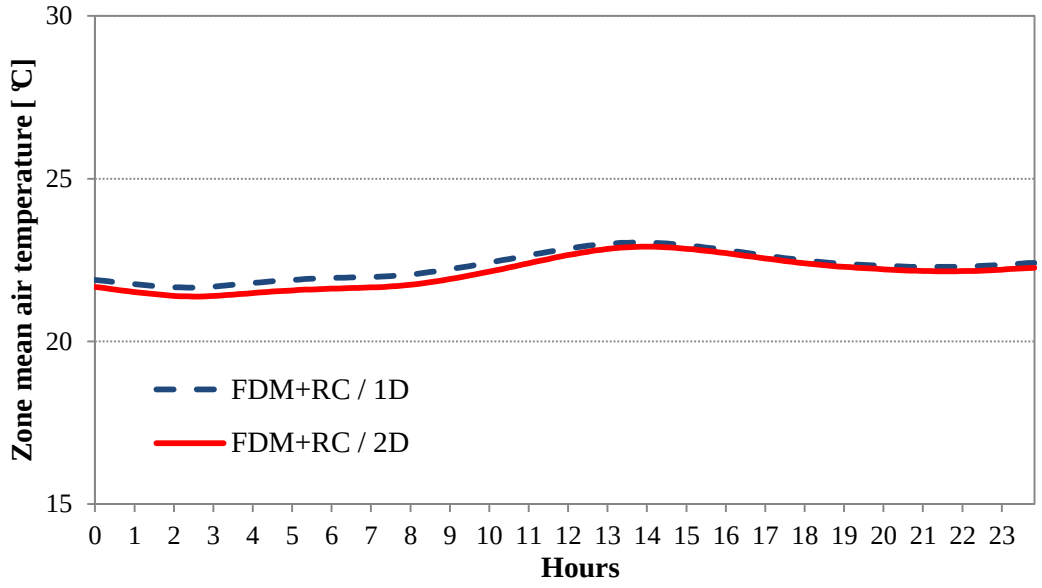

Figure 4.13: Zone mean air temperature time-variation obtained from the developed simulation environment with 1-dimensional and 2-dimensional solutions for the radiant slab model during December 21st in Golden, CO

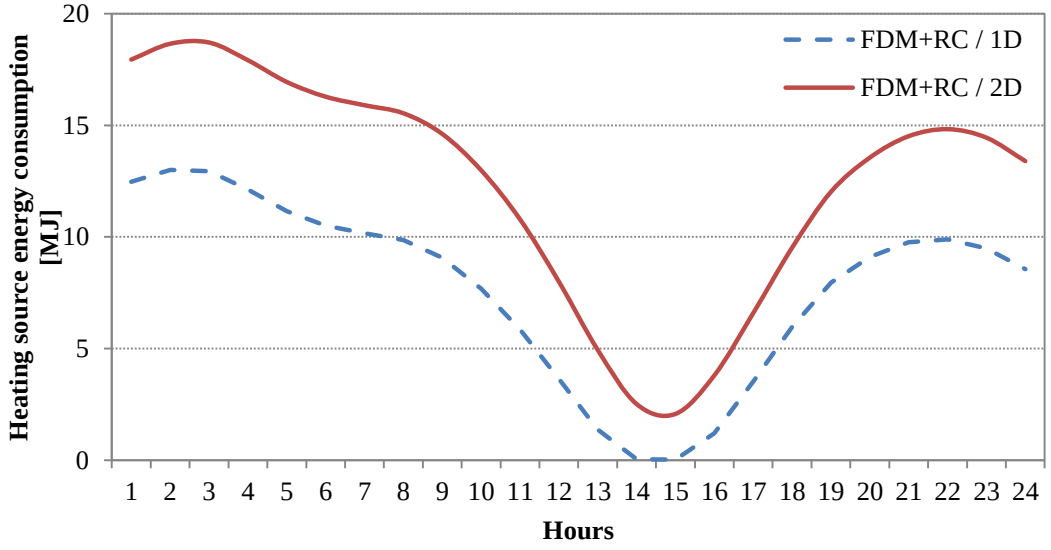

Figure 4.14: Radiant heating energy consumption time-variation obtained from the developed simulation environment with 1-dimensional and 2-dimensional solutions for the radiant slab model on December 21st in Golden, CO

When variable flow control method is used, the uninsulated radiant heating slab without accounting for the thermal bridging effect consumes 185 MJ of heating source energy, meanwhile the same radiant heating slab but with consideration of the thermal bridging effect consumes 251 MJ of heating energy. The energy impact of thermal bridging is therefore about 35 percent more heating energy required by the radiant heating slab system to maintain the required indoor thermal comfort during December 21st.

Table 4.5: Summary of daily radiant heating energy consumption and impact of energy losses due to thermal bridging effect for December 21st

	Daily radiant heating source energy consumption [MJ]	Difference [%]
FDM+RC / 1D	185	-
FDM+RC / 2D	251	35 %

4.5.2. Radiant cooling ceiling performance

In this section, the impact of thermal bridging effects on the energy performance of radiant cooling systems is investigated by evaluating the total daily radiant cooling energy consumption of radiant cooling ceiling operated using variable flow control strategy for various configurations including one-dimensional and two-dimensional heat conduction slab models.

4.6.2.1. Zone indoor temperature

Figure 4.15 and Figure 4.16 show respectively, the time variation profiles for the zone mean air temperature and radiant cooling energy consumption obtained using 1-dimensional numerical solution and 2-dimensional numerical solution for radiant slab ceiling. Based on the results of, zone mean air temperatures obtained using 1-dimensional and 2-dimensional numerical solutions are almost identical. However, the predictions obtained from the 2-dimensional numerical solution indicate that the radiant cooling system consumes about 24 percent more energy when compared to the predictions from the 1-dimensional numerical solution. These results show that 24 percent more energy is consumed by the radiant cooling system is attributed to the increased thermal cooling load caused by thermal bridging effects related to the slab-wall joints.

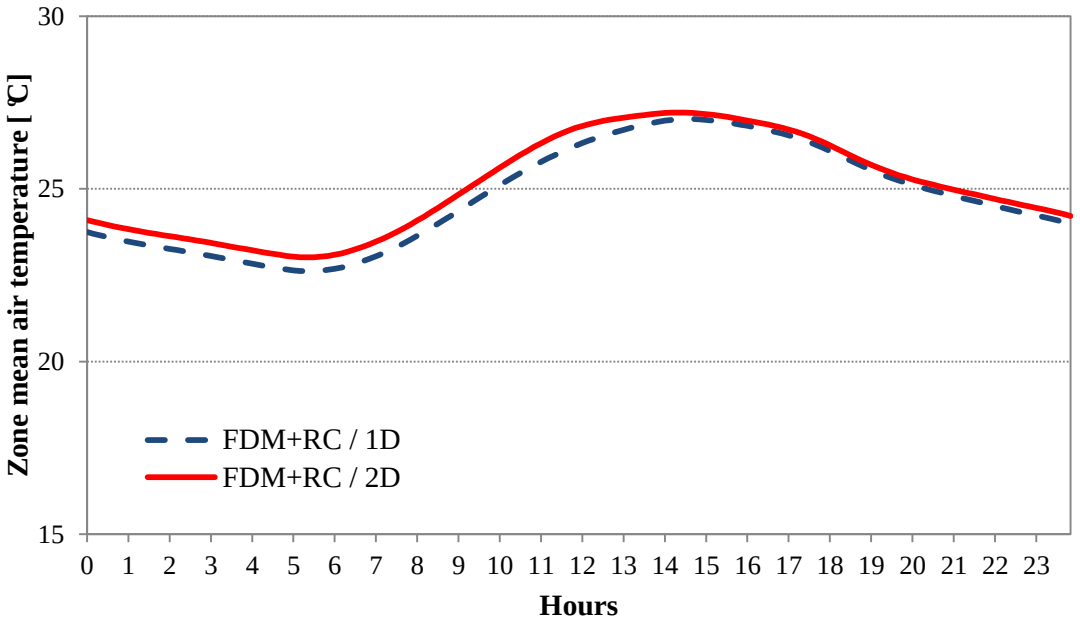

Figure 4.15: Zone mean air temperature time-variation obtained from the developed simulation environment with 1-dimensional and 2-dimensional solutions for the radiant slab ceiling model during July 21st in Golden, CO

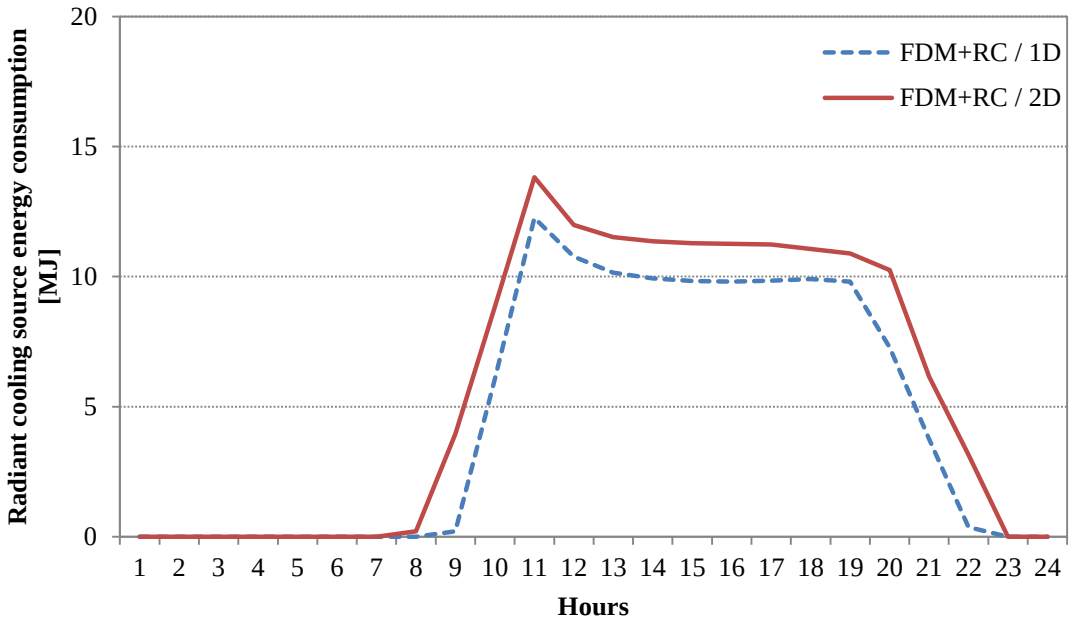

Figure 4.16: Radiant heating energy consumption time-variation obtained from the developed simulation environment with 1-dimensional and 2-dimensional solutions for the radiant slab model on July 21st in Golden, CO

When variable flow control method is used, the radiant cooling ceiling system without the effect of thermal bridging consumes 110 MJ of cooling source energy, meanwhile the same radiant cooling ceiling system but with accounting the thermal bridging effects consumes 137 MJ of cooling energy as summarized in Table 4.6. Thus, the impact of thermal bridging effects results in 24 percent more cooling energy used by the radiant cooling ceiling system.

Table 4.6: Summary of daily radiant cooling energy consumption and energy impact of thermal bridging effects during July 21st

	Daily radiant cooling energy consumption [MJ]	Difference [%]
FDM+RC / 1D	110	-
FDM+RC / 2D	137	24 %

Based on the previous results, energy impact associated with thermal bridging effects can be significant for radiant slab systems. To reduce the energy impact of thermal bridging effects from the slab-wall joints, insulation should be utilized. Using the simulation environment for modeling energy use of radiant slab systems, the impact of adding insulation using various placement configurations is evaluated. Table 4.7 indicates the properties of concrete and insulation materials used for the simulation analysis.

Table 4.7: Properties of materials used for concrete slab and thermal insulation

Material	Conductivity [W/m-K]	Density [kg/m^3]	Specific Heat [J/kg-°C]
Concrete (slab)	1.731	2300	653
Polystyrene (insulation)	0.058	24	1214

Energy consumptions of the radiant system obtained from the 1-dimensional solution (FDM+RC/1D) with no lab insulation are compared to energy consumptions obtained from the 2-dimensional solution (FDM+RC/2D) with vertical insulation placement with various R-values as shown in Figure 4.17. As expected with no insulation, the FDM+RC / 2D

model predicts that the radiant system consumes 35 percent more energy use that that predicted by the FDM+RC / 1D model due to thermal bridging effect. When vertical insulation is considered with R-value of 0.38 [m^2-K/W] (2.2 [hr-ft^2- ℉/Btu]), the impact of thermal bridging effect is reduced by 20 percent during winter season. For an insulation level of R-0.38 SI (R-2.2 IP), the impact thermal bridging effect is further reduced to 15 percent of cooling energy consumption during summer season.

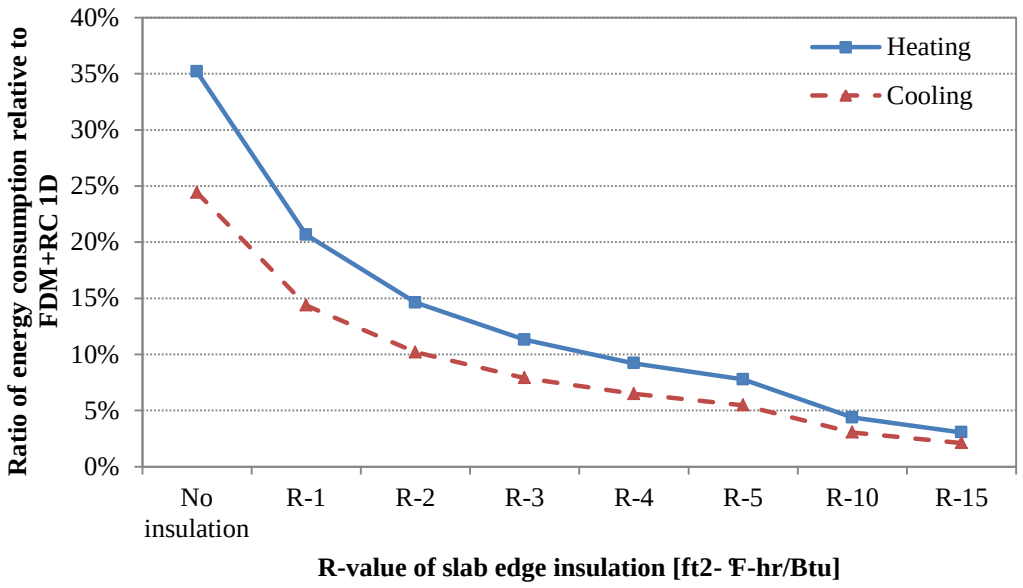

Figure 4.17: Impact of R-value of slab edge insulation on radiant system energy consumption in Golden, CO

Figure 4.18 compares the average heat transfer rate through the slab edges, upper slab surface (i.e., floor), and lower slab surface (i.e., ceiling). As the R-value of the slab edge insulation increases, the average heat losses through the slab edge gradually decrease, but the average heat transfer rate through the upper slab surface and average heat transfer rate

through the lower slab surface are not affected by the R-value. Thus the total heat generation is decreased by reducing heat losses through the slab edges.

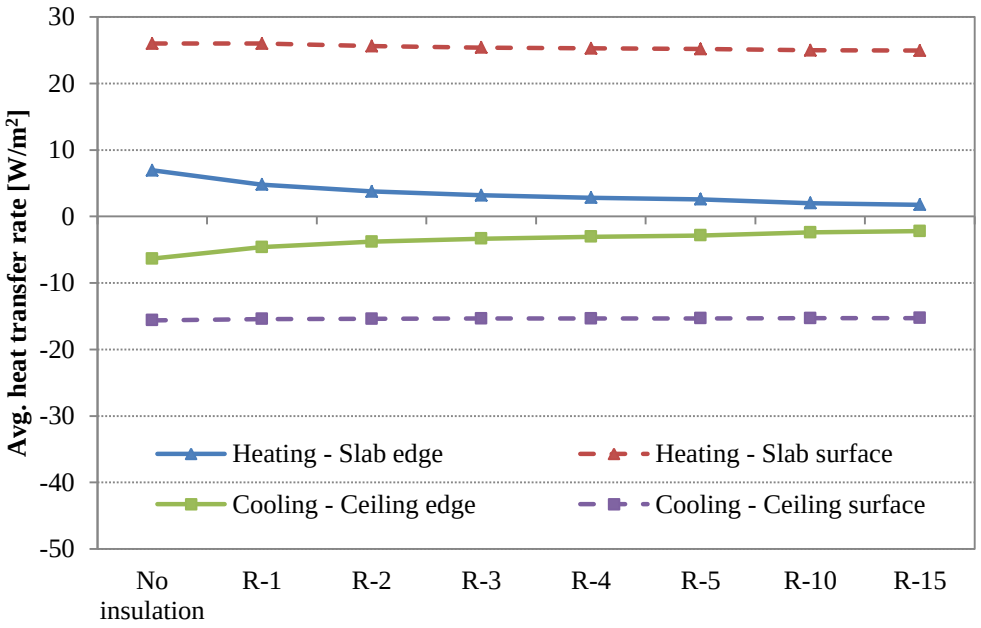

Figure 4.18: Average heat transfer rate through slab edge, upper slab surface (heating), and lower slab or ceiling surface (cooling)

Figure 4.19 compares average heat transfer rates estimated for the upper slab surface (heating), ceiling surface (cooling), and slab edge.

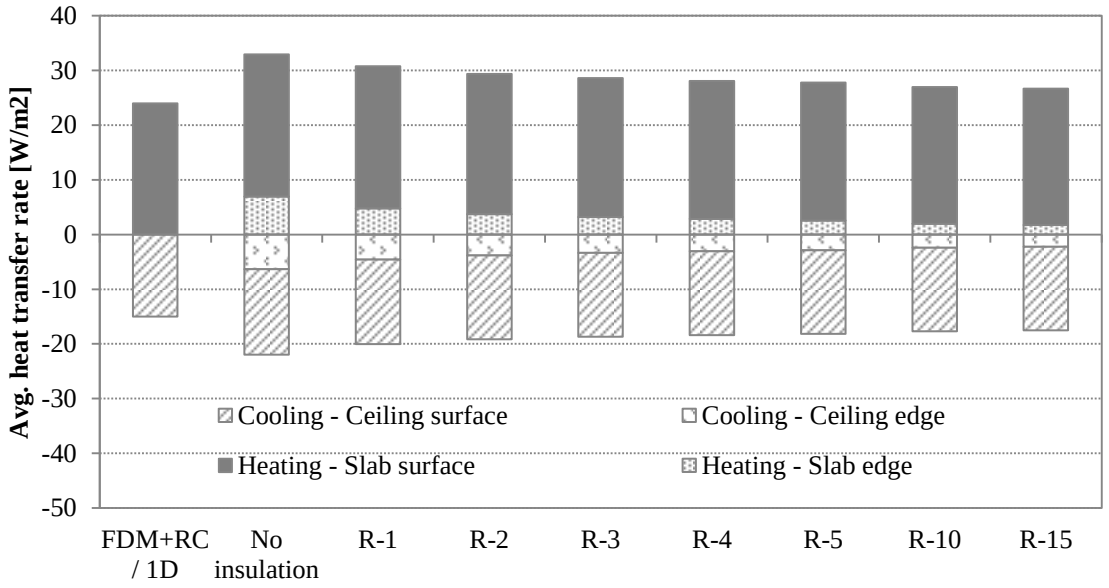

Figure 4.19: Combined average heat transfer rates through slab edge, upper slab surface (heating), and ceiling surface (cooling)

4.6. Summary and Conclusions

In this chapter, a simulation environment is developed based on a two-dimensional numerical solution for radiant slabs combined with RC network model for thermal zones. The predictions from the simulation environment are validated against results obtained from Energyplus simulation tool for specific radiant slab system configurations. In particular, predictions of zone mean air temperature and energy consumption of radiant systems estimated from the developed simulation environment tool are compared against the results obtained from Energyplus for both heating and cooling operations. Then impact of thermal bridging effect on radiant slab heating and cooling systems is explored using the developed simulation environment tool.

It is found that 35 percent of radiant heating energy consumption can be attributed to thermal bridging effects for uninsulated radiant slabs in Golden, CO. Moreover, it is found that radiant cooling slab consumes 24 percent more cooling energy due to thermal bridging when no insulation is used for the radiant slabs in Golden, CO. Detailed simulation tools such Energyplus simulation tool ignores this significant impact of thermal bridges associated with slab-wall joints.

In addition, it is found that the energy consumption of radiant heating energy and cooling systems can be significantly reduced by adding insulation in the edges of the slab. Specifically, energy consumption can be reduced by 15 percent with R-2 slab edge insulation relative to the case where the radiant slab has no insulation. The addition of R-10 slab edge insulation is found to decrease the heating and cooling energy end uses by 30 percent and 20 percent, respectively.

CHAPTER 5: APPLICATIONS

5.1. Introduction

In this section, a series of parametric analyses is performed using the developed simulation environment based on a 2-dimensional FDM solution for radiant slab combined with an RC network model to evaluate the energy performance of radiant slab heating and cooling systems with specific design features. A two-zone building model described in Figure 4.6 is used to perform the parametric analyses. The radiant systems are controlled by a variable flow control scheme as described in Figure 4.2. Table 5.1 is the summary of indoor setpoint temperature and variable for control scheme used in the parametric analyses carried out in this chapter. Selected building design features are considered in the parametric analysis including: insulation placement configuration, conditioned zone vs. unconditioned zone, and mass level and location within the thermal zone. For all the parametric analyses, energy consumption for the radiant system as well as thermal performance is evaluated under representative climatic conditions for both heating and cooling seasons.

Table 5.1: Summary of radiant system features used for the parametric analyses

Category		Input
Radiant floor heating	Zone setpoint temperature	20 ˚C
	Throttling range	2 ˚C
	Water mass flow rate	0 ~ 0.1 kg/s
	Water inlet temperature	45 ˚C

Radiant ceiling cooling	Zone setpoint temperature	26 ˚C
	Throttling range	2 ˚C
	Water mass flow rate	0 ~ 0.1 kg/s
	Water inlet temperature	15 ˚C

5.2. Impact of insulation placement configuration

In this section, the impact of insulation placement for the radiant slab is evaluated. Five different insulation placement configurations are considered for this analysis including no insulation, edge insulation, horizontal insulation, horizontal and edge insulation, and exterior insulation. Figure 5.1 illustrates the five types of insulation placement configurations.

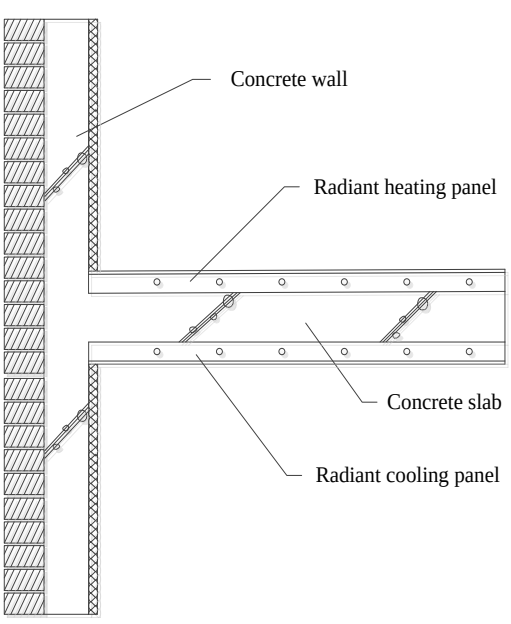

b) No insulation

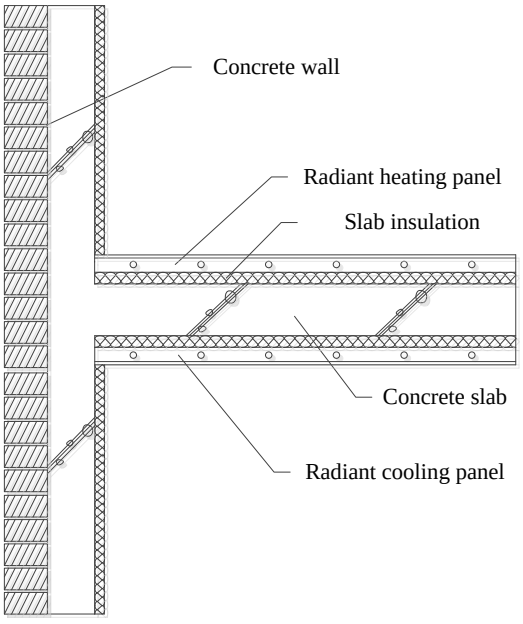

b) Horizontal insulation

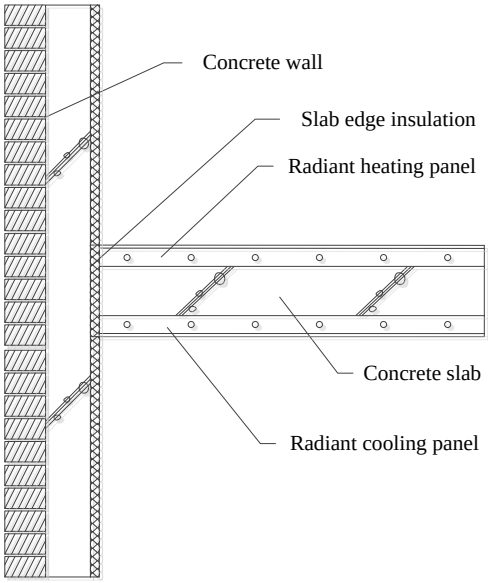

c) Edge insulation

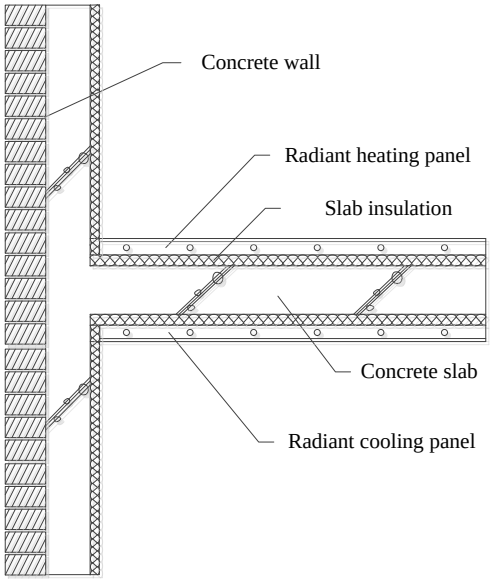

d) Horizontal and Edge insulation

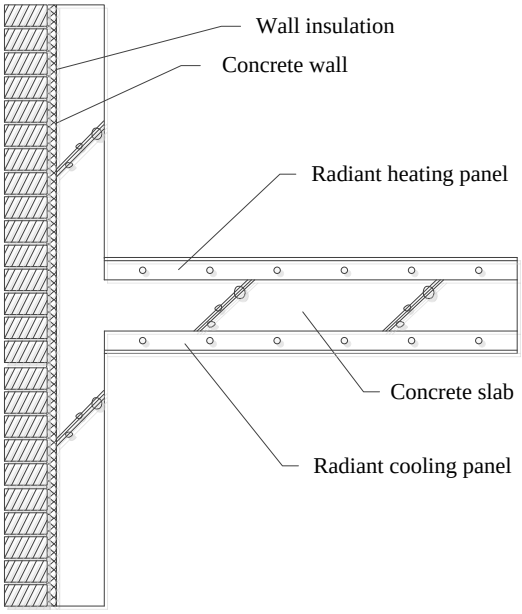

e) Exterior insulation

Figure 5.1: Radiant slab insulation placement configurations

The most effective insulation placement in terms of reducing energy consumption of the radiant system depends on thermal interactions between the two thermal zones separated by

the radiant slab. In this section, two types of zone configurations: (a) the two zones are conditioned, and (b) one of the zones is conditioned with the other is unconditioned such as an attic or a crawlspace. The performance of the insulation placement is evaluated for both zone configurations as outlined in the following sections.

5.2.1. Radiant slab separating conditioned and unconditioned zones

In this section, the performance of radiant slab heating and cooling system is evaluated when one of the adjacent zones is an unconditioned space. Specifically, the adjacent zone is assumed to be a crawl space (for radiant heating floor) or an attic is assumed to be adjacent zone (for radiant cooling ceiling). Figure 1.5 shows the view section of the radiant heating floor with a crawl space and the radiant cooling ceiling with an attic.

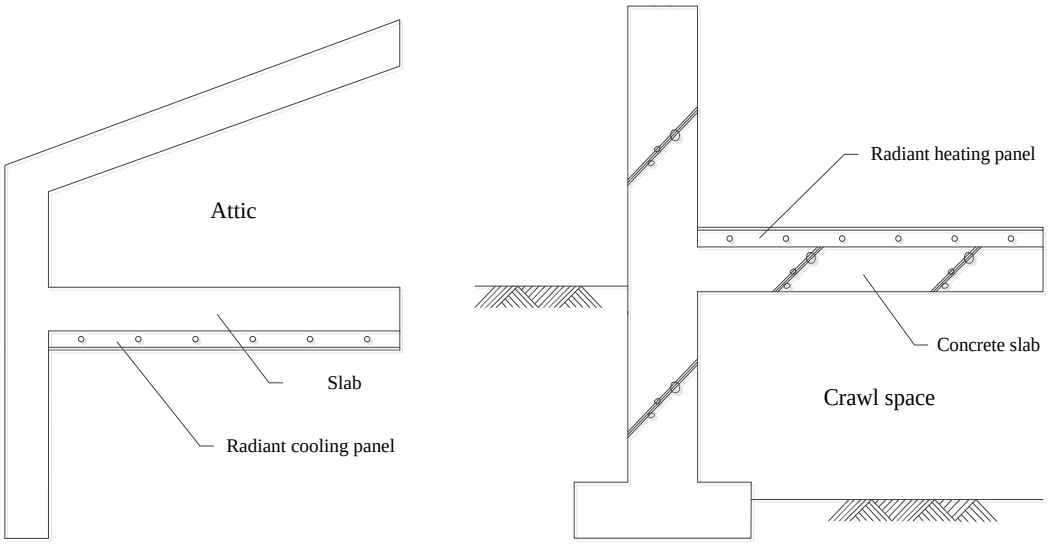

(a) Radiant cooling slab under an attic (b) Radiant heating slab above a crawl space

Figure 5.2: Radiant system serving a conditioned zone adjacent an unconditioned zone: (a) attic or (b) crawl space

Figure 5.3 shows the time variations for the mean indoor air temperature for both conditioned and unconditioned zones (attic for cooling) and crawlspace (for heating) during representative summer and winter days in Golden, CO. The conditioned zone is served by a radiant heating and cooling system with no thermal insulation.

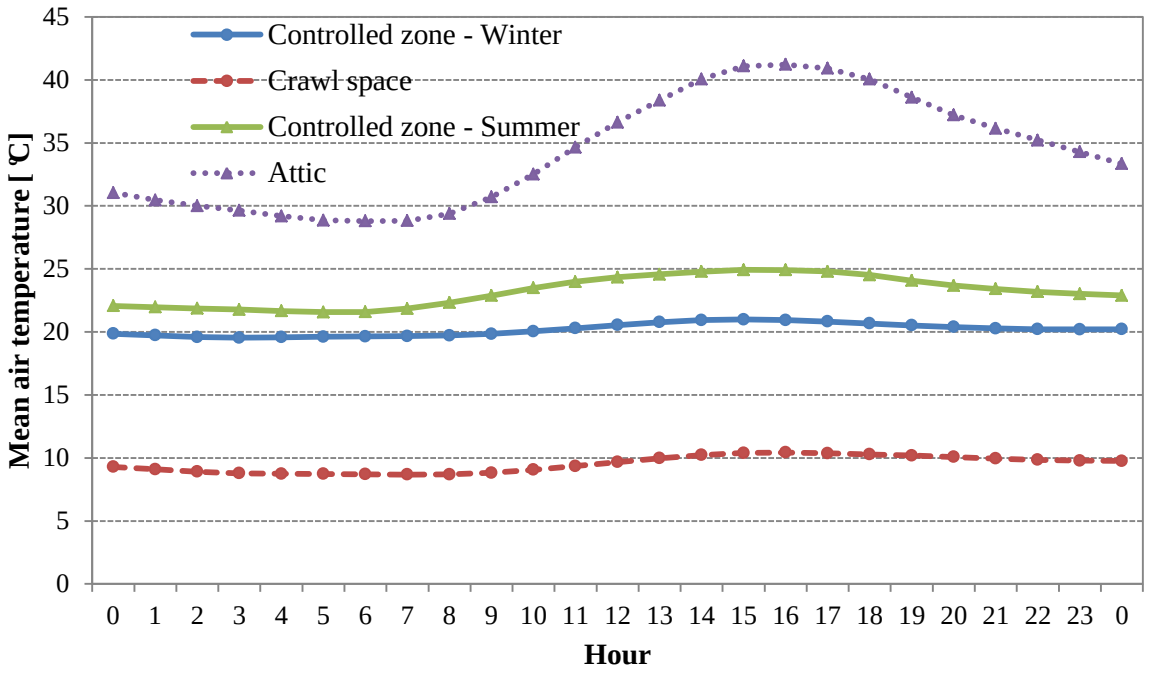

Figure 5.3: Mean air temperature time variation profiles for both conditioned and unconditioned zone (attic and crawl space) for a radiant slab system with no insulation during winter season or summer season representative days in Golden, CO

Figure 5.4 compares source energy consumption of radiant heating and cooling system among various insulation placement configurations. During a representative winter season day (December 21st), edge insulation configuration decreases radiant heating energy consumption by 6 percent compared to the no insulation case. Meanwhile, horizontal insulation reduces radiant heating energy consumption by 27 percent. Radiant heating energy use is reduced by 4 percent with exterior insulation. As clearly shown in Figure 5.4,

the most effective insulation placement configuration for radiant heating system is horizontal and edge insulation. Indeed, daily radiant heating energy consumption is reduced by 33 percent with horizontal and edge insulation compared to no insulation configuration during winter season.

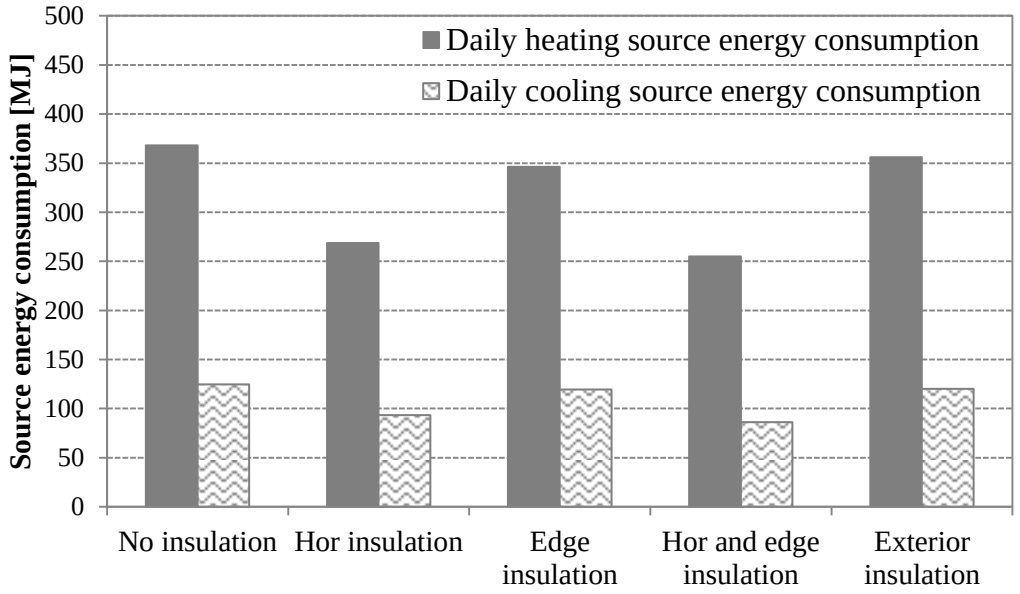

Figure 5.4: Impact of insulation configuration for when radiant controlled zone adjacent attic or crawl space during representative winter season and summer season days in Golden, CO

Table 5.2: Impact of insulation placement configurations for radiant slabs separating conditioned and unconditioned zones during winter season and summer season in Golden, CO

	Daily heating source energy consumption [MJ]	Daily cooling energy consumption [MJ]
No insulation	368	125
Horizontal insulation	269	93
Edge insulation	346	119

Horizontal and edge insulation	255	86
Exterior insulation	356	120

During a summer season day (July 21st), Figure 5.4 indicated that edge insulation configuration decreases radiant cooling energy consumption by 5 percent compared to the no insulation case. Meanwhile, horizontal insulation reduces radiant cooling energy consumption by 25 percent. Radiant cooling energy uses is saved by 4 percent with exterior insulation. As is the case of heating mode, Figure 5.4 shows that the most effective insulation placement to reduce cooling energy use is the horizontal and edge insulation. For this insulation placement, daily energy consumption of the radiant cooling system is reduced by 30 percent during the summer season.

5.2.2. Radiant slab separating two conditioned zones

When two adjacent zones are conditioned in multi-floor building, radiant slab heating and cooling systems can be used to maintain comfort within both zones throughout the year. The energy performance of the radiant slab heating and cooling systems depends on their design and control specifications. In this section, two design types of radiant systems (referred to as Type 1 and Type 2) are considered as illustrated in Figure 5.5. Type 1 uses the radiant floor panel that supplies both heating and cooling meanwhile Type 2 uses the radiant floor panel for heating and radiant ceiling for cooling.

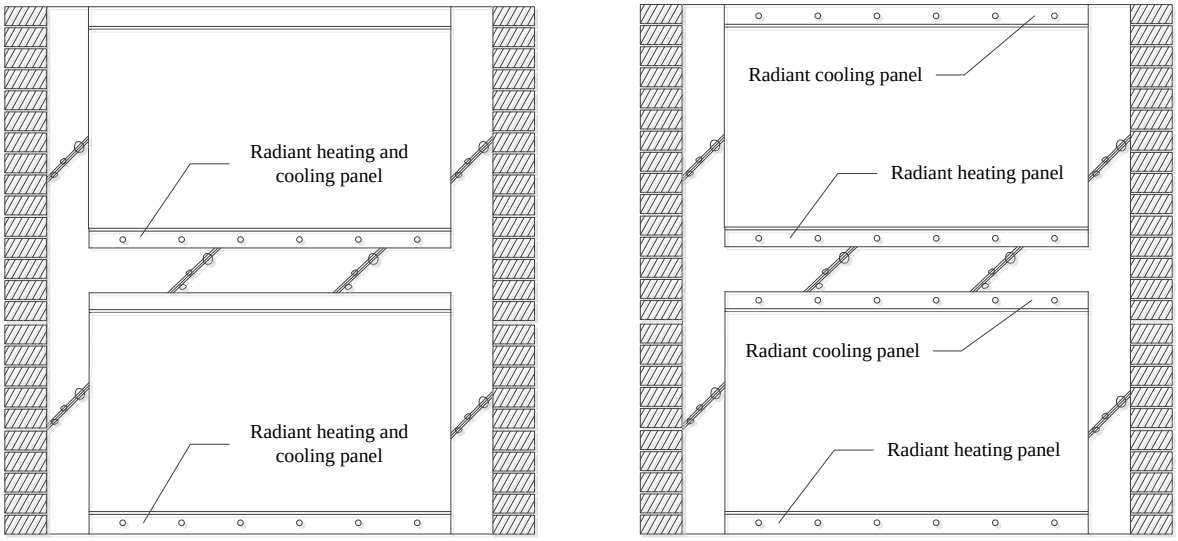

(a) Type 1 (b)Type 2

Figure 5.5: Two design configurations of (a) integrated radiant heating and cooling floor (Type 1) and (b) separate radiant heating floor and radiant cooling ceiling (Type 2)

Source energy consumption for both radiant systems, Type 1 and Type 2, are determined using the developed simulation tool for various insulation placement configurations as summarized in Figure 5.6 for representative days during both cooling and swing seasons. Table 5.3 lists the thermal properties used for various insulation configurations. Note that source energy consumption during the swing season is defined as the sum of radiant heating and cooling energy uses.

Table 5.3: Thermal properties for various insulation placement configurations

	Thickness [m]	Conductivity [W/m-K]	R-value [m^2-K/W]
Horizontal insulation	0.025	0.0648	0.385
Edge insulation	0.010	0.0648	0.154
Horizontal and edge insulation	0.025 (horizontal) 0.010 (edge)	0.0648	0.385 (Horizontal) 0.154(Edge)
Exterior insulation	0.010	0.0648	0.154

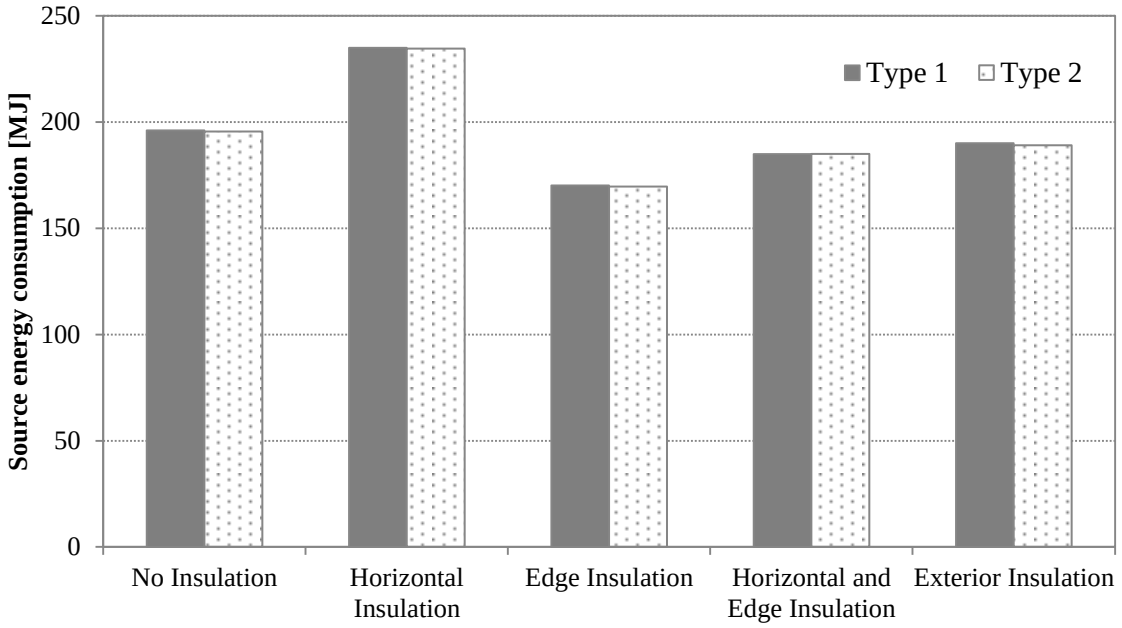

(a) Heating season

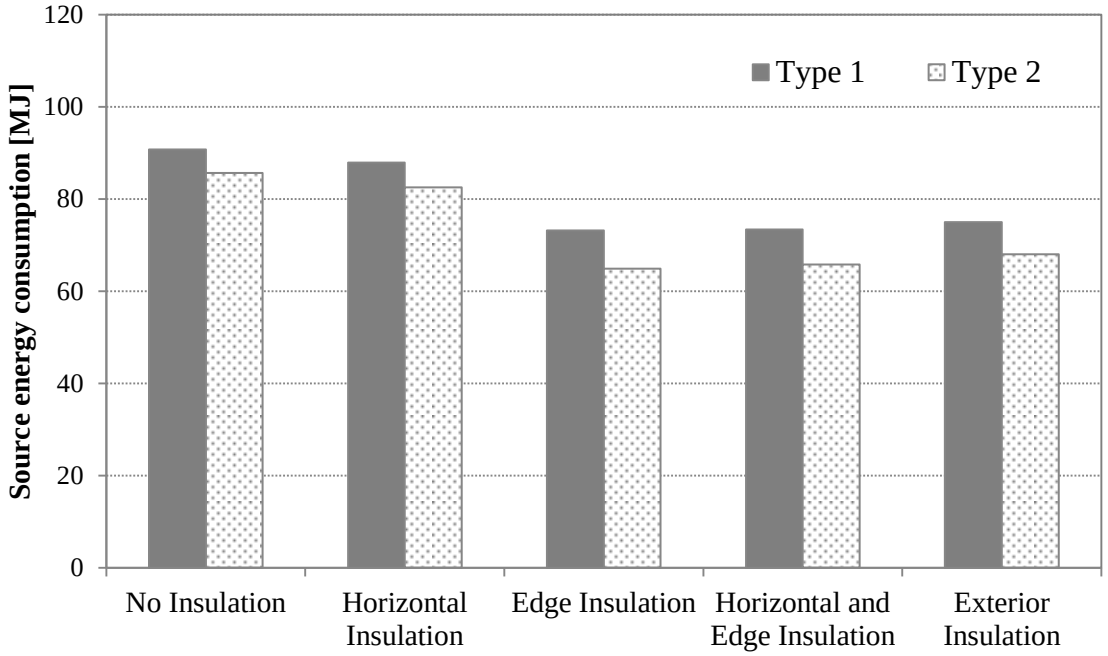

(b) Cooling season

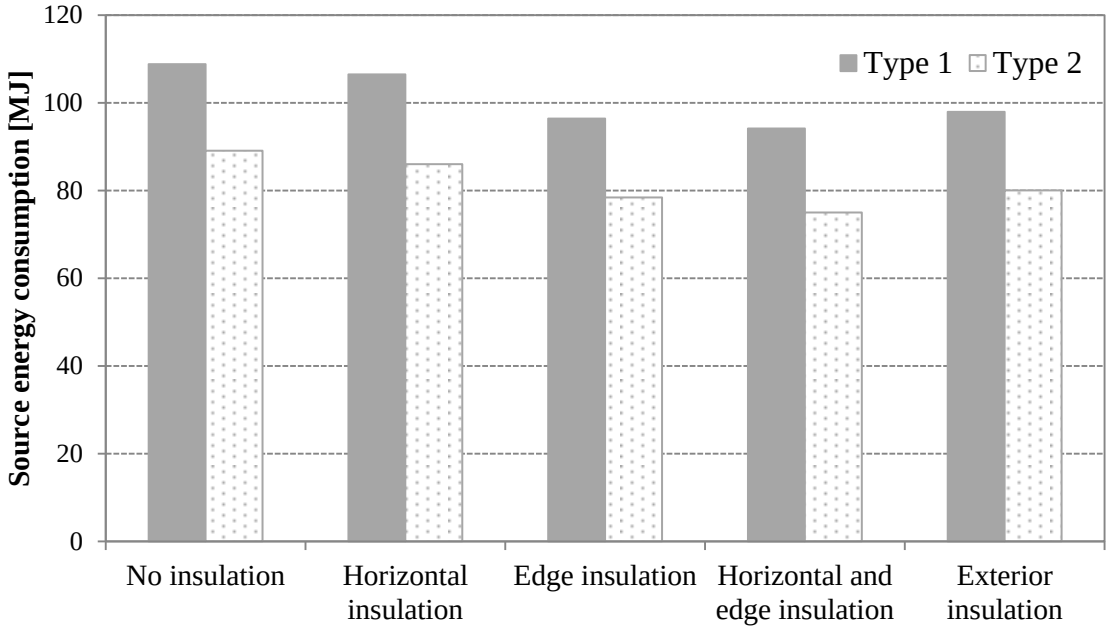

(c) Swing season

Figure 5.6: Comparison of daily source energy consumption for Type 1 and Type 2 radiant systems during heating, cooling and swing seasons in Golden, CO

Unlike in the case of the adjacent zone is unconditioned, horizontal insulation is not effective when the adjacent zone is conditioned. Indeed, the horizontal insulation placement configuration reduces the radiant system energy consumption only by 2 - 5 percent compared to the no insulation case. For the case of two adjacent conditioned zones, slab edge insulation placement is more effective with radiant system energy consumption reduced by 12 - 15 percent.

During the heating season, Type 1 and Type 2 only uses radiant slab floor panel to supply heating energy to both the conditioned zones. Therefore, heating energy consumption during the winter season is the same for both Type 1 and Type 2. During cooling season, Type 2 radiant system provide lower energy consumption of 6 – 11 percent compared to

Type 1 radiant system because cooling provided by the radiant cooling ceiling is more effective than that provide by radiant cooling floor. During swing season, Type 2 radiant system is more effective provides lower energy consumption of 17 – 20 percent compared to Type 1 radiant system.

5.3. Impact of thermal mass

In this section, energy consumption for radiant slab heating and cooling systems is determined for various thermal mass levels. Two locations for the thermal mass are considered including in the slab floor-ceiling and in the exterior walls. Table 5.4 summarizes the thermal properties of lightweight concrete and heavyweight concrete used for the parametric analysis. The analysis is conducted using the weather conditions of Golden, CO. Uniform horizontal and edge insulation configuration for the radiant slab system is used for this analysis.

Table 5.4: The thermal properties of light weight and heavy weight concrete materials

Category	Density [kg/m3]	Specific heat [J/kg-℃]	Ext. wall thickness [m]	Ext. wall Thermal mass [MJ/℃]
Lightweight thermal mass	2300	653	0.15	4
Heavyweight thermal mass	2300	653	0.50	14

During warm summer days, walls with thermal mass will steadily absorb heat, conducting it inwardly, and storing it until exposed to the cooler air during the evening/night periods. At these times, heat will begin to migrate back to the exterior surfaces and be released to the outdoors. This ability of thermal mass to respond naturally to changing conditions helps

stabilize the internal temperature and provides a largely self-regulating environment, reducing the risk of overheating and thus the need for mechanical cooling.

The ability of heavyweight buildings to remain cooler during the summer is fairly well understood. Perhaps less well understood is that this daily cycle of absorbing and releasing heat continues on a year-round basis and can reduce heating energy required to maintain a high mass building comfortable during the heating season. Specifically, the thermal mass captures and recycles heat gains from south facing windows, along with those produced by lighting, people and appliances. As the temperature drops overnight, the stored heat is slowly released back into the building, helping keep it warm and reducing the need for supplementary heating. Whilst lightweight buildings are also capable of storing heat, the extent to which the heat gains can be captured and released increases with the level of thermal mass.

5.3.1. Impact of exterior wall thermal mass

Figure 5.7 provides the daily energy consumption by the radiant slab heating or cooling system as a function of the exterior wall mass level. Based on the results of Figure 5.7, high wall thermal mass can significantly reduce heating and cooling loads. Specifically, a wall thermal mass of 7 MJ/℃ can reduce source heating and cooling energy consumption for radiant slab heating and cooling system by 20 percent and 29 percent, respectively compared to exterior wall with 2 MJ/℃ thermal mass.

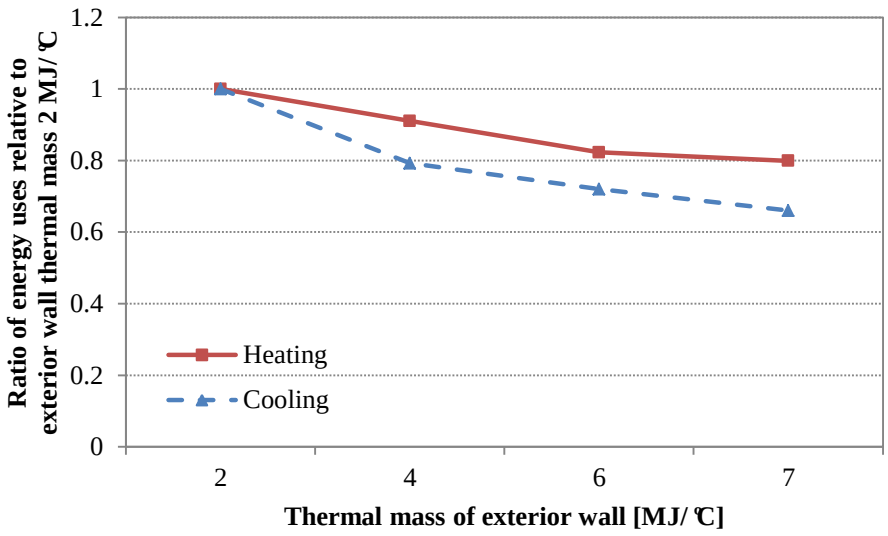

Figure 5.7: Impact of exterior wall thermal mass level on energy consumption for radiant system with slab edge insulation in Golden, CO

Table 5.5: Source heating and cooling energy consumption for radiant slab heating and cooling system for various thermal mass levels within exterior walls

Exterior wall thermal mass [MJ/℃]	Heating source energy use [MJ]	Cooling source energy use [MJ]
2	110	88
4	100	70
6	90	63
7	88	58

5.3.2. Impact of slab thermal mass

In this section, the impact of slab thermal mass level on energy consumption for integrated radiant slab heating and cooling system is analyzed using the simulation environment tool as outlined in Figure 5.5. Zone air temperature is set to be 20 ℃ for heating and 26 ℃ for cooling. For the analysis, a maximum hot water flow rate of 0.15 kg/s is used for heating, a maximum chilled water flow rate of 0.15 kg/s for cooling is considered. To evaluate the impact for thermal mass within the slab floor, two pipe depths are considered. In the first

case, the pipe is embedded at a fixed shallow depth of 0.03 meter within the slab regardless of the mass level. In the second case, the pipe is embedded in the middle of the slab thickness which varies with the thermal mass level of the slab.

Figure 5.8 compares the daily source energy consumption of integrated radiant slab system for various slab thermal mass levels using the two pipe depth options. The results indicate that as the slab thermal mass increases source energy use required by the radiant system is gradually reduced for both pipe depth cases. Note that when the pipe is placed in the middle of the slab thickness, it consumes more source energy compared to the shallow depth of 0.03 m case since it requires more energy to charge the slab, which is to increase or reduce the surface temperature of the slab to the desired set-point.

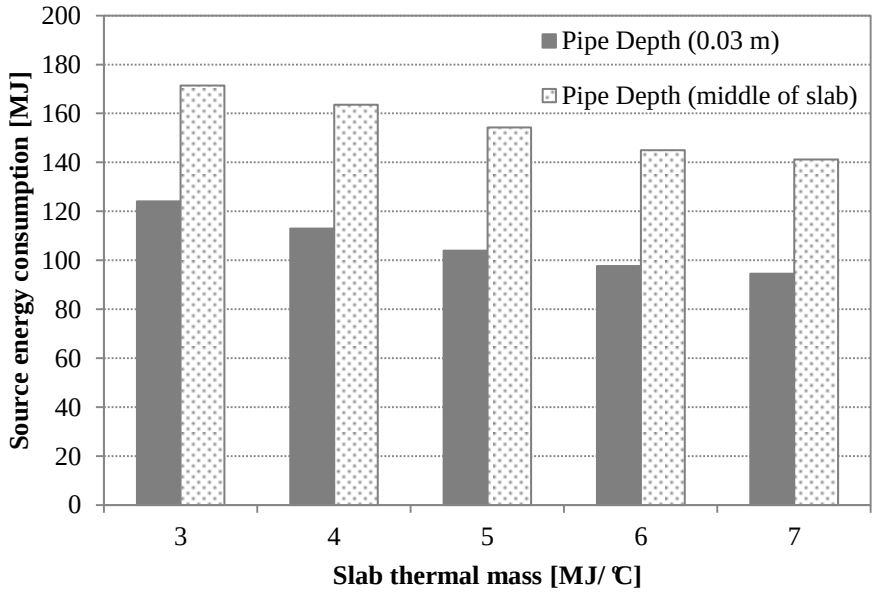

(a) Heating

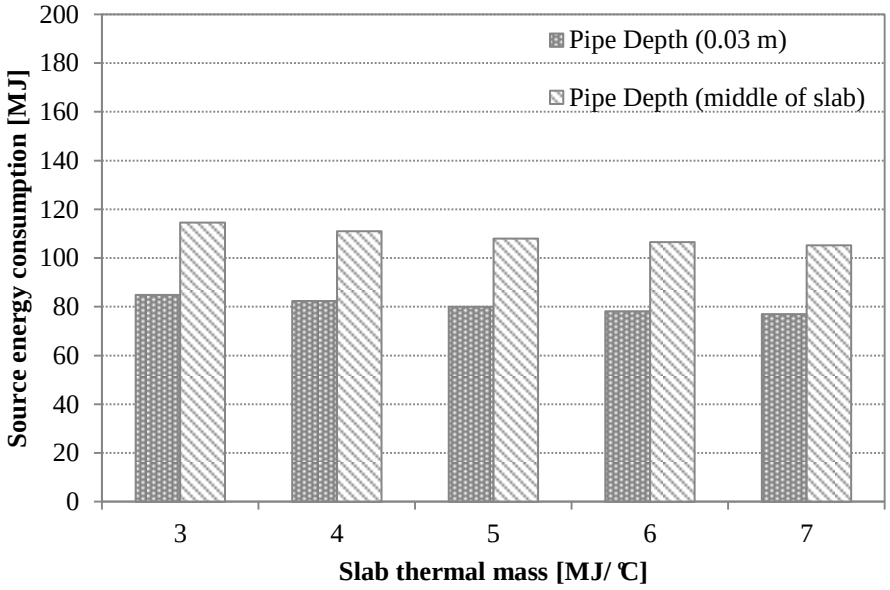

(b) Cooling

Figure 5.8: Comparison of daily source energy consumption of integrated radiant system for (a) heating and (b) cooling for two pipe depth options as a function of slab thermal mass in Golden, CO

As the slab thermal mass increases, the required heating or cooling source energy use starts decreasing. When slab thermal mass is larger than 6 MJ/ ℃, the source energy use remains unchanged as illustrated in Figure 5.9 for both pipe depth options. In particular, the results shown in Figure 5.9 indicated that when the embedded pipe depth is fixed at 0.03 m (i.e., near the slab surface), higher thermal mass levels are more effective in reducing heating than cooling thermal loads since the differences between desired indoor air temperature and outdoor air temperature during the winter season are larger than those observed during the summer season. Comparing the results of Figure 5.7 and Figure 5.9, it seems that when the pipe depth is fixed at 0.03 m, thermal mass associated with the slab medium is more effective than thermal mass associated with exterior walls especially during the heating

mode. In particular, the integrated radiant system with fixed pipe depth of 0.03 m, a thermal mass level of 7 MJ/ ℃ for exterior walls can result in a reduction of 19 percent in the heating source energy consumption. The same 7 MJ/℃ thermal mass level but within the slab floor can decreases the heating energy consumption by 23 percent. However, when the pipe is embedded in the middle of the slab, the thermal mass associated with exterior walls is more effective than that embedded in the slab floor during cooling mode. Indeed, the integrated radiant system with fixed pipe depth of 0.03 m, a thermal mass level of 7 MJ/ ℃ attributed to the exterior walls can reduce by 32 percent the cooling source energy consumption, the same 7 MJ/℃ thermal mass level but embedded in the slab floor reduces the cooling energy consumption by a mere 10 percent.

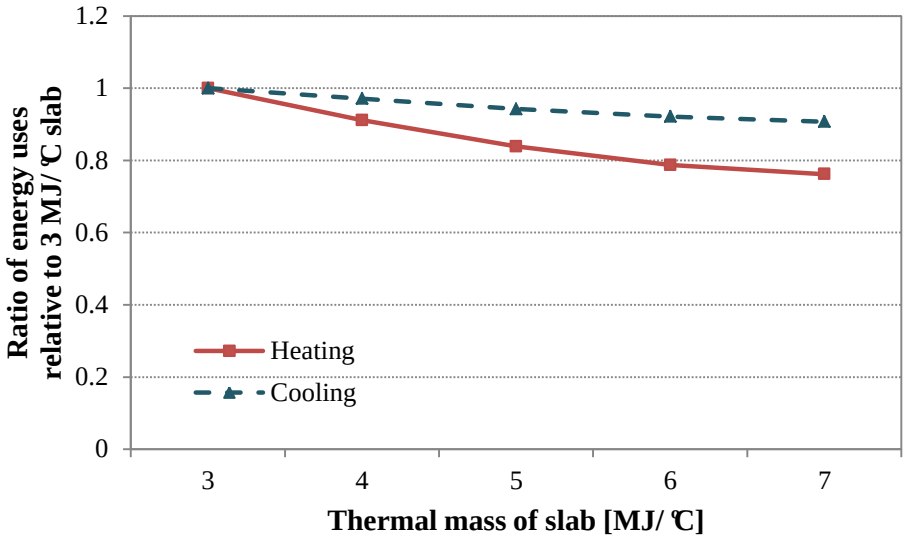

(a) Embedded pipe with fixed depth (0.03 meter)

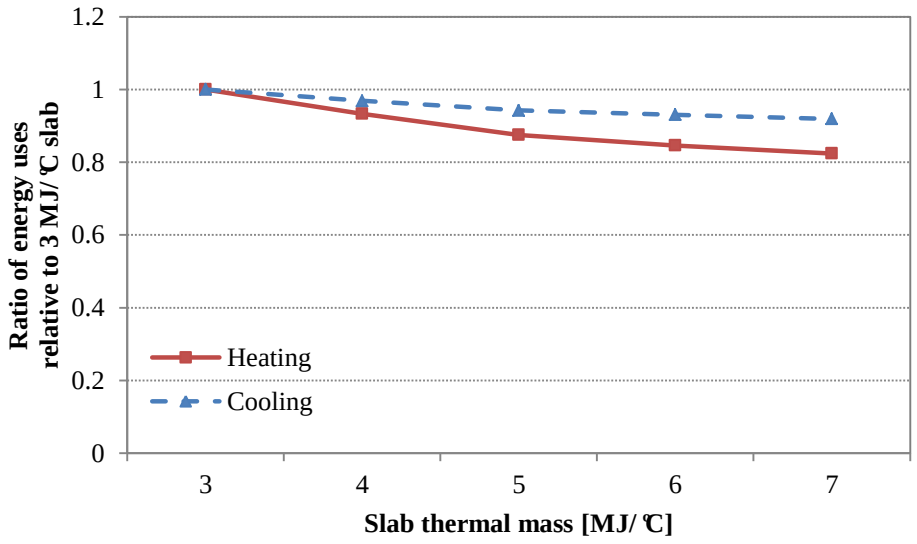

(b) Embedded pipe in the middle of the slab thickness

Figure 5.9: Normalized source energy consumption of radiant heating floor and radiant cooling ceiling with (a) fixed pipe depth of 0.03 m and (b) pipe placed in the middle of the slab thickness as a function of slab thermal mass level in Golden, CO

Table 5.6: Daily heating and cooling energy consumption for the radiant slab systems with various thermal mass levels within the slab medium

Slab thermal mass [MJ/℃]	Heating source energy use [MJ]		Cooling source energy use [MJ]	
	Pipe Depth (0.03 m)	Pipe Depth (middle of slab)	Pipe Depth (0.03 m)	Pipe Depth (middle of slab)
3	124	171	85	115
4	113	164	82	111
5	104	154	80	108
6	98	145	78	107
7	94	141	77	105

Figure 5.10 compares the hourly source energy consumption of radiant heating slab system for various slab thermal mass levels and the two pipe depth options during December 21st in Golden, CO. Figure 5.11 presents the time variation of the slab surface temperature for the same mass level and pipe depth configurations. The results show that as the thermal mass level within the slab medium is increased, the floor surface temperature increases. As indicated in Figure 5.10, when the slab thermal mass increases, the starting operation time of the radiant heating system is delayed, and the peak thermal load is significantly lowered compared to the case when the slab has a light thermal mass level. The analysis results clearly indicate that the peak thermal loads are generally higher when the pipe is embedded in the middle of the slab compared to the case when the pipe depth is set at 0.03 m.

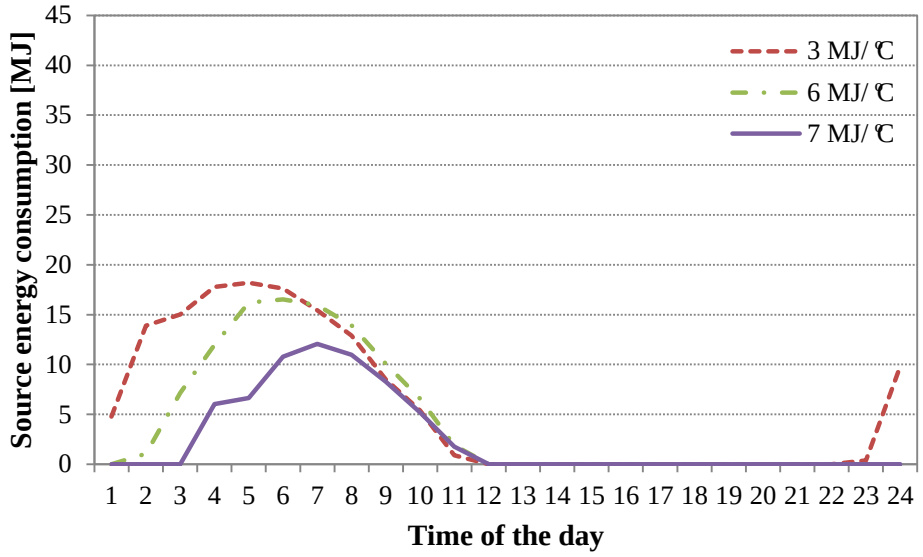

(a) Embedded pipe with fixed depth (0.03 meter)

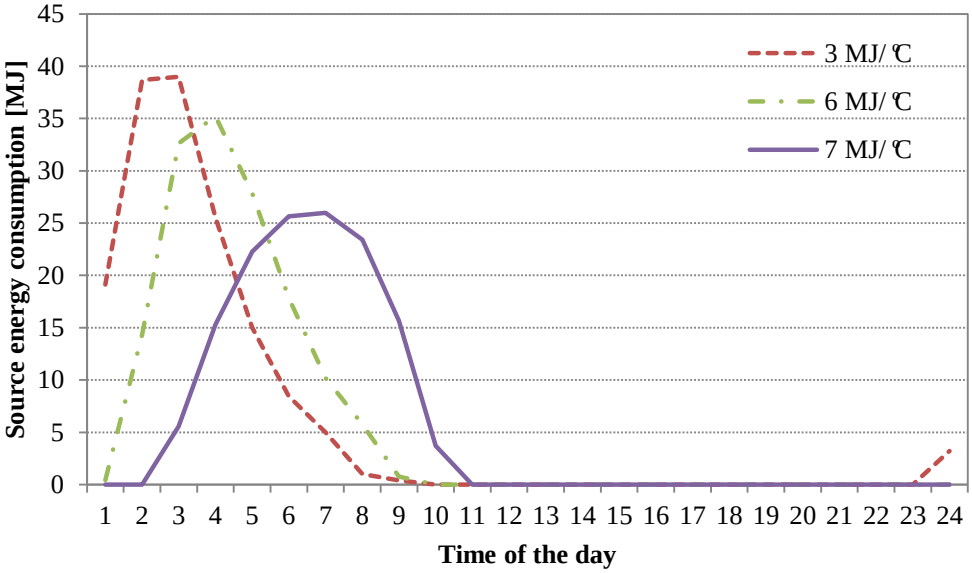

(b) Embedded pipe in the middle of the slab thickness

Figure 5.10: Hourly heating source energy consumption variation of radiant heating slab with (a) fixed pipe depth of 0.0 3 m and (b) pipe placed in the middle of the slab thickness as a function of thermal mass levels during December 21st in Golden, CO

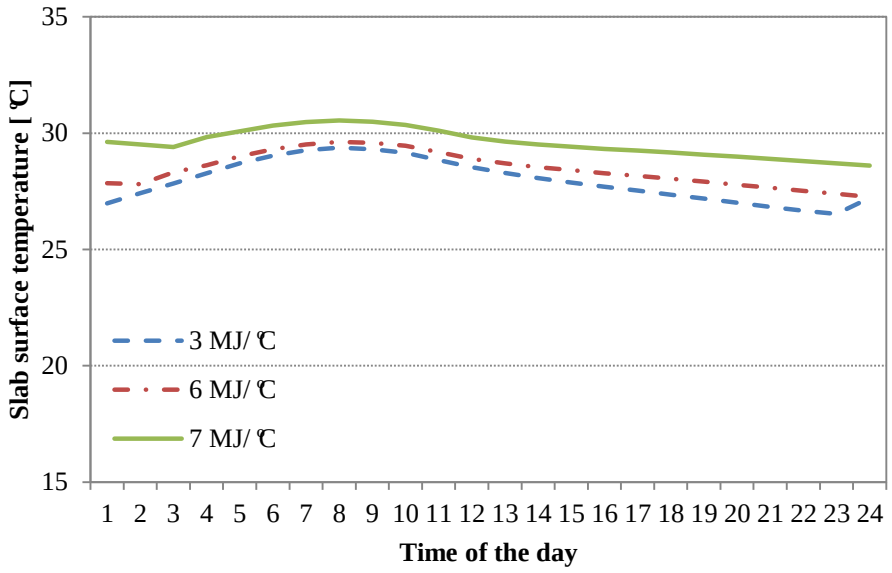

(a) Embedded pipe with fixed depth (0.03 meter)

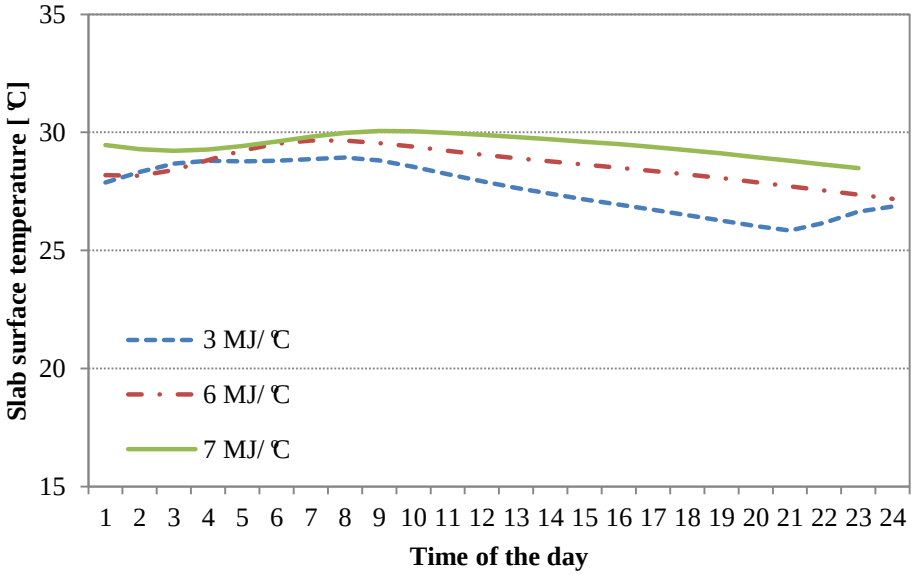

(b) Embedded pipe in the middle of the slab thickness

Figure 5.11: Hourly slab surface temperature variation for radiant heating floor with (a) fixed pipe depth of 0.03 m and (b) pipe placed in the middle of the slab as a function of thermal mass levels during December 21st in Golden, CO

Figure 5.12 compares the hourly source energy consumption of the radiant cooling ceiling system for various slab thermal mass levels using the two pipe depth options during July 21st in Golden, CO. Figure 5.13 illustrates the time variation of the ceiling surface temperature for the same slab thermal mass levels and pipe depth options. As the slab thermal mass increases, the ceiling surface temperature is maintained lower. As indicated in Figure 5.12, when the slab thermal mass level increases, the starting operation time of the radiant cooling ceiling is delayed, and peak thermal load is significantly reduced compared to the case when the slab has a light thermal mass independently of the pipe depth option.

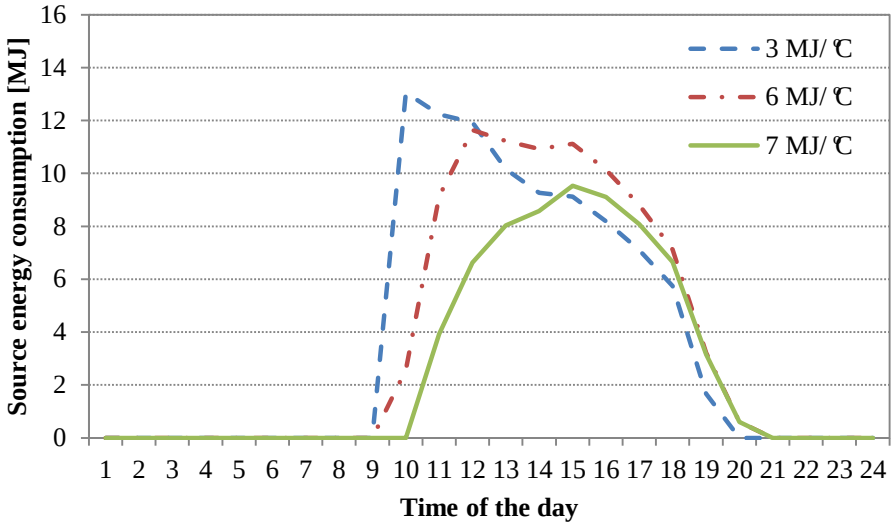

(a) Embedded pipe with fixed depth (0.03 meter)

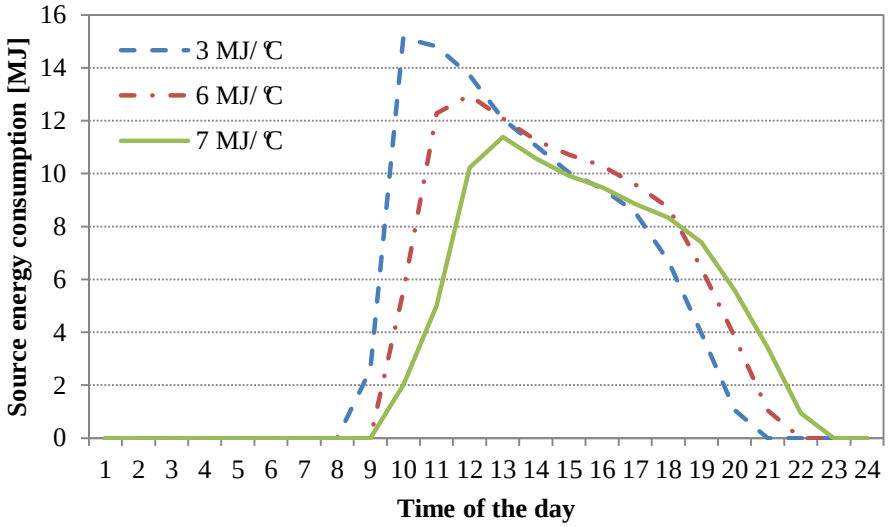

(b) Embedded pipe in the middle of the slab thickness

Figure 5.12: Hourly cooling source energy consumption variation of radiant cooling ceiling with (a) fixed pipe depth of 0.03 m and (b) pipe placed in the middle of the slab as a function of thermal mass levels during July 21st in Golden, CO

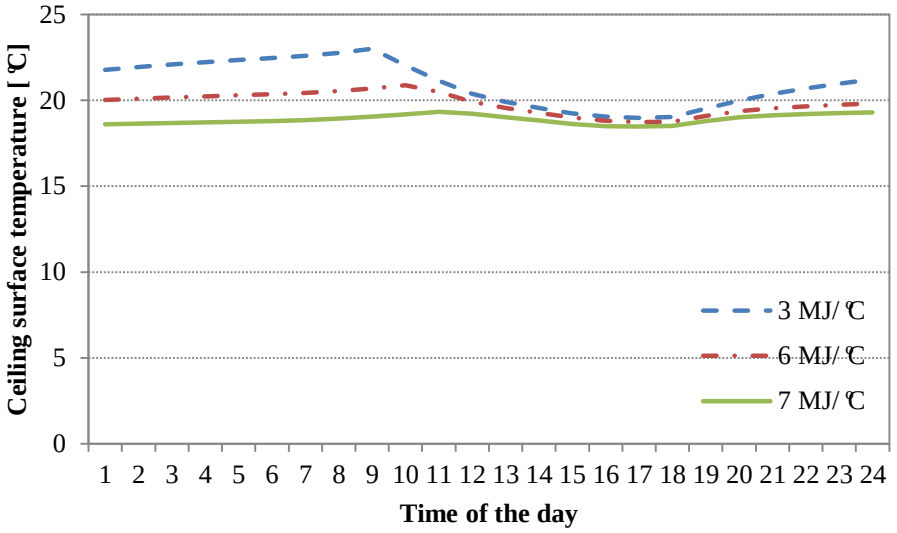

(a) Embedded pipe with fixed depth (0.03 meter)

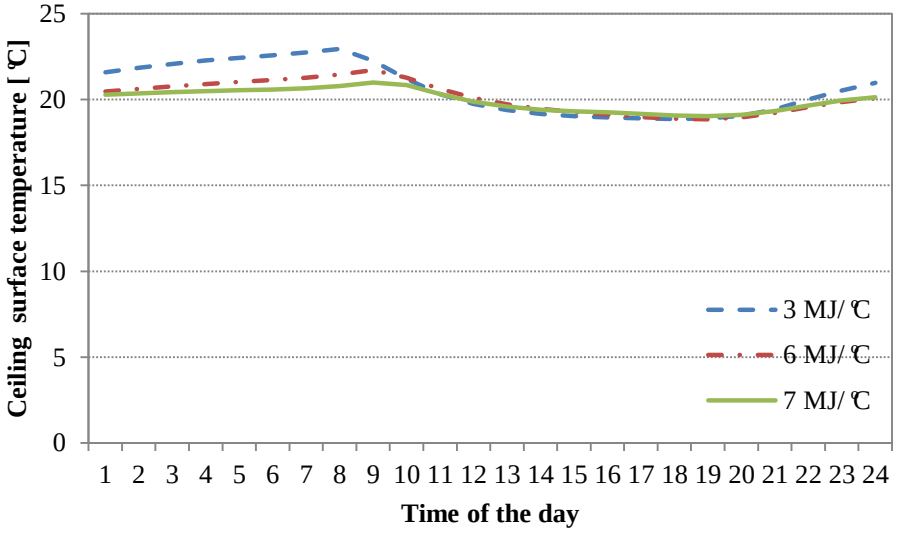

(b) Embedded pipe in the middle of the slab thickness

Figure 5.13: Hourly slab surface temperature variation for radiant cooling ceiling with (a) fixed pipe depth of 0.03 m and (b) pipe placed in the middle of the slab thickness as a function of thermal mass levels during July 21st in Golden, CO

5.4. Climate Sensitivity

In this section, the performance of radiant slab heating and cooling systems is evaluated for three different US climates. Specifically, climates for Chicago (IL), Golden (CO), and Phoenix (AZ) are selected to perform the climatic sensitivity analysis. The three cities belong to three different climate conditions as defined by ASHRAE standard 90.1. Indeed, ASHRAE defines Chicago as cool-humid climate, Golden as cool-dry climate, and Phoenix as warm-dry climate.

Figure 5.14, Figure 5.15, and Figure 5.16 illustrate the outdoor dry bulb temperature variations during winter season, summer season, and swing season in Chicago, Golden, and Phoenix, respectively.

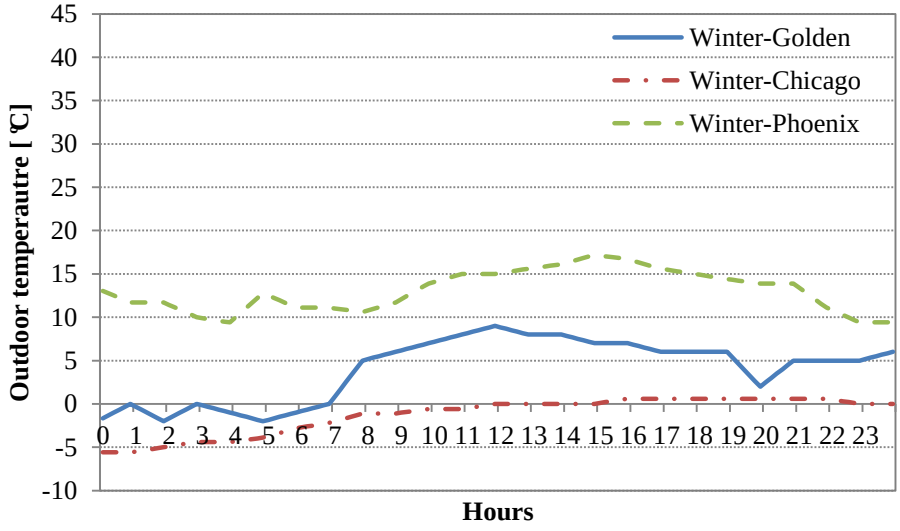

Figure 5.14: Outdoor dry bulb temperature variations during December 21st (winter season) in three US locations considered in the parametric analysis

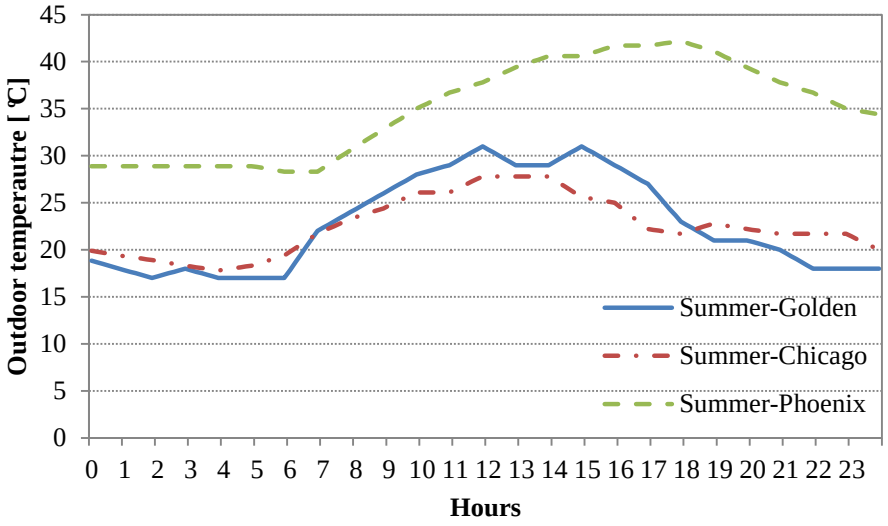

Figure 5.15: Outdoor dry bulb temperature variations during July 21st (summer season) in three US locations considered in the parametric analysis

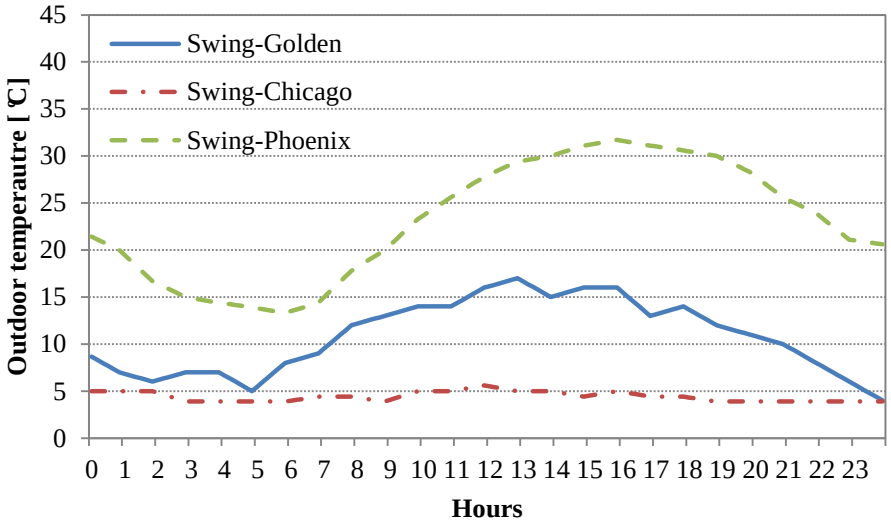

Figure 5.16: Outdoor dry bulb temperature variations during April 21st (swing season) in three US locations considered in the parametric analysis

Monthly source energy consumption variations obtained for Type 1 and Type 2 radiant slab systems in Golden, CO are compared in Figure 5.17. During the winter season, as expected

the monthly energy consumption is almost the same for both radiant system types. However Type 2 conserves around 17 % during the swing season, and Type 2 reduces cooling energy consumption approximately by 10 % during the cooling season compared to Type 1. Even if edge insulation or horizontal insulation is added, similar results are obtained.

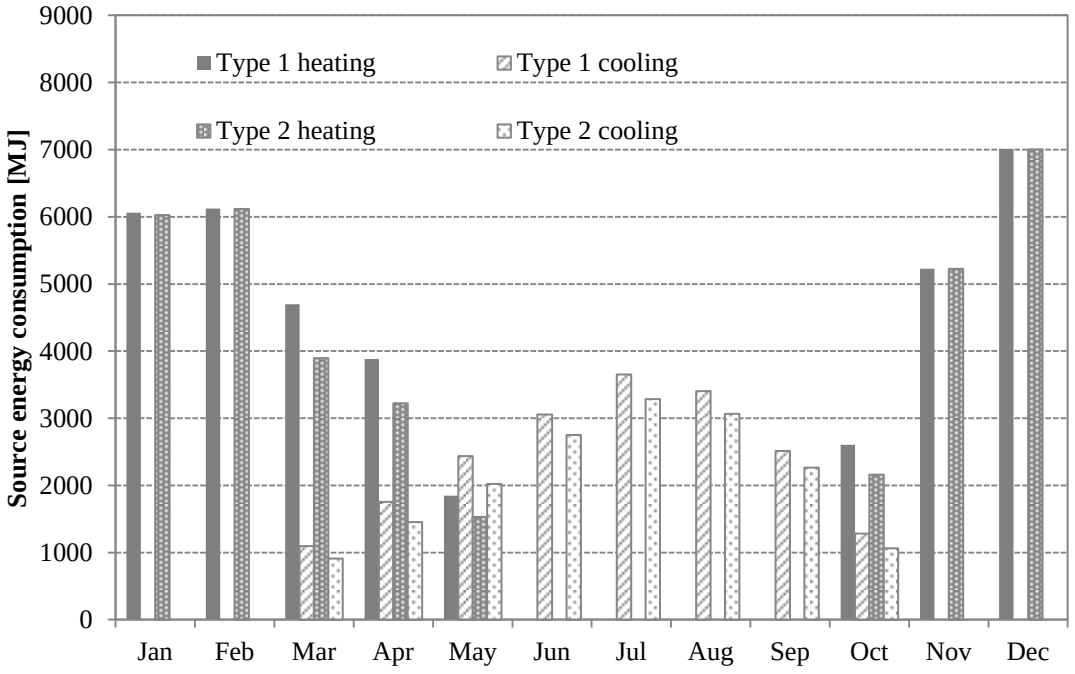

Figure 5.17: Monthly radiant heating and cooling source energy consumption for Type 1 and Type 2 with horizontal and edge insulation configuration in Golden, CO

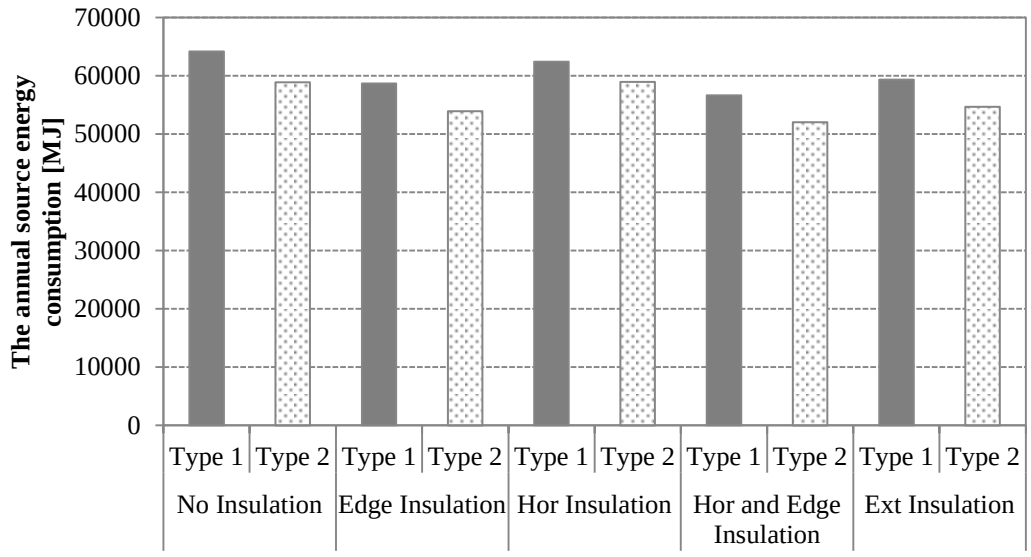

Figure 5.18: Comparison of the annual source energy consumption with various insulation placement configurations in Golden, CO

Monthly source energy consumption variations obtained for Type 1 and Type 2 radiant slab systems in Phoenix, AZ are compared as illustrated in Figure 5.19. During the winter season, monthly energy consumption is almost the same for both types of radiant slab systems. Type 2 reduces cooling energy consumption approximately by 19 % during the cooling season compared to Type 1. Even if edge insulation or horizontal insulation is added, similar results are obtained.

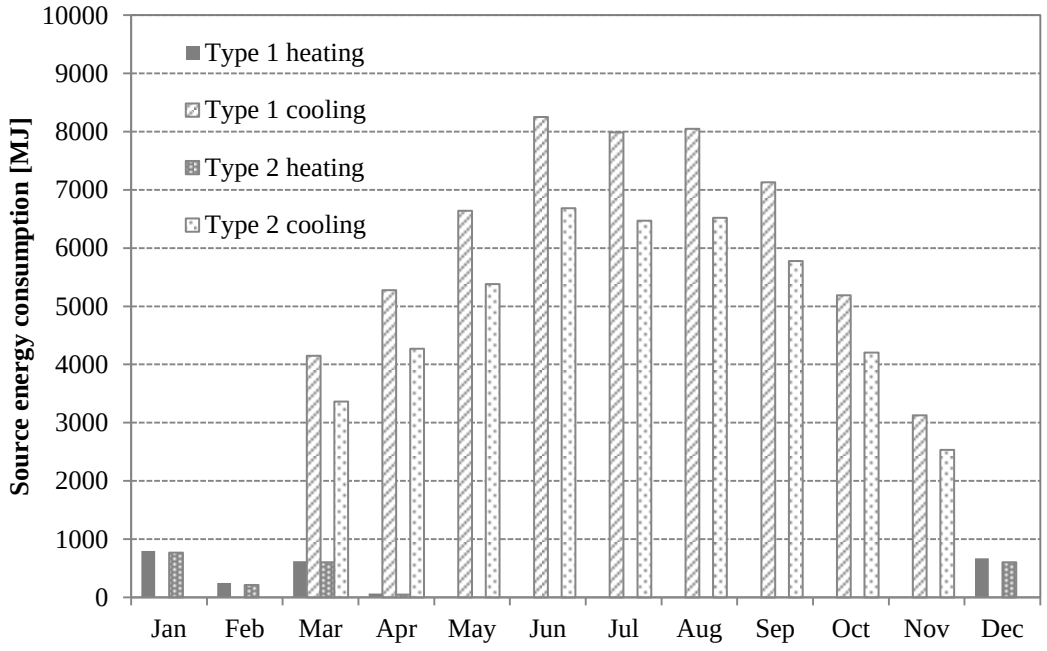

Figure 5.19: Monthly radiant heating and cooling source energy consumption for Type 1 and Type 2 with horizontal and edge insulation configuration in Phoenix, AZ

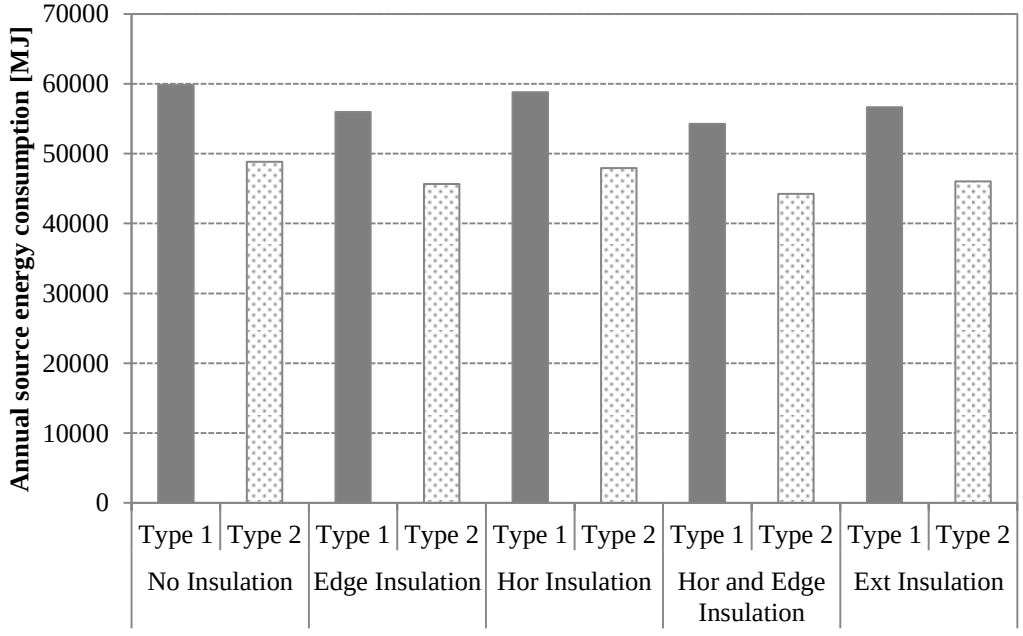

Figure 5.20: Comparison of the annual source energy consumption with various insulation placement configurations in Phoenix, AZ

Monthly source energy consumption variations obtained for Type 1 and Type 2 radiant slab systems in Chicago, IL are compared as shown in Figure 5.21. During the winter season, the monthly energy consumption remains almost the same for both system types. However, Type 2 uses 6 % less energy during the swing season, and Type 2 reduces cooling energy consumption approximately by 8 % during the cooling season compared to Type 1. Even if edge insulation or horizontal insulation is added, similar results are obtained.

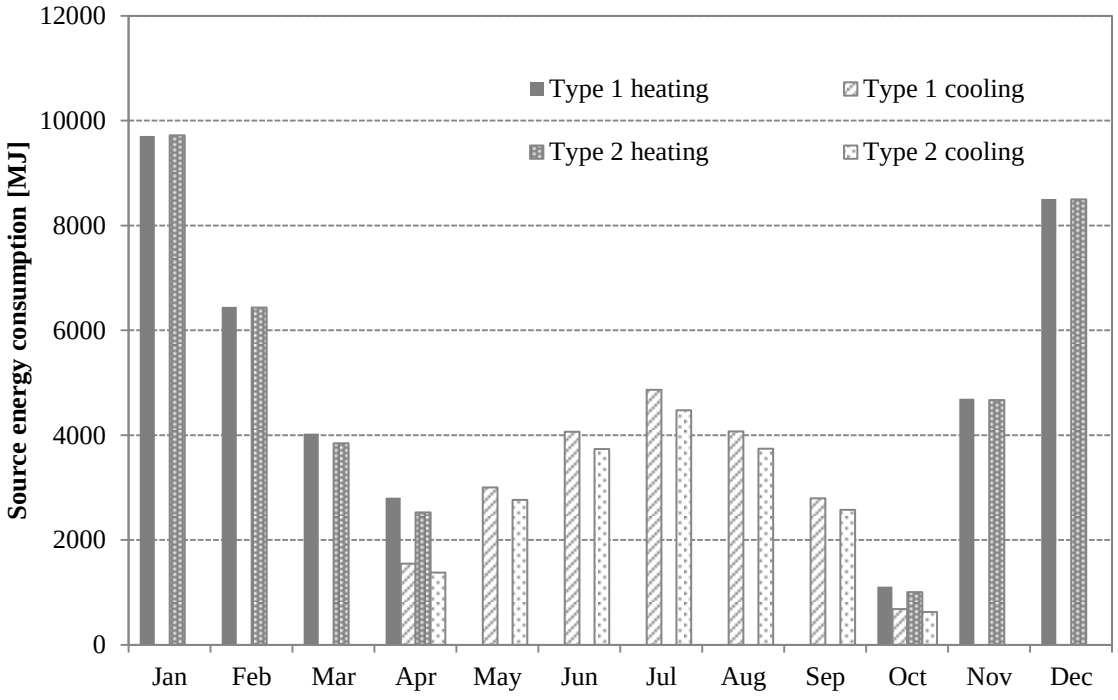

Figure 5.21: Monthly radiant heating and cooling source energy consumption for Type 1 and Type 2 with horizontal and edge insulation configuration in Chicago, IL

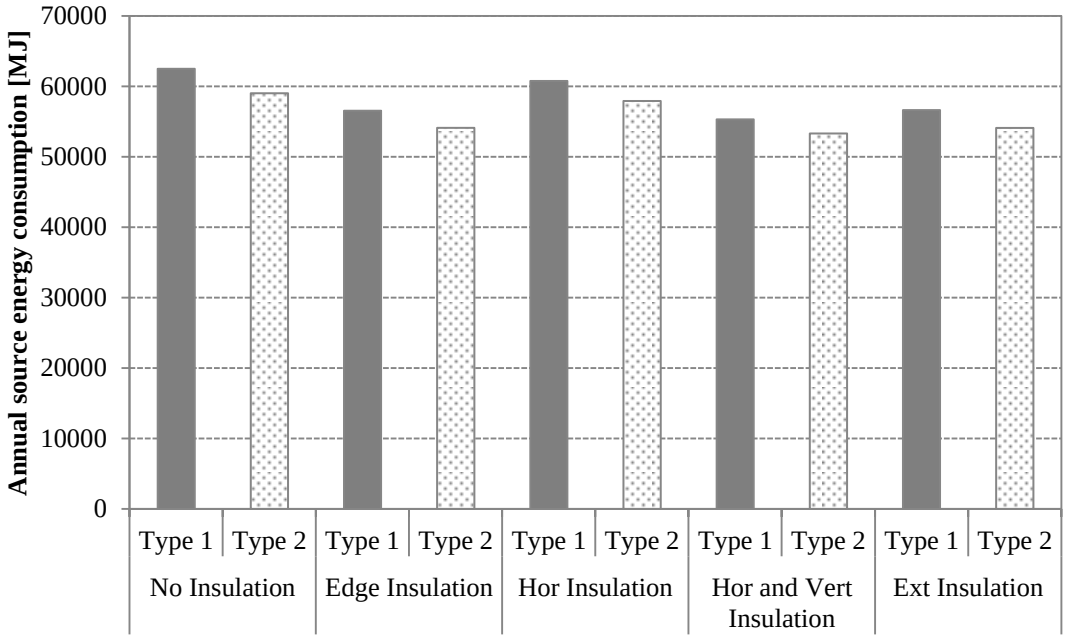

Figure 5.22: Comparison of the annual source energy consumption with various insulation placement configurations in Chicago, IL

5.5. Summary and Conclusions

In this chapter, thermal and energy performance of radiant slab heating and cooling systems are evaluated using the developed simulation environment that includes a two-dimensional numerical solution for the radiant slab combined with an RC network model for conditioned zones. The analyses include the impact of insulation placement configurations depending on the thermal interactions between two adjacent thermal zones (conditioned with unconditioned zones as well as two adjacent conditioned zones) the impact of thermal mass located in the exterior walls and slab floor medium , and the effect of the climate on energy consumption for radiant systems .

It is found that when an adjacent zone is unconditioned such as an attic or a crawl space, uniform horizontal insulation for the radiant slab is more effective than slab edge insulation. For the case of a conditioned zone adjacent to an unconditioned zone, the most effective insulation placement for the radiant slab system is horizontal and edge insulation. For this insulation configuration, daily radiant heating energy consumption and radiant cooling energy consumption can be reduced by 33 percent and 30 percent compared to the slab system with no insulation.

In addition, when the adjacent zone is conditioned, slab edge insulation is found to be more effective more slab horizontal insulation in reducing energy use. Indeed, energy consumption can be reduced by 12 - 15 percent with slab edge insulation and by only 2 - 5 percent of with horizontal insulation.

Energy performance of integrated radiant floor heating and cooling systems (Type 1) and separate radiant floor heating and radiant ceiling cooling system (Type 2) is evaluated. During the heating season Type 1 and Type 2 only uses radiant floor panel to

supply heating energy to the conditioned zone. Therefore, the heating energy consumption during the winter season is the same for Type 1 and Type 2. During the cooling season, Type 2 radiant system reduces energy consumption by 6 – 11 percent compared to Type 1 because cooling energy provided by the radiant cooling ceiling is more effective due to better convective heat transfer. During the swing season, Type 2 reduces energy consumption by 17 – 20 percent compared to Type 1. Thus, during the swing season, Type 2 is more energy efficient than Type 1.

It is found that an increase in the slab thermal mass decreases the source energy required by the integrated radiant slab systems. In particular, it is also found that when the embedded pipe depth is fixed to be near the slab surface (i.e., 0.03 m), increasing the slab thermal mass is more effective than adding thermal mass in the exterior walls during heating operation. However and during cooling operation, thermal mass within the exterior walls is more effective in reducing cooling energy consumption that thermal mass embedded in the slab floor.

Performance of radiant floor heating and radiant ceiling cooling system is evaluated in three different US climates including Chicago (IL), Golden (CO), and Phoenix (AZ). During the winter season, it is found that the monthly energy consumption is the same for Type 1 and Type 2 radiant slab systems.

Type 2 radiant system reduces source energy use by 17 percent compared to Type 1 during the swing season. Moreover, it is found that Type 2 reduces cooling energy consumption by 10 percent during the cooling season compared to Type 1 in Golden, CO. The same Type 2 radiant system is found to reduce cooling energy consumption approximately by 19 percent during the cooling season compared to Type 1 in Phoenix, AZ. Finally, it is found that Type 2 radiant system saves 6 percent in energy use during the swing season, and 8 percent

during the cooling season compared to Type 1 in Chicago, IL. Generally, radiant ceiling cooling systems are more effective in cooling dominated climates compared to heating dominated climates.

CHAPTER 6: CONCLUSIONS AND FUTURE WORK

6.1. Summary and Conclusions

The study presented in this thesis consists of a detailed thermal analysis of the radiant slab heating and cooling systems with two embedded water pipes. In particular, the study investigated the thermal interaction between radiant slab system and the building indoor environment utilizing a newly developed simulation environment that integrates an RC thermal network with an FDM numerical model for the radiant slab. Several analyses have been carried out using developed FDM numerical model as well as the integrated RC+FDM simulation environment. Throughout the thesis, the results of the analyses are provided and discussed. An outline of the scope and the major focus as well as the main findings of each chapter is briefly presented in the following sections.

In Chapter 2, general simulation procedures for building envelope systems are described including numerical models for radiant slab systems. In addition, a literature review of previous reported studies including those utilizing numerical modeling techniques to evaluate radiant systems are briefly introduced. Both one-dimensional and two-dimensional numerical solutions utilizing the implicit finite difference method (FDM) for the radiant slab with two heat sources ate developed to assess thermal interactions between radiant slab system and indoor environment including thermal bridging effects associated with the slab floor-exterior wall joints.

The predictions obtained from the FDM solution are verified against the results from an analytical solution for the case of a simplified slab model. The verification analysis

indicates that the developed numerical model can accurately predict thermal performance of radiant heating and cooling slabs.

Chapter 3 presents the results obtained from developed two-dimensional numerical FDM model for the radiant slab system with two heat sources. The analysis included evaluation of the thermal bridging effects between the radiant slab floor and the exterior walls. In particular, zone mean air temperatures, temperature distributions within slab, and total slab heat losses/gains are analyzed for various slab insulation placement configurations.

Comparative analyses are performed to examine the performance of radiant slab heating and cooling systems under various design and operating conditions. Specifically, the analyses included the effect of pipe pitch size, the effect of supplied hot or cold water temperature, the effect of hot or cold water mass flow rate, the effect of depth of embedded pipe, and the effect of insulation configuration.

The results of the sensitivity analyses have indicated that the pipe pitch has a minimal effect on the performance of the radiant slab systems. It is found that the total radiant heat transfer from the slab increases proportionally to increase in supplied hot water temperature.

When the water mass flow rate is larger than 0.15 kg/s, the total slab heat transfer rate to the indoor space is not significantly affected by the mass flow rate for both heating and cooling operation modes.

As the depth of embedded heating pipe increases, the total slab heat transfer rate on upper slab surface was found to decreases, but the total slab heat transfer rate on lower slab surface increases. During cooling mode, the total slab heat transfer rate into the upper zone was found to increases proportionally to the increase of the depth of cooling pipe.

It was also found that radiant heat losses obtained from the two-dimensional numerical model are higher than those predicted by the one-dimensional model, regardless of the type of slab insulation configuration. The results have indicated that heat losses from radiant slab are significantly reduced when vertical edge and horizontal uniform insulation configurations are used. In addition, horizontal uniform insulation was found to be more effective in reducing thermal bridging effects than vertical edge insulation configuration. In Chapter 4, a simulation environment for estimating energy consumption of radiant heating and cooling systems to maintain thermal comfort within spaces is developed. The simulation environment is based on an RC thermal network model of zones integrated to the developed two-dimensional numerical solution presented in chapter 3 to model radiant slab floor with embedded hot and cold water pipes. In this chapter, radiant floor heating and cooling systems operated with a variable flow control strategy is evaluated. Using the developed simulation environment with the combined RC and FDM models, the impact of thermal bridging effects, associated with the joints between the radiant floor slab and the exterior walls, on energy consumption for radiant floor heating and ceiling cooling system are evaluated.

It was found that an increase of 35 percent of radiant heating energy consumption can be obtained due to accounting for thermal bridging effects when the no insulation is utilized. Similarly, it was also found that radiant ceiling cooling panel consumes 24 percent more cooling energy when thermal bridging occurs. Existing simulation tools such as Energyplus ignore the impact of thermal bridging effects and therefore may underestimate both heating and cooling energy use related to radiant slab systems.

Chapter 5 presents some specific applications of developed simulation environment to model radiant heating and cooling slab systems using the two-dimensional numerical

solution for heat conduction within the slab-wall joints. The analyses include impact of insulation placement configurations on radiant heating and cooling energy consumption for various design and operating conditions. They also include the interaction between two conditioned or unconditioned thermal zones, the thermal mass level of the slab floor and the exterior wall, and the climate conditions.

It was found that when one of the adjacent zones is not conditioned such as an attic or a crawl space, uniform horizontal insulation placed along the slab floor has a larger impact on reducing radiant energy consumption when compared to slab edge insulation placement. The most effective placement configuration is to add horizontal and edge insulation. Indeed, for this insulation placement configuration daily radiant heating energy consumption and radiant cooling energy consumption were found to be reduced by 33 percent and 30 percent compared to the case of no insulation. In addition, it was found that when the adjacent zones are conditioned and utilizing radiant heating and cooling systems, slab edge insulation placement is more effective than uniform horizontal insulation in reducing energy use for both heating and cooling. Indeed, it was found that heating and cooling energy consumption can be reduced by 12 - 15 percent with slab edge insulation compared to the case of no insulation. Meanwhile, horizontal insulation placement was found to only reduce radiant energy consumption by 2 - 5 percent.

Energy performance of radiant floor heating and cooling systems is evaluated for two types of designs, Type 1 and Type 2. Type 1 consists of separate radiant floor heating system and radiant ceiling cooling system while Type 2 has two the same slab has a radiant heating and a radiant cooling system is also evaluated. During the heating season, both Type 1 and Type 2 systems rely on radiant floor panel to supply heating energy to the controlled thermal zones. Therefore, the heating energy consumption during the winter

season is the same for Type 1 and Type 2 systems. During cooling season, however, Type 2 reduces the energy consumption by 6 – 11 percent compared to Type 1 because cooling energy provided by radiant cooling ceiling is more effective through convective heat transfer. During the swing season, Type 2 radiant system reduces energy consumption by 17 – 20 percent compared to Type 1.

It is found that an increase in the slab thermal mass decreases the source energy required by the integrated radiant slab systems. In particular, it is also found that when the embedded pipe depth is fixed to be near the slab surface (i.e., 0.03 m), increasing the slab thermal mass is more effective than adding thermal mass in the exterior walls during heating operation. However and during cooling operation, thermal mass within the exterior walls is more effective in reducing cooling energy consumption that thermal mass embedded in the slab floor.

It is found that an increase in slab thermal mass decreases source energy consumption by radiant slab heating and cooling systems. It is also found that when the embedded pipe depth is fixed shallowly at certain depth, the effective of thermal mass associated with slab medium can be maximized. For heating scenario, increasing a slab thermal mass is more effective than adding a thermal mass associated with exterior wall. On the other hand, exterior wall thermal mass is more effective to reduce cooling energy consumption compared to the increase of the slab thermal mass for cooling scenario.

The performance of radiant floor heating and radiant ceiling cooling systems is evaluated in three different US climates including Chicago (IL), Golden (CO), and Phoenix (AZ). It is found that in Golden, CO, Type 2 radiant system utilizes less energy compared to Type 1 system by 17 percent during swing season, and 10 percent during the cooling season. Similarly, it is found that in Phoenix, AZ, Type 2 reduces energy consumption

compared to Type 1 by 19 percent during the cooling season and by 6 percent during the swing season,. Finally, in Chicago, IL, it found that Type 2 radiant system can reduce energy consumption compared to Type 1 by 8 percent during the cooling season.

6.2. Future Work

In this thesis, only stand-alone simulation environment that combines RC network and FDM models is used to analyze the performance of radiant slab heating and cooling systems, radiant slab with two heat sources. Even though the developed simulation environment adapted some algorithms from Energyplus including zone heat balance and control strategies, it still has limited capabilities due to the inherent assumptions specific to the RC thermal network modeling technique. However, the developed FDM model can be integrated directly in Energyplus, especially that the source code for the simulation tool is now readily available. As shown in this work for radiant slab heating and cooling system, it is important to consider the effect of thermal bridge on the performance of radiant slab system. Unlike developed combined model, current Energyplus does not consider thermal bridge effect on radiant slab system; it tends to under-estimate the energy consumption of the radiant slab system.

The radiant slab model developed and evaluated in the presented study considers only embedded hot or cold water pipes. Slab with electric wires for heating can be easily added and considered in the developed simulation environment for evaluating the thermal performance of radiant heating and cooling slab systems. Furthermore, various control strategies including variable temperature control and optimal control based on main radiant temperature, operative temperature, or predicted mean value can be modeled and analyzed to achieve the most effective performance of the radiant slab systems.

In this thesis, radiant slabs with embedded water pipes radiant system are considered. Future work would include other fluids for radiant slab systems including circulating conditioned air through embedded ducts or channels. For instance, hollow

core slab systems, also known as ventilated slab systems, utilize channels within precast slabs to cool or heat thermal zones. Compared to conventional air systems, hollow core slab systems have the potential to significantly reduce energy use to heat and cooling both residential and commercial buildings. The simulation environment developed and presented in this thesis energy, can be modified and adapted to model the thermal performance of hollow core slab systems.

REFERENCES

ANSI/ASHRAE/IESNA Standard 90.1-2007 (2007), ASHRAE energy standard for buildings except low-rise residential buildings.

ASHRAE (2005). Handbook of Fundamentals, American Society of Heating, Refrigerating and Air-Conditioning Engineers, Atlanta, GA.

ASHRAE (2011). Handbook of HVAC Applications, American Society of Heating, Refrigerating and Air-Conditioning Engineers, Inc., Atlanta, GA.

ASHRAE (2008). Handbook of Systems and Equipment, American Society of Heating, Refrigerating and Air-Conditioning Engineers, Inc., Atlanta, GA.

Athientis, A. K. (1994), Numerical Model of Floor Heating System, ASHRAE Transactions, 100(1), 1024-1030.

Athientis, A. K. and Chen T.Y. (1997), Numerical Study of Thermostat Setpoint Profiles for Floor Radiant Heating and the Effect of Thermal Mass, ASHRAE Transactions, 103(1).

Awbi, H.B. and Hatton. A. (1999), Natural convection from heated room surfaces, Energy and Buildings 30: 233-244.

CADDET (1999), Radiant Heating Panels Save Energy in Homes, Centre for the Analysis and Dissemination of Demonstrated Energy Technologies, US-1999-502, Result 337.

Chen T. Y. (2002), Application of Adaptive Predictive Control to a Floor Heating System with a Large Thermal Lag, Energy and Buildings, 34, 45-51.

Clarke J. A. (2001), *Energy Simulation in Building Design Second Edition*, Oxford, Betterworth-Heinemann.

Conroy C., Mumma, S. (2001), Ceiling radiant cooling panels as a viable distributed parallel sensible cooling technology integrated with dedicated outdoor air systems. ASHRAE Transactions, 107, 578-585.

Department of Energy (2010), Building Energy Data Book, DOE.

EnergyPlus User's Guide (2010), Engineering Reference, DOE.

EnergyPlus User's Guide (2010), Input Output Reference, DOE.

Gwerder M., Lehmann B., J. Tödtli, V. Dorer and F. Renggli (2008), "Control of thermally-activated building systems (TABS)". Applied Energy 85 (7): 565–581.

Ho, S.Y., R. E. Hayes, and R. K. Wood. (1995), Simulation of the dynamic behavior of a hydronic floor heating system, Heat Recovery Systems & CHP 15(6): 505–19.

Ihm P. C. (2003), *Modeling and Optimization in Slab-on-grade Radiant Heating Floor Systems*, Ph.D Thesis, University of Colorado at Boulder.

Imarani, T., T. Omori, and K. Bogaki. (1999), Thermal comfort and energy consumption of the radiant ceiling panel system: Comparison with the conventional all-air system. Energy and Buildings 30: 167–75.

Incorpera, F.P., D. DeWitt, T. Bergman, and A. Lavine. (2006), Fundamentals of Heat and Mass transfer, 6th ed. John Wiley & Sons.

Karadag R. (2009), New approach relevant to total heat transfer coefficient including the effect of radiation and convection at the ceiling in a cooled ceiling room. Applied Thermal Engineering 29: 1561-1565.

Krarti M. (2000), *Energy Audit of Building Systems*, CRC.

Krarti M. and Park B. (2011), Analysis of Design Features of Walking Box Ranch Project, Final Report to RMI, University of Colorado at Boulder.

Kreith F. and Bohn M. S. (2001), *Principle of Heat Transfer Sixth Edition*, Cengage Learning.

Laouadi, A. (2004), Development of a radiant heating and cooling model for building energy simulation software, Building and Environment 39: 421–31.

MacCluer C. R. (1989), The Control of Radiant Slabs, ASHRAE Journal, September, 28-33.

Miriel J., Serres L., Trombe A. (2002), Radiant ceiling panel heating-cooling systems: experimental and simulated study of the performances, thermal comfort and energy consumptions, Applied Thermal Engineering 22: 1861–1873.

Mumma S.A. (2001), Ceiling panel cooling systems, ASHRAE Journal, November, 28–32.

Mumma, S.A. (2002). Chilled ceilings in parallel with dedicated outdoor air systems: Addressing the concerns of condensation, capacity, and cost, ASHRAE Transactions 108 (2): 220–231.

Olesen, B.W. (1994), Comparative Experimental Study of Performance of Radiant Flow-Heating Systems and Wall Panel Heating System under Dynamic Conditions, *ASHRAE Transaction*, vol. 100, pt. 1, pp. 1011-1023.

Olesen, Bjarne W. (2008), Hydronic Floor Cooling Systems, ASHRAE Journal, September.

Pantankar S. V. (1980), *Numerical Heat Transfer and Fluid Flow*, New York, Hemisphere.

Simmonds, P. (1994), Control Strategies for Combined Heating and Cooling Radiant Systems, ASHRAE Transaction, vol. 100, pt. 1, pp. 1031-1039.

Stanley A Mumma (2001), Condensation issues with radiant cooling panels, IAQ Applications, Fall, 16–8.

Stetui C., (1998), Radiant Cooling in US Office Buildings: Towards Eliminating the Perception Climate Imposed Barriers, Energy and Resources Group, University of California Berkeley, CA 94720.

Strand, R.K. and C.O. Pedersen. (1997), Implementation of a Radiant Heating and Cooling Model into an Integrated Building Energy Analysis Program, ASHRAE Transaction, vol. 103, pt. 1, pp. 949-958.

Watson, R.D., and Chapman. K.S. (2002), Radiant Heating & Cooling Handbook, Chapter 4.5, Radiant hydronic heating systems, New York, McGraw-Hill.

Weitzman, P., J. Kragh, P. Roots, and S. Svendesn. (2005), Modeling floor heating systems using a validated two-dimensional ground-coupled numerical model, Building and Environment 40: 153–63.

Wilcox, S. and W. Marion. (2008), User's Manual for TMY3 Data Sets, NREL/TP-581-43156, April 2008, Golden, Colorado: National Renewable Energy Laboratory.

Yunus A. Cengel and Afshin J. Ghajar (2001), *Fundamentals of thermal-fluid sciences*, McGraw Hill.

Zaheer-uddin, M. and Cho, S. H. (2002), Augmented Control Strategies for Radiant Floor Heating Systems, International Journal of Energy Research, 26, 79-92.

Zaheer-uddin, M. and Cho, S. H. (1999), An Experimental Study of Multiple Parameter Switching Control for Radiant Floor Heating Systems, International Journal of Energy Research, 24, 433-444.

Zhang, Z. and Pate. M. B. (1989), A New Approach for Designing Heating Panels with Embedded Tubes, ASHRAE Transactions, 95(1).

Zhang, Z.L. January (2001), Temperature control strategies for radiant floor heating systems, Master’s Thesis, Concordia University, Montreal, Quebec, Canada.

APPENDIX A

Energyplus timestep sensitivity analysis

1. Zone mean air temperature

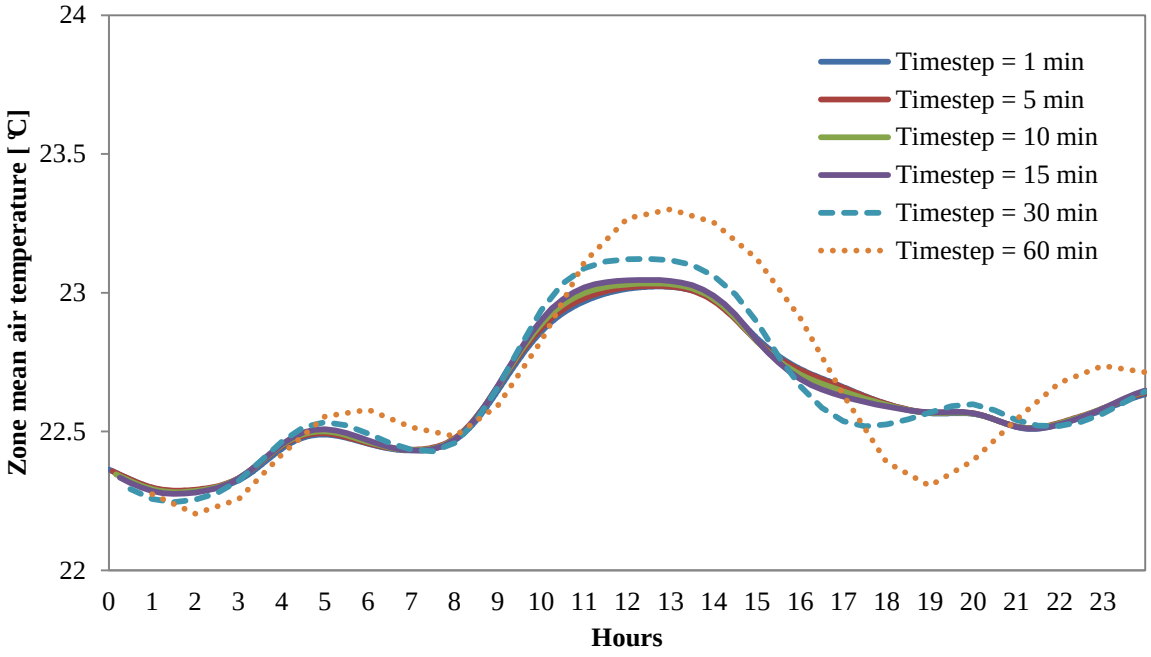

Zone Mean Air Temperature	Average % Diff.
Timestep = 1 min	-
% Diff.	-
Timestep = 5 min	-
% Diff.	**0.0%**
Timestep = 10 min	-
% Diff.	**0.0%**
Timestep = 15 min	-
% Diff.	**0.0%**
Timestep = 30 min	-
% Diff.	**-0.1%**
Timestep = 60 min	-
% Diff.	**-0.2%**

2. Water mass flow rate

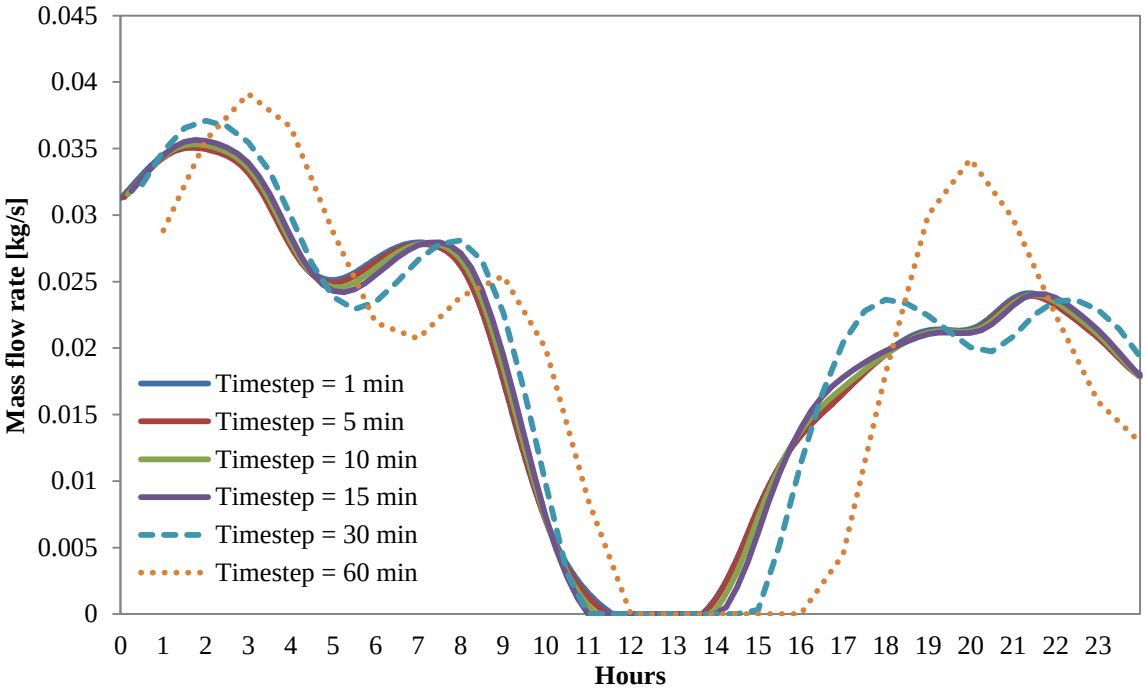

Zone Mean Air Temperature	Average % Diff.
Timestep = 1 min	-
% Diff.	-
Timestep = 5 min	-
% Diff.	**1.6%**
Timestep = 10 min	-
% Diff.	**5.9%**
Timestep = 15 min	-
% Diff.	**8.7%**
Timestep = 30 min	-
% Diff.	**8.5%**
Timestep = 60 min	-
% Diff.	**-14.8%**

3. Water outlet temperature

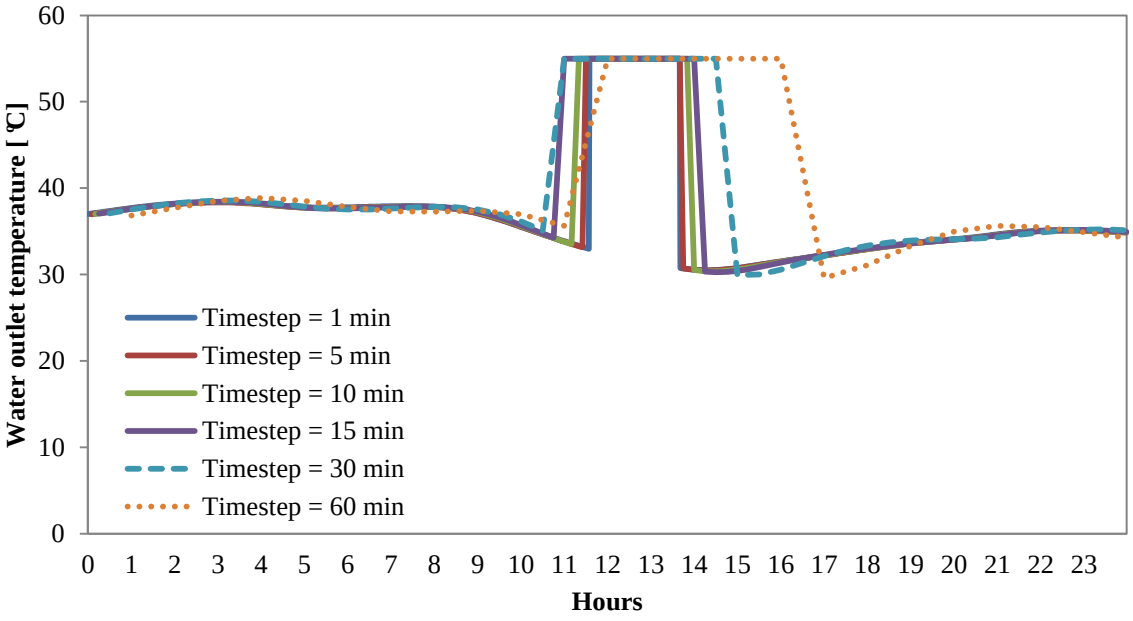

Zone Mean Air Temperature	Average % Diff.
Timestep = 1 min	-
% Diff.	-
Timestep = 5 min	-
% Diff.	**0.1%**
Timestep = 10 min	-
% Diff.	**0.1%**
Timestep = 15 min	-
% Diff.	**-6.1%**
Timestep = 30 min	-
% Diff.	**-6.1%**
Timestep = 60 min	-
% Diff.	**-10.1%**

4. Slab edge insulation

Insulation product introduced by Schöck Ltd which can be used in outer joint of exterior wall and slab edge.